Report No. BD545 RPWO #57 Date: July 2007
FINAL REPORT

Contract Title: Development of Hurricane Resistant Traffic Signal Hangers and Disconnects
UF Project No. 00054246
Contract No. BD545 RPWO #57

DEVELOPMENT OF HURRICANE RESISTANT CABLE SUPPORTED TRAFFIC SIGNALS

Principal Investigator: Ronald A. Cook, Ph.D., P.E.

Graduate Research Assistant: Eric V. Johnson, Jr.

Project Manager: Marcus H. Ansley, P.E.

Department of Civil & Coastal Engineering
College of Engineering
University of Florida
Gainesville, Florida 32611

DISCLAIMER

The opinions, findings, and conclusions expressed in this publication are those of the authors and not necessarily those of the State of Florida Department of Transportation.

Technical Report Documentation Page

1. Report No. BD545 RPWO #57	2. Government Accession No.	3. Recipient's Catalog No.
4. Title and Subtitle Contract Title: Development of Hurricane Resistant Traffic Signal Hangers and Disconnects Report Title: Development of Hurricane Resistant Cable Supported Traffic Signals		5. Report Date July 2007 6. Performing Organization Code
7. Author(s) R. A. Cook and E. Johnson		8. Performing Organization Report No. 00054246
9. Performing Organization Name and Address University of Florida Department of Civil Engineering 345 Weil Hall / P.O. Box 116580 Gainesville, FL 32611-6580		10. Work Unit No. (TRAIS) 11. Contract or Grant No. BD545 RPWO #57
12. Sponsoring Agency Name and Address Florida Department of Transportation Research Management Center 605 Suwannee Street, MS 30 Tallahassee, FL 32301-8064		13. Type of Report and Period Covered Final Report 14. Sponsoring Agency Code
15. Supplementary Notes		

16. Abstract

Performance of traffic signal support systems during hurricanes has indicated that the current dual cable system often experiences substantial damage. Damage to these signal support systems typically occurs in the hanger or quick disconnect box near the connection to the messenger cable. Because there is widespread use of single cable support systems in hurricane prone regions of other states, this project investigated the performance of both dual cable and single cable support systems under high velocity winds.

Thirty-one wind load tests were performed using both dual cable and single cable support systems. The weight, orientation, and type of signal support hardware were modified to show the effects of various signal configurations. Test results indicate:

- The difference in signal rotation is insignificant between dual cable and single cable systems.
- The tension in the catenary cable does not significantly increase for either system; however, in the dual cable system, the increase in tensile force is substantial in the messenger cable resulting in increased flexural loading in the pole support structure.
- Cable supported traffic signals should be designed using both the drag and lift coefficients rather than just the drag coefficient since the signal rotates.

17. Key Word signals, signal support, cables, wind	18. Distribution Statement No restrictions		
19. Security Classif. (of this report) Unclassified	20. Security Classif. (of this page) Unclassified	21. No. of Pages 109	22. Price

Form DOT F 1700.7 (8-72) Reproduction of completed page authorized

DEVELOPMENT OF HURRICANE RESISTANT CABLE SUPPORTED TRAFFIC SIGNALS

Contract No. BD545 RPWO #57
UF No. 00054246

Principal Investigator: Ronald A. Cook, Ph.D., P.E.

Graduate Research Assistant: Eric V. Johnson, Jr.

FDOT Technical Coordinator: Marcus H. Ansley, P.E.

Engineering and Industrial Experiment Station
Department of Civil and Coastal Engineering
University of Florida
Gainesville, Florida

July 2007

ACKNOWLEDGMENTS

The authors acknowledge and thank the Florida Department of Transportation for providing the funding for this research project. The development and planning for the full-scale wind load tests performed on single and dual cable supported traffic signals was a collaborative effort between the University of Florida, the FDOT Structures Design Office, and the FDOT Traffic Operations Office. The successful implementation of the full-scale wind load test program resulted from a collaborative effort between the University of Florida, the City of Gainesville Public Works Department, Florida International University, and Gainesville Regional Utilities. Over 80 individuals from these organizations and state-wide traffic engineering, operations, and maintenance organizations were present on the very hot and humid July day when the tests were performed – thanks to all who attended and many thanks to those that helped develop and implement this project. Hopefully, this research project will result in improved performance of cable supported traffic signals in future hurricanes.

EXECUTIVE SUMMARY

The performance of traffic signal support systems during hurricanes has indicated that the current dual cable system often experiences substantial damage. Damage to these signal support systems typically occurs in the hanger or quick disconnect box near the connection to the messenger cable. Because there is widespread use of single cable support systems in hurricane prone regions of other states, this project investigated the performance of both dual cable and single cable support systems under high velocity winds.

The objective of this project was to evaluate both dual cable and single cable traffic signal support systems under high velocity winds. The evaluation included:

- Full-scale wind tests to 115 miles per hour on both single and dual cable systems supporting a five-head traffic signal
- Measurement of signal rotation, signal weight, cable tensions, and cable translations
- Evaluation of test data to determine the appropriate drag and lift coefficients for design
- Development of a recommendation to the Florida Department of Transportation regarding which type of support system would result in improved performance in hurricanes.

Thirty-one wind load tests were performed using both dual cable and single cable support systems. The weight, orientation, and type of signal support hardware were modified to show the effects of various signal configurations. Test results indicated:

- Regarding signal rotation, both dual and single cable support systems maintained 50% visibility of the signal to a wind velocity equal or exceeding 54 miles per hour. The average wind velocity for 50% visibility was 72 miles per hour for the dual cable system tests and 68 miles per hour for the single cable system tests.
- Tests of the single cable system experienced an insignificant increase in cable tension with increased wind load indicating that the system acts similar to a simple pendulum
- Tests of the dual cable system exhibited a significant increase in the tension of the messenger cable with increased wind load and with the accompanying increase in stresses in the hanger/disconnect and moment in the pole support structure.
- For dual cable support systems, the design of the support poles must include the large increase in moment with the resulting increase in cost of the pole support structure. Single cable support systems do not require this since the cable force remains relatively constant.

- Cable supported traffic signals should be designed using both drag and lift coefficients rather than just the drag coefficient since the signal rotates.
- For the single cable system, the results of this study indicate that for a five-head signal, a maximum drag coefficient of 0.7 and maximum lift coefficient of 0.4 would be reasonable.

Based on previous field performance in hurricanes, the dual cable system is unreliable in high wind environments. The results of the tests performed in this project indicate that the dual cable system increases the likelihood of failure of hangers/disconnects, cables, and poles with increased wind speed. Test results for the single cable system indicate that it operates as a simple pendulum resulting in no significant increase in the forces carried by the hanger, cables, and poles with increased wind speed over those carried in the dead load condition. The single cable system should be adopted to minimize failures associated with span wire support systems.

Implementation of the single cable support system will likely result in significantly less hurricane damage to cable supported traffic signals. This will result in a more reliable post-storm traffic system that should improve the time response for restoration of other critical services. In addition, the lower forces observed in the single cable system will result in decreased cost of construction of single cable support systems rather than the traditional dual cable support systems.

TABLE OF CONTENTS

1.0 INTRODUCTION

Performance of traffic signal support systems during hurricanes has indicated that the current dual cable system performs inadequately under high velocity winds. As investigated in "Structural Qualification Procedure for Traffic Signals and Signs" after Hurricane Andrew, failures in traffic signal support systems occur in the hanger or quick disconnect box near the connection to the messenger cable (Cook et al. 1996). Experience has shown that the current support system needs improvement. Because there is widespread use of single cable support systems in hurricane prone regions, this project investigates the performance of both dual cable and single cable support systems under high velocity winds.

Several actions were performed in order to evaluate the performance and design of both the single and dual cable support systems. Codes provided by the American Society of Civil Engineers (ASCE) and the American Association of State Highway Transportation Officials (AASHTO), as well as previous research by the Florida Department of Transportation, were investigated to determine the expected wind forces in extreme wind events. Testing of both systems was performed to determine how the signal support systems behave in high winds. Results from design methods were compared to the results observed from testing to verify accuracy.

This report summarizes the results of the design code review, testing of traffic signals, and comparison between test results and design methods.

2.0 BACKGROUND

The response of traffic signals to high velocity winds has previously been studied at the Virginia Polytechnic Institute and State University under James F. Marchman, III (Marchman 1971). Because of the complexities of the shape of traffic signals and their support systems, empirical data was determined to be best suited for finding the design wind loads on traffic signals. Testing of 3-head signals took place with varying signal orientation, hood shapes, and number of signals on each support. Graphs depicting wind pressure versus the force applied by the signal illustrated how the signals responded to winds that reached 160 mph.

The research conducted at Virginia Tech in the late 1960s remains as background in the 2001 version of "Standard Specifications for Structural Supports for Highway Signs, Luminaires and Traffic Signals" (AASHTO 2001). A few other projects, as discussed below, were carried out to further understand the behavior of traffic signal structures under wind loads before the current version of the code was adopted.

Florida is prone to high winds from tropical cyclones, and widespread damage to traffic signal structures was experienced in South Florida during Hurricane Andrew in 1992. As a result, the following projects sponsored by Florida Department of Transportation in the 90's were geared towards understanding how traffic signals respond to wind loading. One project, "Computer Aided Design Program for Signal Pole and Span Wire Assemblies with Two Point Connection System," was completed in two phases. Phase one included the development of a computer program—Analysis of Traffic Lights and Signs (ATLAS)—to model the behavior of traffic signals supported by the two-cable system used in Florida (Hoit et al. 1994). ATLAS includes a

nonlinear analysis of the signal support system and can verify that components are not overstressed. The second phase included the testing of dual cable support systems for comparison of results between ATLAS and the tests.

The other project, "Structural Qualification Procedure for Traffic Signals and Signs," was conducted to understand the failures of the dual cable traffic signal system that occur during hurricanes and to create a method of testing dual cable systems for adoption of standards into the FDOT Product Approval List (Cook et al. 1996). "Standards for Windborne Debris Impact Tests" by Southern Building Code Congress International (SBCCI) specifies tests that expose structures to cyclic loads; Table 2-1 shows the load application for testing according to the standards. The maximum force was determined after examination of both ASCE 7-95 and

Table 2-1. Number of cycles and fraction of maximum force applied according to SBCCI.

Load Cycle	Load Range			Cycles
1	0.2 F_{max}	to	0.5 F_{max}	3500
2	0.0 F_{max}	to	0.6 F_{max}	300
3	0.5 F_{max}	to	0.8 F_{max}	600
4	0.3 F_{max}	to	1.0 F_{max}	100
5	-0.3 F_{max}	to	-1.0 F_{max}	50
6	-0.5 F_{max}	to	-0.8 F_{max}	1050
7	0.0 F_{max}	to	-0.6 F_{max}	50
8	-0.2 F_{max}	to	-0.5 F_{max}	3350

AASHTO 1985. The design procedure in ASCE 7-95, "Minimum Design Loads for Buildings and Other Structures," was selected for computation of the wind force because it was the more current document. The total force was altered, however, according to the anticipated motion of traffic signals in high velocity wind events. Unlike fixed structures, cable supported signals rotate when exposed to wind. As a result, the profile of the signal exposed to the wind changes,

resulting in drag and lift coefficients that vary. Using "Wind Forces on Structures" published by the ASCE Wind Force Committee, the anticipated drag and lift coefficients were selected (ASCE 1961; Cook et al. 1996). The drag and lift were computed, and using vector addition of the perpendicular forces, the total anticipated force was determined through 90 degrees of rotation for the signals. Figure 2-1 shows the expected drag and lift coefficients for 3 head and 5 head traffic signals. ATLAS was used to model the rotation of the traffic signal at varying wind velocities with rigid hardware, and this angle was added to the angle of rotation experienced by a

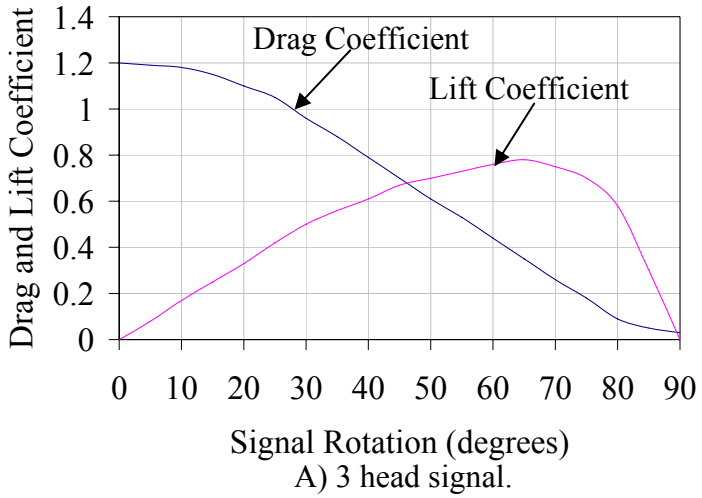

A) 3 head signal.

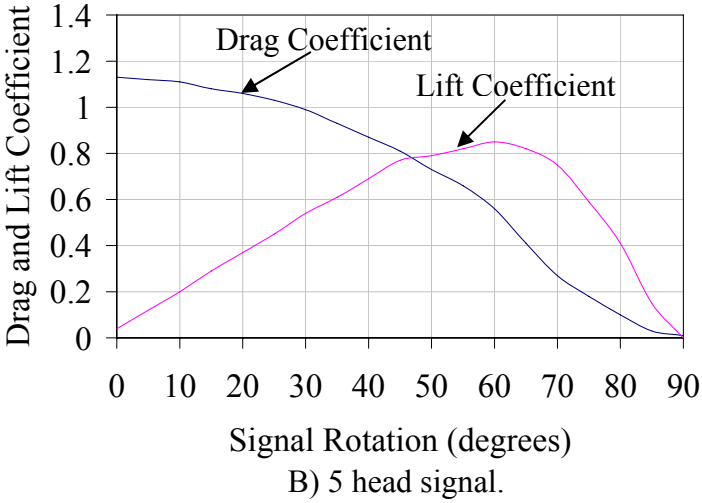

B) 5 head signal.

Figure 2-1. Drag and lift coefficients from ASCE Task Committee on Wind Forces.

signal in the test apparatus. The total angle expected for the change in wind velocity was then used to find the anticipated rotation at various wind speeds. Where the anticipated wind force from ASCE 7-95 matched the wind force measured from the actuator arm attached to the signal, the value was considered the applied force F_{max} and was used for testing. The test apparatus, as shown in Figure 2-2, applies the force to the centroid of the signal using an actuator arm. When the load cell reaches the appropriate force, the actuator retracts. The cycles may be altered, but the program allows for typical factors of F_{max} based on SBCCI standards. For the negative pressures, the signal is rotated 180 degrees for the actuator arm to apply the force in the negative direction. The testing summary reveals the number of cycles, F_{max}, and when failure occurred, when necessary. This method of testing could be used to qualify signal components while using widely accepted loading criteria for structural engineering.

Figure 2-2. Test apparatus created for testing of traffic signal components.

The New York Department of Transportation investigated the affects of winds on support poles for single cable systems (Alampalli 1998). NYDOT attached an anemometer atop one pole to record wind speed and direction, and load cells were placed on opposite ends of the cable to measure tension in the single cable assembly. The instrumentation was programmed to collect

data when wind speeds exceeded 10 miles per hour; testing took place over 6 months. Wind speeds rarely exceeded 40 miles per hour, and the loads placed on the poles were compared to results from AASHTO design methods. The results were within 10% of design loads at low wind velocities, but design values were much higher than measured at higher velocities (see Figure 2-3). Note that the measured field data for pole load (i.e., cable tension) shown in Figure 2-3 did not change appreciably between the no wind condition and 50 mph (85 km/hr). The author concluded that the dead and wind loads on the pole calculated from AASHTO design method are conservative. NYDOT surveyed other transportation agencies around the United States before conducting research, and of the 17 respondents, only Florida and West Virginia experienced failures of the span wire assemblies. West Virginia experienced failures of the wire clamps, while Florida experienced failures of the dual cable system from high winds during hurricanes.

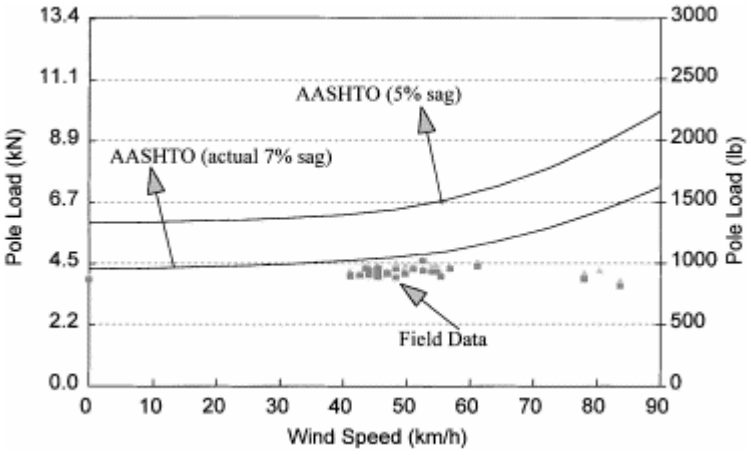

Figure 2-3. Comparison of field data with AASHTO design procedure (Alampalli 1998).

The current code provisions for determination of wind forces are provided by ASCE and AASHTO. ASCE 7-05, "Minimum Design Loads for Buildings and Other Structures," offers extensive information for the determination of wind forces on various structures (ASCE 2005).

Traffic signals would apply to section 6.5.15, which provides a computational method for determining wind forces on structures other than buildings. The determination of wind forces according to ASCE is given by the Bernoulli expression, and Equation 2-1 describes the expected wind force, where q_Z is the dynamic wind pressure at elevation z, G is the gust effect factor, C_f is the force coefficient, and A_f is the projected area of the object perpendicular to the wind unless the force coefficient is specified for the total surface area (ASCE 2005).

$$F = q_Z \, G \, C_f \, A_f \tag{2-1}$$

The dynamic wind pressure can be determined from the design wind speed, and the projected area of the signal is known. The gust factor would need to be determined from Section 6.5.8, which provides an analytical procedure for determining the factor for either rigid or flexible structures (ASCE 2005). Force coefficients are provided for solid freestanding walls and solid signs in Figure 6-20; other shapes and structures have coefficients provided in Figures 6-21 through 6-23 of the specifications (ASCE 2005).

AASHTO 2001 is the current specification that determines wind forces for transportation related structures. The calculation of wind forces is governed by Equation 2-2 where K_z is the height and exposure factor, G is the gust effect factor, V is the basic wind speed to be determined from the wind speed map, I_r is the importance factor, and C_d is the drag coefficient (AASHTO 2001).

$$P_z = 0.00256 \, K_z \, G \, V^2 \, I_r \, C_d \tag{2-2}$$

Recommended design values for traffic signals are found within the code, including the gust effect factor—which has a recommended value of 1.14—and the drag coefficient, which may be taken as 1.2 unless more detailed information is provided, as recommended by Marchman (Marchman, 1971; AASHTO 2001).

In Florida the use of cable supported traffic signals is widespread as it is a lower-cost alternative to cantilever mast arm structures. The dual cable system is the primary system in use around the state; however, these have been shown to perform poorly in high velocity winds. This report includes a comparison of the dual and single cable systems.

3.0 DEVELOPMENT OF WIND TESTING PROGRAM

Wind tests provide the unique opportunity to develop an understanding of the response of a traffic signal structure to extreme winds. The intent is to compare expectations provided by design codes with test data and verify the adequacy of design procedures. The response of traffic signals to high winds was measured, and comparisons between dual cable and single cable systems were made for a large scale assembly. Testing was conducted at the Eastside Campus of the University of Florida in July 2006 cooperatively between the Florida Department of Transportation, City of Gainesville, University of Florida, and Florida International University.

3.1 TEST SETUP

A full scale signal system was deemed necessary in providing an accurate assessment of response to wind loads.

The span between support poles was determined with the help of ATLAS, the computer software program developed at the University of Florida. Many traffic signals span intersections at least 100 feet, and a span of 72 feet was previously deemed adequate to verify the accuracy of ATLAS (Hoit et al. 1994). However space was limited at the test site, and a span of 50 feet was proposed. Studies were conducted using ATLAS to determine if the results of testing are comparable between the spans of 50 feet and 72 feet. ATLAS was run using a wind speed of 120 mph, which is the approximate highest wind speed that could be developed. Figure 3-1 shows the rotations and translations for a five-head signal suspended on spans of 50 feet and 72 feet, respectively, and on hangers of 15 inches and 40 inches. Computer outputs indicated that essentially the same signal rotations occur as with the 72 ft span, and because the differences in

displacement and rotation are minimal, the 50 foot span was considered acceptable for obtaining data. A schematic of the test setup is provided in Figure 3-2.

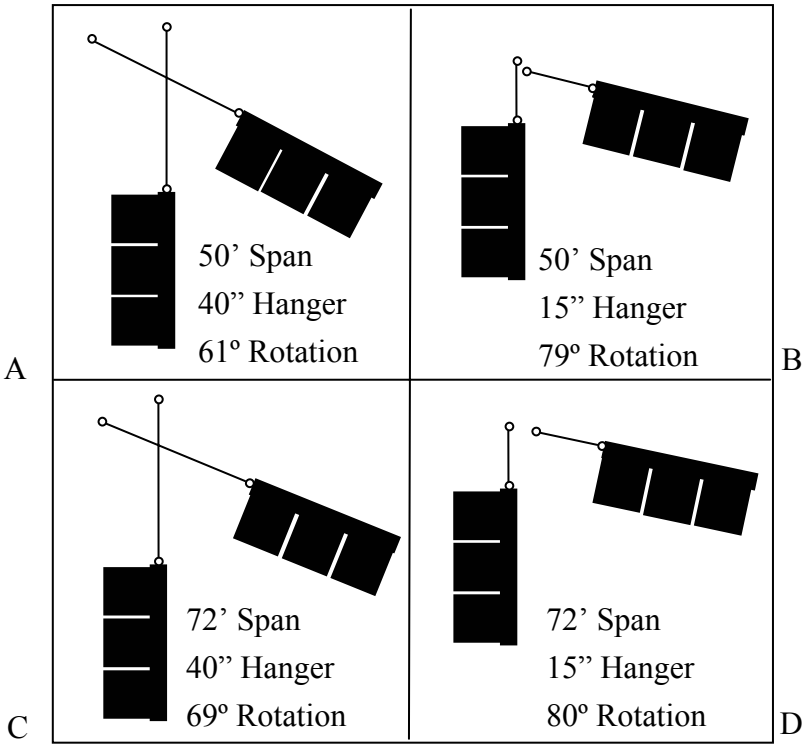

Figure 3-1. ATLAS results for rotations.

Two 18” x 18” Class 6 concrete poles were obtained from a traffic intersection undergoing improvements in Gainesville, Florida. As previously done in “Static and Dynamic Tests on Traffic Signal and Sign Dual Cable Support Systems,” holes were dug approximately 7 feet into the ground, the poles were set into place, and the holes were backfilled with soil (Hoit et al. 1994). No concrete was used as a foundation, and to verify that the poles moved negligibly, their displacement was measured at the connection of the catenary cable parallel to the wind direction.

Alampalli mentions the cable sag as having a large effect on the tension observed in each cable (Alampalli 1998). A sag of 5% is typical (AASHTO 2001). Systems with both 2% and 5% sags

were tested in order to understand the behavior of a common structural system, as well as a high-tension situation. In order to achieve both sags while maintaining the position of the signal during various tests, the poles had to be modified to handle various cable configurations, and the location of the additional eyebolts are illustrated in Figure 3-2.

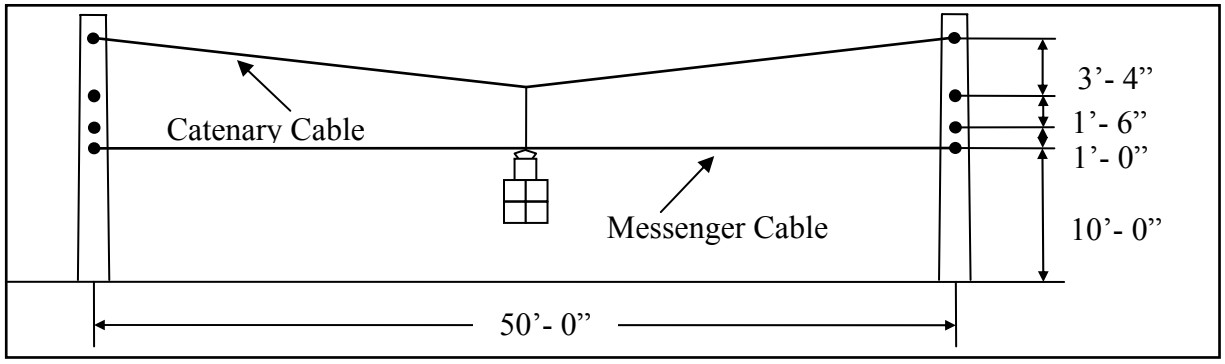

A) 40" aluminum hanger, 5% sag.

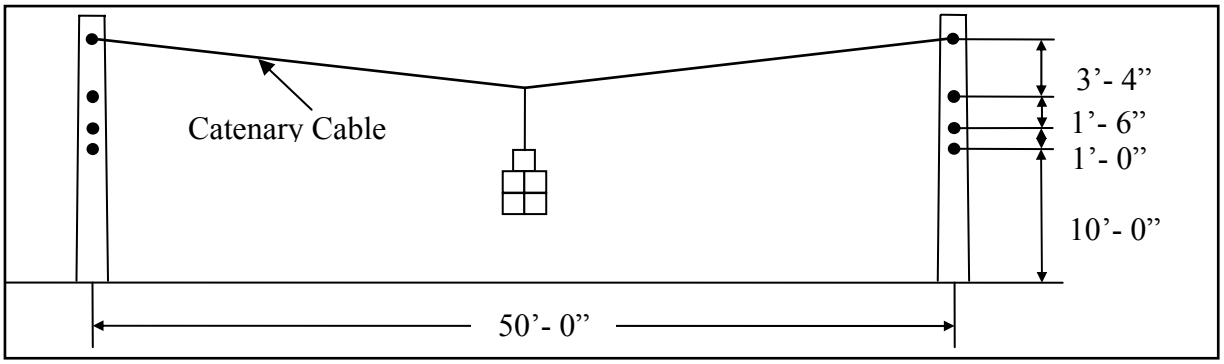

B) 40" pipe hanger, 5% sag.

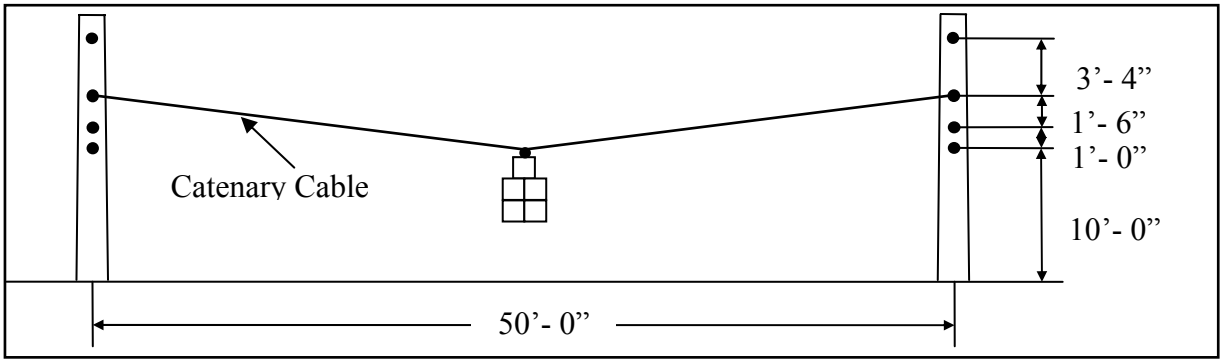

C) Direct connection, 5% sag.

Figure 3-2. Layout of test setup.

In Florida the catenary cable supports the gravity load of the traffic signal whereas the signal wiring is attached to the messenger cable that extends between poles below the catenary cable. Minimum span cable diameter in Florida is 3/8 inches, and ATLAS verified that this is an adequate diameter for an applied wind velocity of 120 mph. For the dual cable system, the catenary cable supports the weight of the signal at rest and the messenger cable supports the electrical wiring. For the single cable system, the catenary cable supports the wiring. Figure 3-2 shows both cables for the various tests performed. The catenary and messenger cables were provided by the City of Gainesville Traffic Operations. The 7-wire strand was manufactured by the Hubbell Power Group and has a minimum breaking strength of 7,400 pounds.

Five-head traffic signals have a larger surface area exposed to wind and, therefore, were used because they would experience a higher wind force than a three head signal. This would also provide results not previously studied in wind tests for comparison. Only one signal could be mounted in the wind field because of the limited width, and this signal was located in the middle of the span. The signal had to be no lower than 6 feet from the ground and within a 6 foot wide wind field to completely be enveloped in the constant wind stream with negligible drag effects from the ground. Figure 3-3 shows a diagram of the 62 pound five-head signals used in testing. The aluminum signals, as well as aluminum extender material, were provided by the Florida Department of Transportation and the City of Gainesville Traffic Operations Department. The wind was applied using the Wall of Wind Phase 1 provided by the International Hurricane Research Center of Florida International University, as shown in Figure 3-4. The Wall of Wind Phase 1 is a system with two fans, each featuring counter-rotating propellers capable of producing wind speeds up to approximately 120 miles per hour.

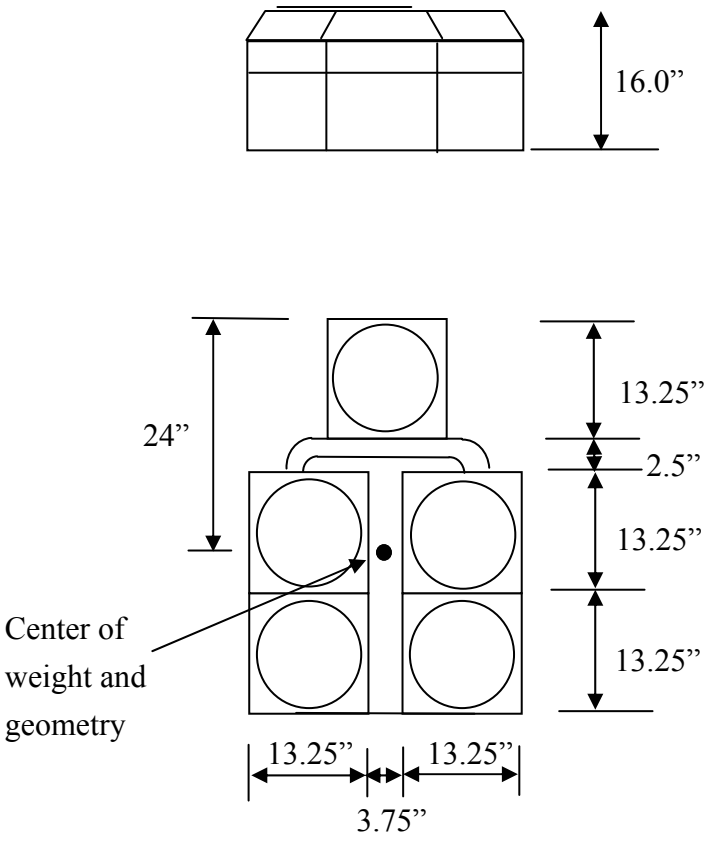

Figure 3-3. Details of 5-head traffic signal without support hardware.

Figure 3-4. Wall of Wind, Phase 1.

3.2 INSTRUMENTATION

Quantifying the behavior of the traffic signal to wind forces required instruments that monitored several variables. Attached at the center of gravity of the signal were 2 sensors produced by Microstrain. Both were model 3DM-GX1 gyro enhanced orientation sensors; one was used as an accelerometer while the other measured the orientation of the signal in three axes. The anemometer—produced by R. M. Young Company—monitored wind speed approximately 7 feet in front of the signal. The cable translations were measured by string potentiometers attached to a nearby aluminum structure. UniMeasure model HX-P1010-80 measured the large translations at the midpoint of the cables where the traffic signal was attached. An additional string pot, Ametek Rayelco Linear Motion Transducer model P-2A, was attached to the eyebolt at the uppermost cable to measure the movement of the pole in the direction of the wind. The tension of the cables was measured directly. Model LCCA-10K load cells—which are tension and compression "s-type" load cells—were manufactured by Omega and placed in line with the cables to measure tension. Data was acquired at a rate of 50 hertz.

3.3 TEST METHODS

For each test, the cable configuration was first set, and the traffic signal was then suspended at midspan. For testing, the instrumentation began to take readings before the application of wind load. The engines either gradually brought the wind speed from 20 miles per hour on initial startup to approximately 115 miles per hour over the course of 2.5 minutes, or they brought the wind speed up to an assigned value and oscillated around that for two minutes. When tests were complete, the engines receded to idle and were finally shut down for installation of a new cable setup.

Figure 3-5 shows a typical wind speed graph over time for the wind speed applied by both a ramp function and oscillating function. The ramp function is modeled by a linear function as shown in Figure 3-5 A. The oscillating velocity is shown in Figure 3-5 B.

Figure 3-6 shows typical measured data for signal rotation and cable tension relative to the wind speed along with best-fit linear trend lines. Appendices B-E provide figures showing measured data and accompanying best-fit linear trend lines.

Table 3-1 presents the tests that were conducted. Street name signs were mounted in lieu of traffic signals in tests 29-31. The ramp loading function is the easiest to analyze for it provides a direct relationship to the other parameters.

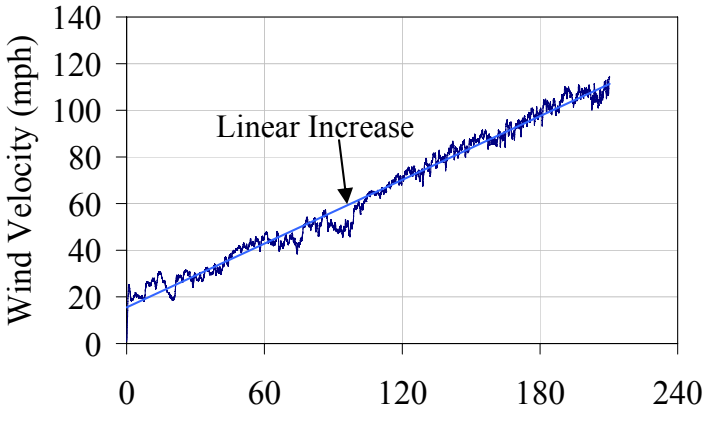

A) Linear increase in velocity.

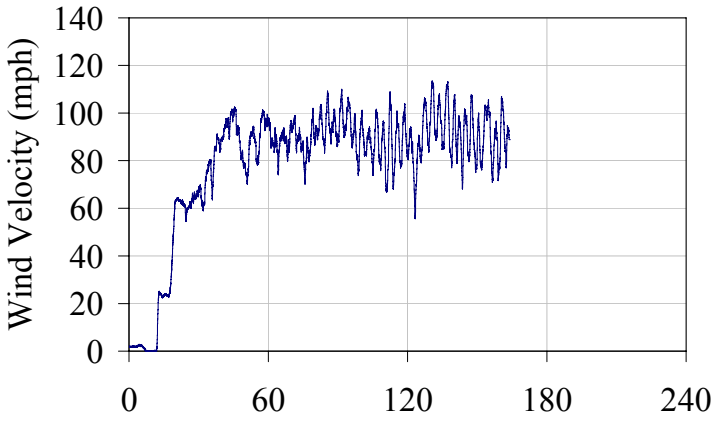

B) Oscillating velocity.

Figure 3-5. Wind loading function.

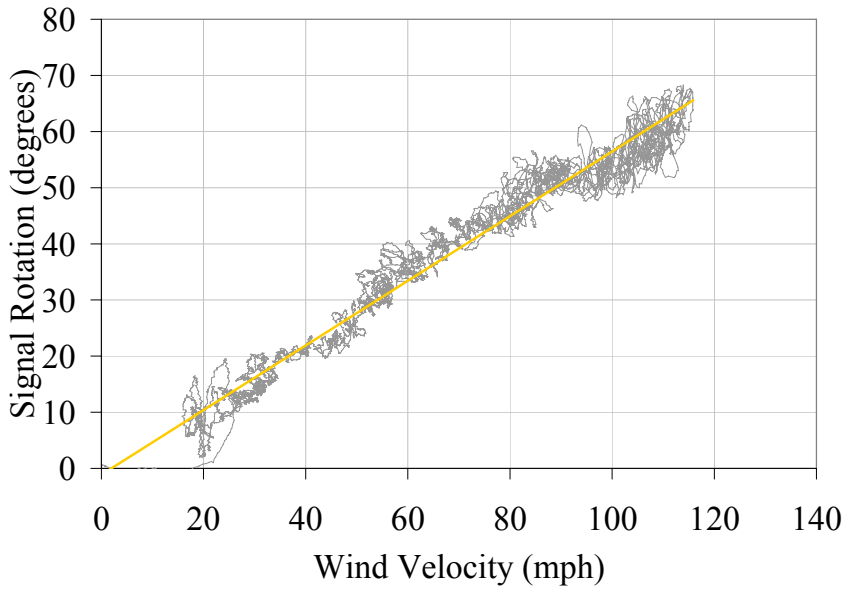

A) Signal rotation relative to wind speed (test 13).

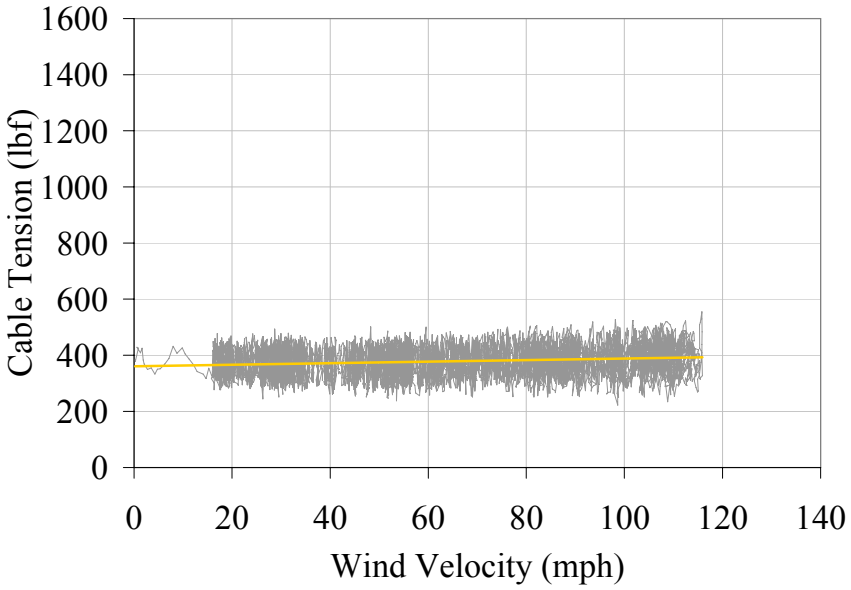

B) Cable tension relative to wind speed (test 13).

Figure 3-6. Typical results for signal rotation and cable tension relative to the wind speed.

Table 3-1. Tests performed.

Date	Test	Orientation	Number of Cables	Connection Hardware	Desired Catenary Sag	Weight	Notes
7/17/2006	1	Forward	2	40” Strap	5%	62 lbs	None
7/17/2006	2	Forward	1	40” Strap	5%	62 lbs	None
7/17/2006	3	Forward	1	40” Pipe	5%	62 lbs	Oscillating Load
7/17/2006	4	Diagonal	1	40” Pipe	5%	62 lbs	None
7/17/2006	5	Forward	1	40” Pipe	5%	62 lbs	Oscillating Load
7/17/2006	6	Forward	2	40” Strap	5%	62 lbs	Oscillating Load
7/18/2006	7	Backward	1	40” Strap	5%	62 lbs	None
7/18/2006	8	Forward	1	40” Pipe	5%	62 lbs	None
7/18/2006	9	Diagonal	1	40” Pipe	5%	62 lbs	None
7/18/2006	10	Backward	1	40” Pipe	5%	62 lbs	None
7/18/2006	11	Forward	1	40” Pipe	5%	82 lbs	None
7/18/2006	12	Forward	1	40” Pipe	5%	102 lbs	None
7/18/2006	13	Forward	1	Direct	5%	62 lbs	None
7/18/2006	14	Forward	1	Direct	5%	82 lbs	None
7/18/2006	15	Forward	1	Direct	5%	102 lbs	None
7/18/2006	16	Forward	1	Direct	5%	62 lbs	Oscillating Load
7/18/2006	17	Diagonal	1	Direct	5%	62 lbs	None
7/18/2006	18	Backward	1	Direct	5%	62 lbs	None
7/19/2006	19	Forward	1	Direct	2%	62 lbs	None
7/19/2006	20	Diagonal	1	Direct	2%	62 lbs	None
7/19/2006	21	Backward	1	Direct	2%	62 lbs	None
7/19/2006	22	Forward	1	Direct	2%	82 lbs	None
7/19/2006	23	Forward	1	Direct	2%	102 lbs	None
7/19/2006	24	Forward	2	15” Strap	7%	62 lbs	None
7/25/2006	25	Forward	2	40” Strap	5%	62 lbs	None
7/25/2006	26	Forward	1	40” Pipe	5%	62 lbs	None
7/25/2006	27	Forward	1	Direct	2%	62 lbs	None
7/25/2006	28	Forward	1	Direct	2%	67 lbs	Backplate
7/25/2006	29	Forward	1	Direct	2%	15 lbs	Street Sign
7/25/2006	30	Forward	1	Direct	2%	15 lbs	Street Sign
7/25/2006	31	Forward	1	Direct	2%	15 lbs	Street Sign

4.0 TEST RESULTS

Wind tests provide the unique opportunity to understand how signals behave in high winds. A total of 31 tests were conducted over the course of 4 days. The final day was open to the public and traffic signal operation and maintenance agencies throughout Florida were invited to observe the tests. The measurable data was compiled and data are presented to help understand the nature of traffic signal behavior under extreme wind conditions. The test number is presented for each data series. The figures provided in this chapter are based on a linear trend line fit to the actual test data. Individual figures for each test showing actual data with the accompanying linear trend line are presented in the Appendices B-E.

4.1 SIGNAL ROTATIONS

The rotation of the signal head is related to signal visibility. This study measured the rotation of the signal head to determine the relationship to wind speed and compare visibility between single cable and dual cable systems. The figures shown in this section all originate at the start-up wind speed of 20 mph (prior to start-up the signal rotation was zero). The linear trend lines presented in these graphs represent all data acquired between 20 mph and the maximum wind speed.

4.1.1 Single Cable System

Figure 4-1 shows the rotation experienced by forward facing signal heads with increasing wind speed for direct connect and 40” hanger and 5% and 2% cable sags. As shown in Figure 4-1, for the forward facing signals without any hanger, the sag of the cable did not play a significant role in the rotation of the signal. However, the signal supported by the pipe hanger did rotate less than the signals connected directly to the cable.

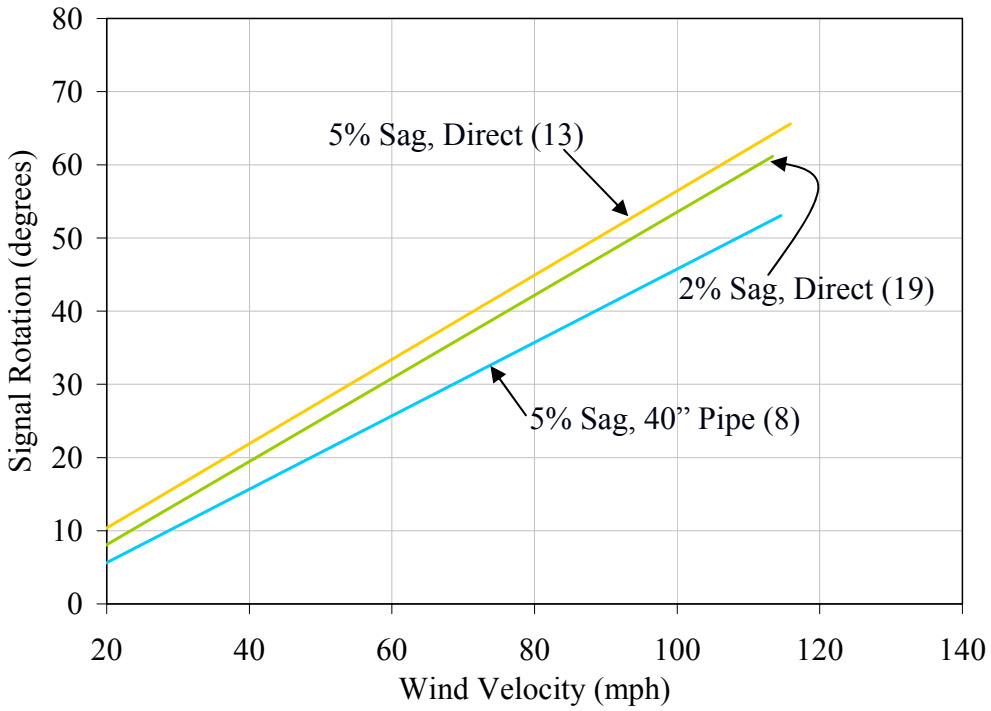

Figure 4-1. Rotation of forward facing signal supported by single cable system.

4.1.1.1 Effect of Signal Orientation on Rotation

The previous section presented the rotations for forward facing signals with a 40 inch pipe hanger on a cable with 5% sag, as well as a signal connected directly to cables with 5% and 2% sag. Because the wind may come at a signal from any direction, the previous tests were repeated with varying orientations of the signal. The additional testing angles are presented in Figure 4-2.

Figure 4-3 shows signal rotation for the forward facing signals presented in Section 4.1.1, as well as for the signals rotated at angles of 45 degrees and 180 degrees. In all cases, the diagonal signals rotated less than the forward facing signals. For the rear facing signal with 40 inch pipe hanger, the signal rotated very similarly to the forward facing case; in the case of the directly

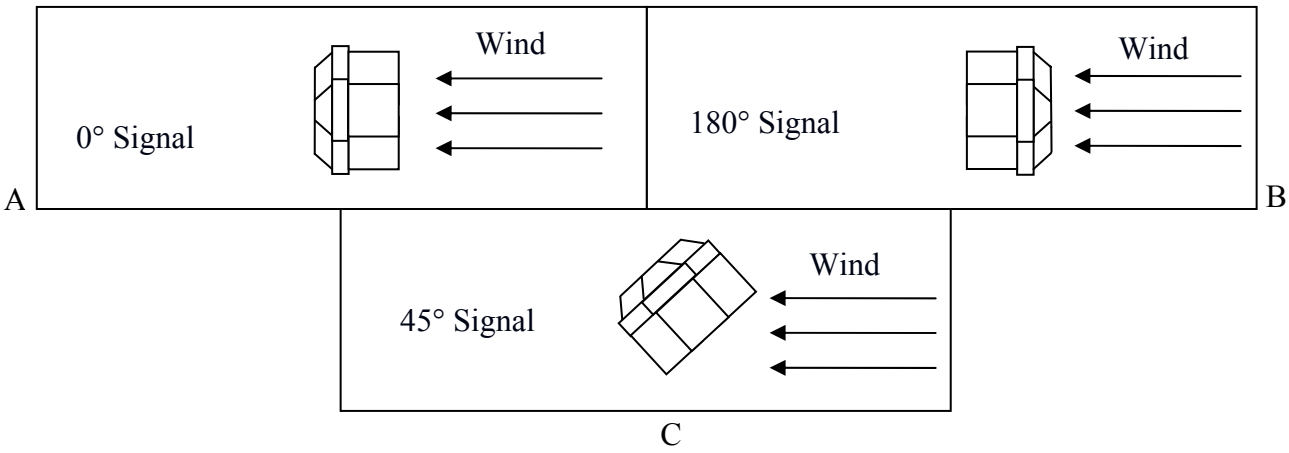

Figure 4-2. Top view of traffic signal with respect to oncoming wind. A) Forward facing signal. B) Backward signal. C) Diagonal signal.

connected systems, the rear facing signals experienced slightly smaller rotations. The diagonal signals measured rotation in line with the front face of the signal heads, which is parallel to the view experienced by drivers but at a 45 degree angle with respect to the oncoming wind. The directly connected signals experienced a different reaction to the wind when exposed from different angles; the signals supported by the pipe hanger experienced consistent results when the orientation was altered.

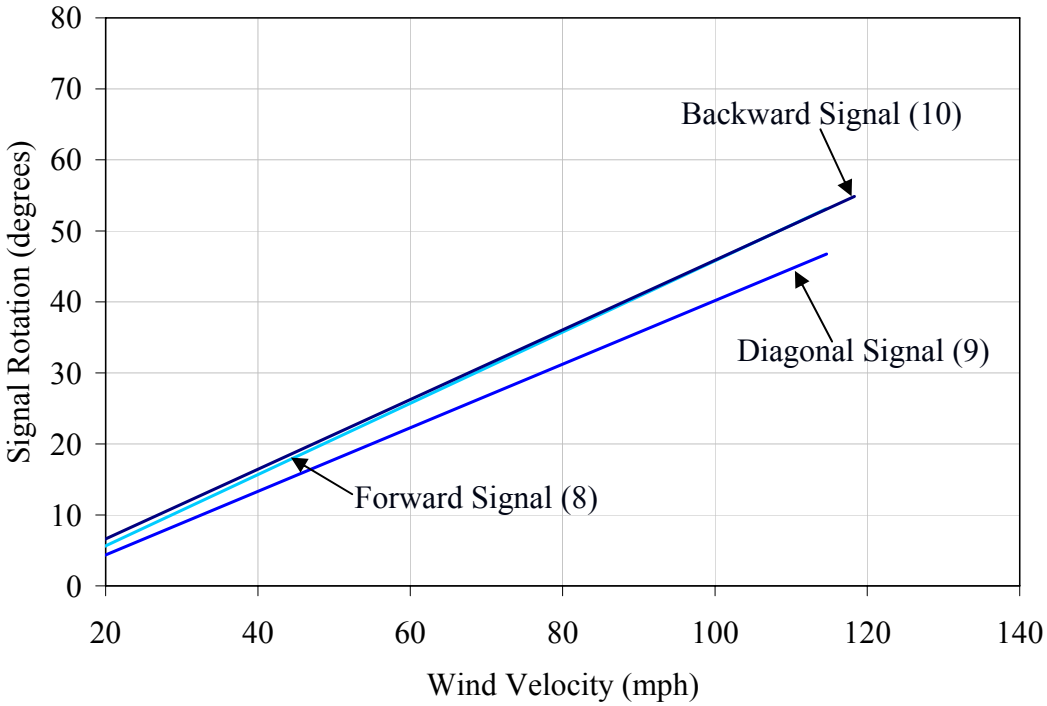

A) 40” pipe hanger with 5% sag.

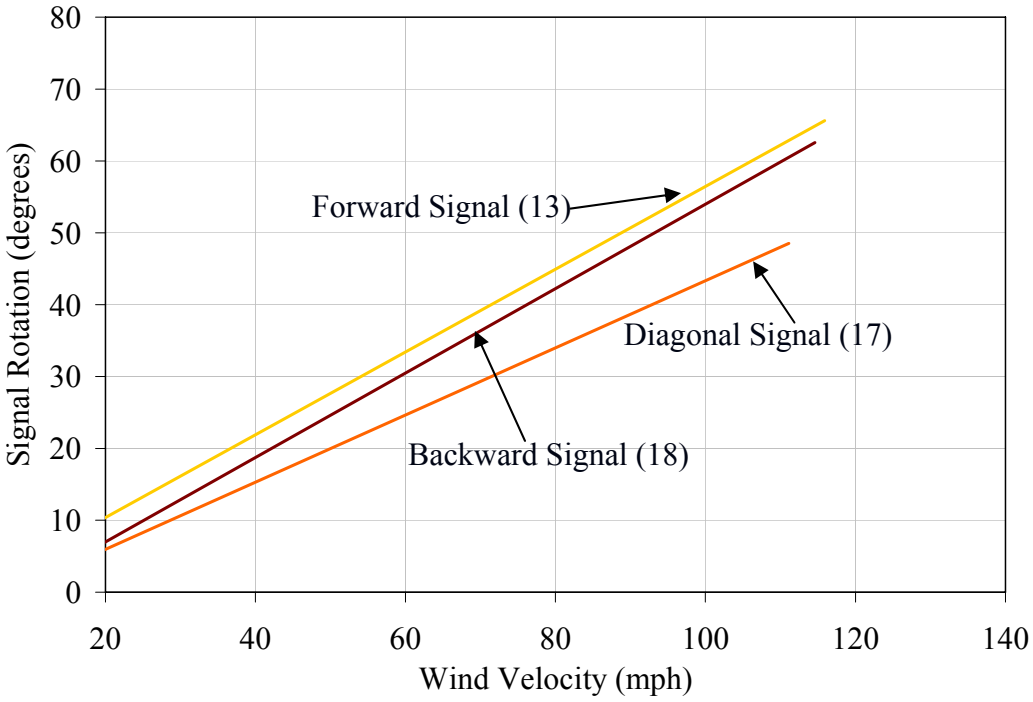

B) Direct connection with 5% sag.

Figure 4-3. Rotation of signal with different orientation supported by single cable system.

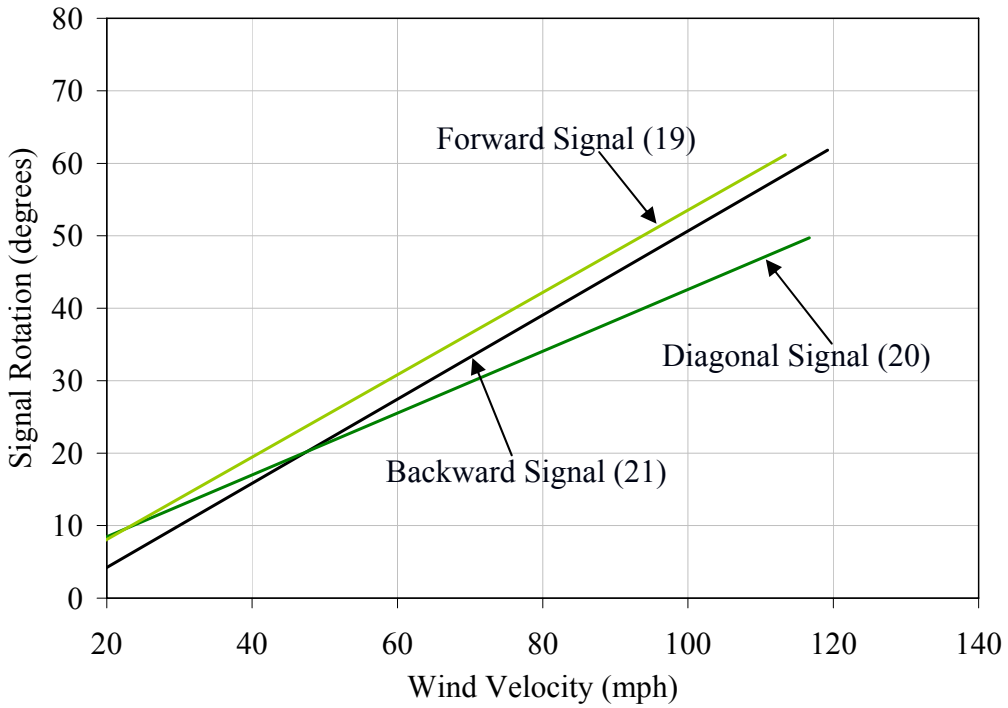

C) Direct Connection with 2% sag.

Figure 4-3. Rotation of signal with different orientation supported by single cable system, continued.

4.1.1.2 Effect of Additional Weight on Rotation

Because aluminum signal heads are heavier than their polycarbonate counterparts, the tests were conducted with the single point tests to observe the role of weight in rotation.

To test the reaction of heavier signals to wind speed, the forward facing tests were repeated adding weights of 20 pounds and 40 pounds to the bottom of the 62 pound aluminum signal head. For the test with the pipe hanger, the signal without weight performed similarly to the signal with an additional 20 pounds as shown in Figure 4-4 A. The signal with the additional 40 pounds, however, did experience less rotation. In Figure 4-4 B, which represents the signal with a catenary sag of 5% and no pipe hanger, additional weight lessened the rotation incrementally at high wind velocities. Figure 4-3 C shows that for the system with 2% sag, the additional weight

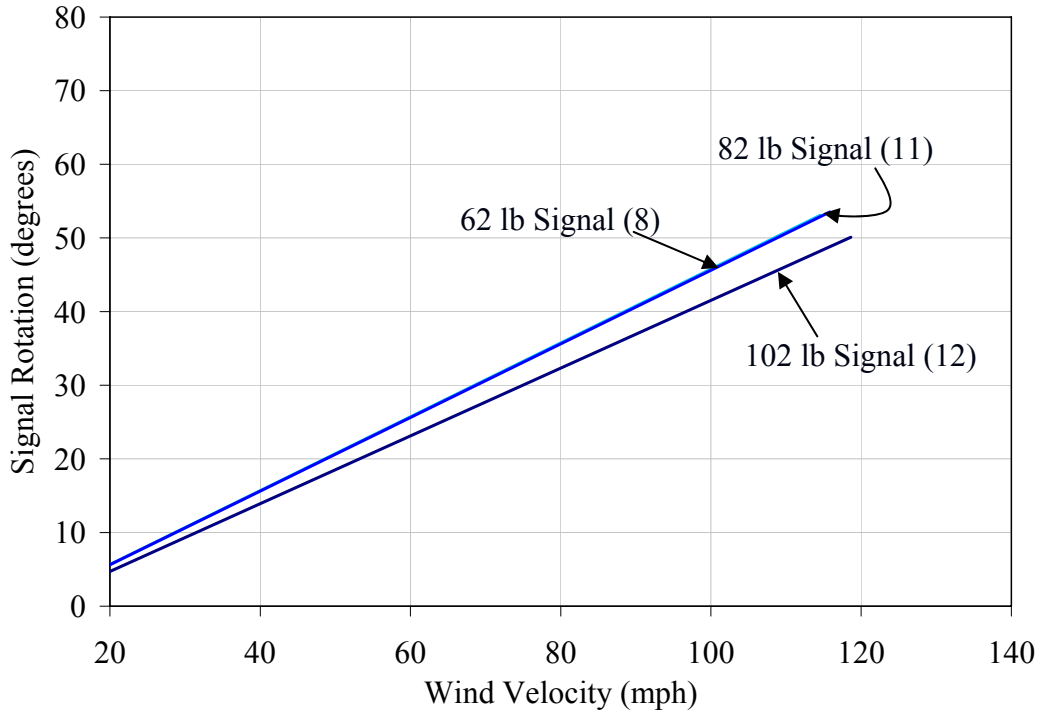

A) 40” pipe hanger with 5% sag.

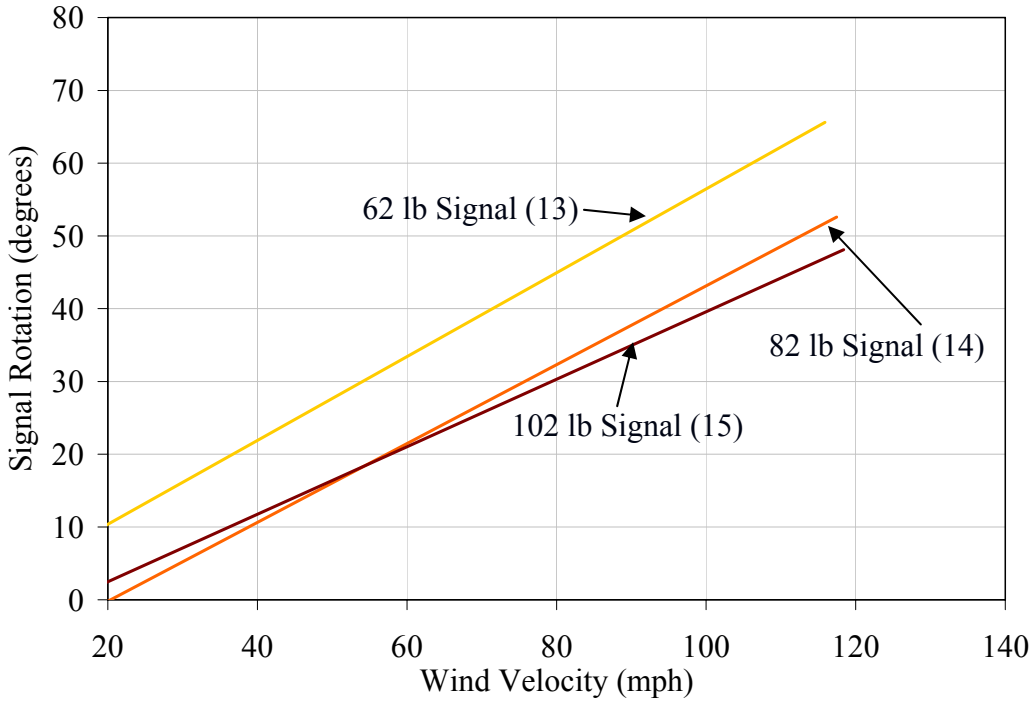

B) Direct connection with 5% Sag.

Figure 4-4. Rotation of signal with varying weight supported by single cable system.

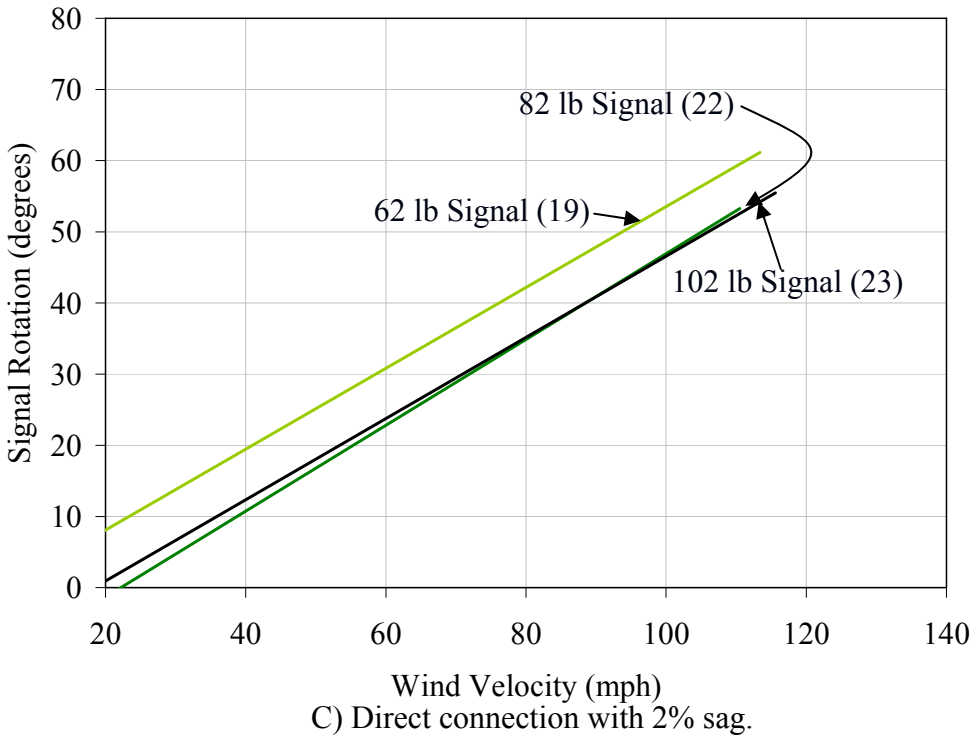

C) Direct connection with 2% sag.

Figure 4-4. Rotation of signal with varying weight supported by single cable system, continued.

influenced rotation similar to the directly connected signal with 5% sag. The system with pipe hanger and 5% catenary sag was the only configuration to lack variation in rotations that appear to be directly associated with the increased weight; the other two cases had lower rotations as a result of the addition of weight.

4.1.2 Dual Cable System

The dual cable system widely used in Florida was tested for comparison to the single cable system. In the tests that featured both a messenger and catenary cable, an aluminum hanger was used to provide 40 inches or 15 inches of separation between the cables, producing a catenary sag of 5% or 7%, respectively.

Figure 4-5 shows the rotation experienced by the signal with a 15 inch hanger and a 40 inch

hanger. The signal with the longer hanger rotated slightly more, but both are within 5 degrees of one another at all velocities, with lower variation at high wind speeds.

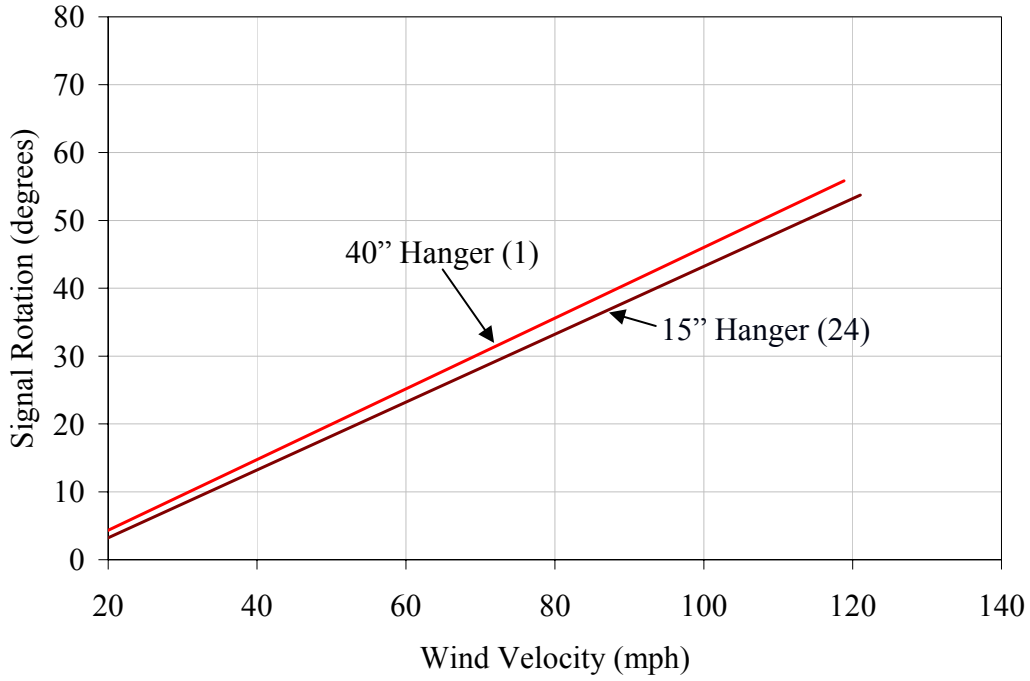

Figure 4-5. Rotation of forward facing signal supported by dual cable system.

4.1.3 Repeated Tests

Several tests were performed twice. The single cable system was redone with a catenary sag of 5% and pipe hanger, as well as with a 2% catenary sag and no hanger. Figure 4-6 A represents the test with the pipe hanger while Figure 4-6 B represents the test without the hanger. Figure 4-6 C shows the rotation experienced by the dual cable system.

Only slight variations occurred between the first and second test in all cases. The variation was within 5 degrees between tests, showing that similar tests performed consistently by yielding similar results, regardless of signal support system.

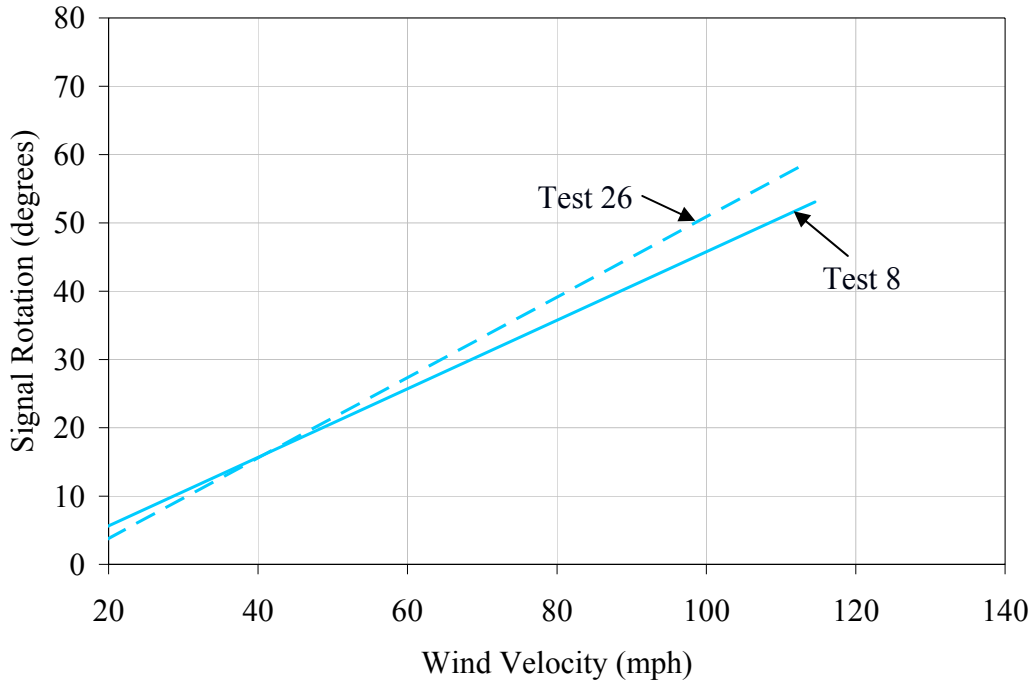

A) Single cable system with 5% sag and 40” pipe hanger.

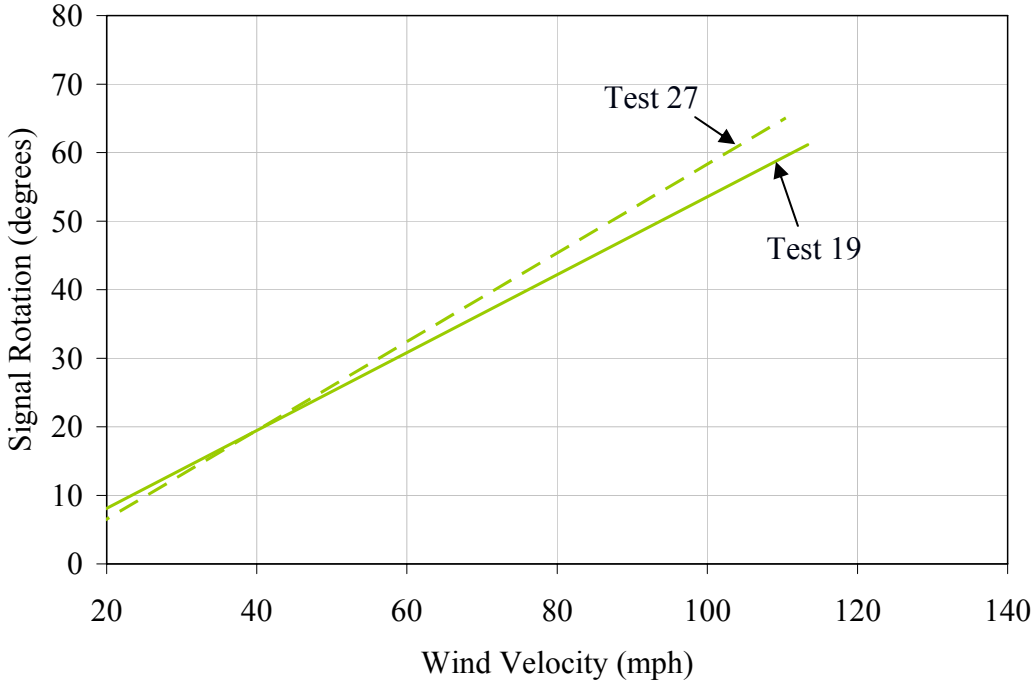

B) Single cable system with 2% sag and direct connection.

Figure 4-6. Rotation of forward facing signal—repeated tests.

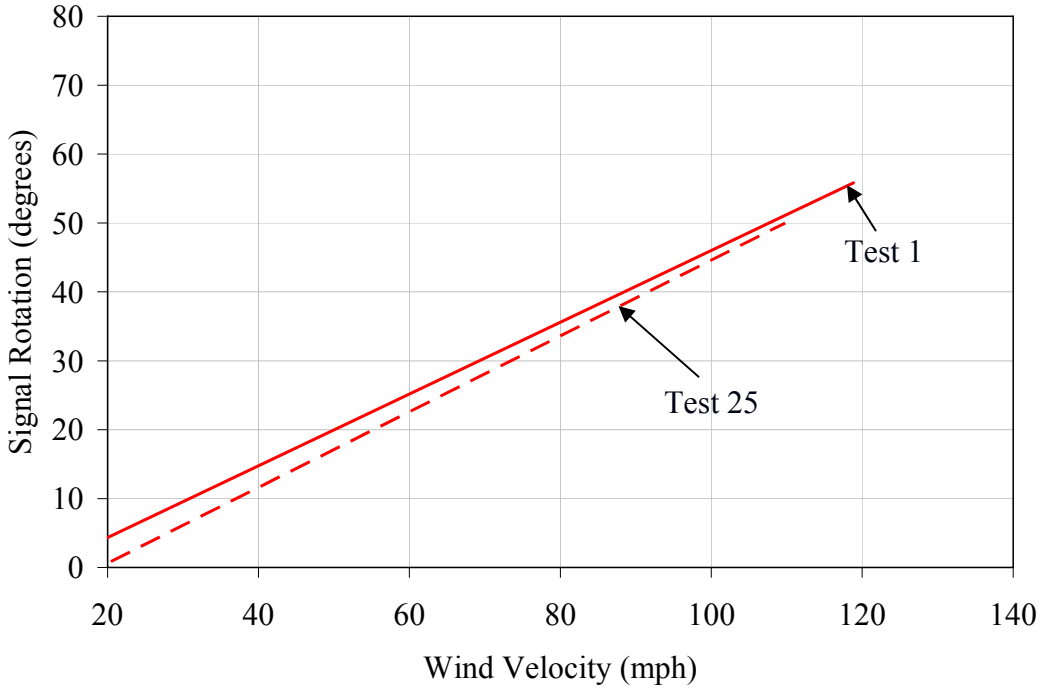

C) Dual cable system with 5% sag and 40" aluminum hanger.

Figure 4-6. Rotation of forward facing signal—repeated tests, continued.

4.1.4 Discussion of Signal Rotation

In all cases, a linear correlation existed between the wind speed and signal rotation. This direct proportionality allows for direct comparison between the single cable and dual cable systems.

The data suggest that although there is a difference between the rotations at the highest wind speed, all values fall between 45 and 70 degrees. The dual cable system, as well as the single cable system with pipe hanger performed comparably, rotating approximately 45 to 60 degrees with little variation between orientation and weight for the single cable system. The signals without hangers varied more with changes in orientation and weight.

The maximum rotation may not be a critical factor as long as the system does not break. No

hardware fractured during testing; however, the aluminum hanger used in the dual cable system did yield. The rotation of the signal head at maximum winds does not play any significant hazard during normal operation because drivers will not be present during extreme events. Signal rotation does play a role in normal operating conditions.

As presented by Hoit, the signal was deemed to be no longer visible when more than half of the bulb cannot be seen by oncoming motorists, occurring at a rotation of 30 degrees (Hoit et al. 1994). Table 4-1 indicates the wind speed from testing when this visibility criterion is no longer met. The maximum wind speed was 79 miles per hour for the 102 pound signal supported by a single cable system with 5% sag and direct connection. A wind speed of 54 miles per hour was the smallest for the forward facing single cable system with direct connection and 5% cable sag. The average wind velocity for 50% visibility was 72 miles per hour for the three dual cable system tests and 68 miles per hour for the nineteen single cable system tests shown in Table 4-1. The single cable systems have a wider variation of wind speed to cause the signal to lose visibility, but the dual cable system does not perform particularly better overall. It should also be noted that the for the dual-cable system, rotational restraint comes from the cables themselves (see Figure 3-1). This resistance is affected by both the distance between the cables and the length of the span. Since the span length was relatively short for these tests, the results should be considered an upper bound for the wind velocity that will result in 50% signal visibility for the dual cable system.

Table 4-1. Wind velocity at limiting angle.

Test	Hanger Length (in)	Sag (%)	Number of Cables	Note	Wind Velocity at 50% Signal Visibility (mph)
1	40” Strap	5	2	None	69
25	40” Strap	5	2	None	73
8	40” Pipe	5	1	None	69
26	40” Pipe	5	1	None	65
19	Direct	2	1	None	59
27	Direct	2	1	None	56
7	40” Strap	5	1	Backward	75
2	40” Strap	5	1	None	56
24	15” Strap	7	2	None	74
9	40” Pipe	5	1	Diagonal	77
10	40” Pipe	5	1	Backward	71
11	40” Pipe	5	1	82 lb Signal	69
12	40” Pipe	5	1	102 lb Signal	74
13	Direct	5	1	None	54
17	Direct	5	1	Diagonal	71
18	Direct	5	1	Backward	59
14	Direct	5	1	82 lb Signal	76
15	Direct	5	1	102 lb Signal	79
20	Direct	2	1	Diagonal	70
21	Direct	2	1	Backward	64
22	Direct	2	1	82 lb Signal	72
23	Direct	2	1	102 lb Signal	71

4.2 CABLE TENSION

Alampalli found that the catenary sag of the catenary cable was the primary factor in determining cable tension (Alampalli 1998). The results indicate that for the single point system, this is accurate; however, the dual cable system reacts differently when wind loads are applied. The figures shown in this section all originate at the initial cable tension with linear trend lines representing all data acquired.

4.2.1 Single Cable System

The forward facing signal with single point attachment is presented in Figure 4-7. As expected

the cable with the smaller sag experienced a larger initial tension. All cases, regardless of initial sag, experienced a small linear increase in tension as the wind increased. In addition to the direct proportionality to wind speed, all also prove to be nearly parallel; this indicates that the systems behave similarly regardless of the initial tension. Both tests featuring a cable sag of 5% experienced similar forces throughout testing.

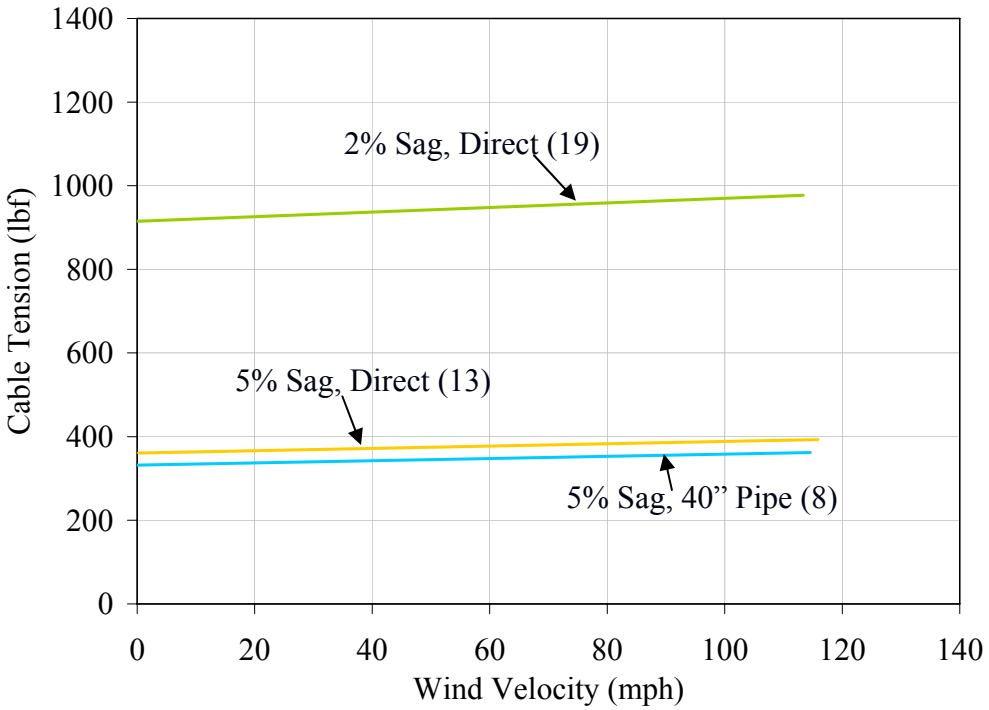

Figure 4-7. Cable tension for forward facing signal supported by single cable system.

4.2.1.1 Effect of Signal Orientation on Cable Tension

Figure 4-8 shows the cable reactions while the signal experienced high wind speeds from various angles of attack. In all cases the orientation has a minimal effect on the measured tension. The 2% forward signal did experience a slightly different increase of tension with respect to the other two cases as indicated by the slope of the tension increase. Otherwise, the change in signal profile did not alter the tension perceived by the cable.

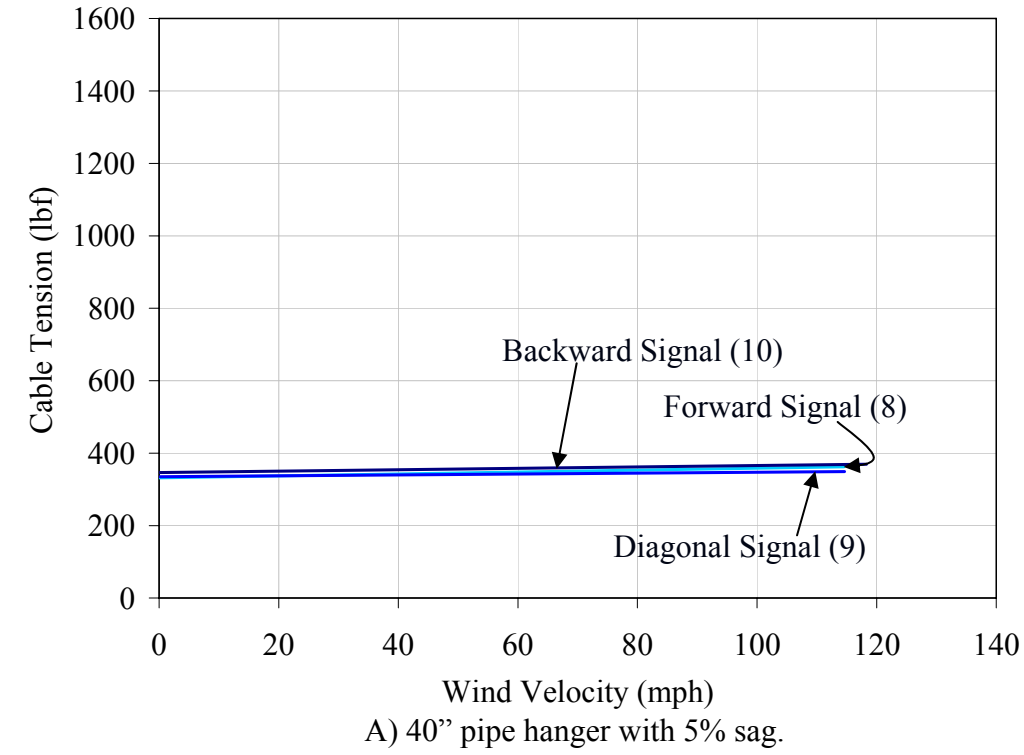

A) 40” pipe hanger with 5% sag.

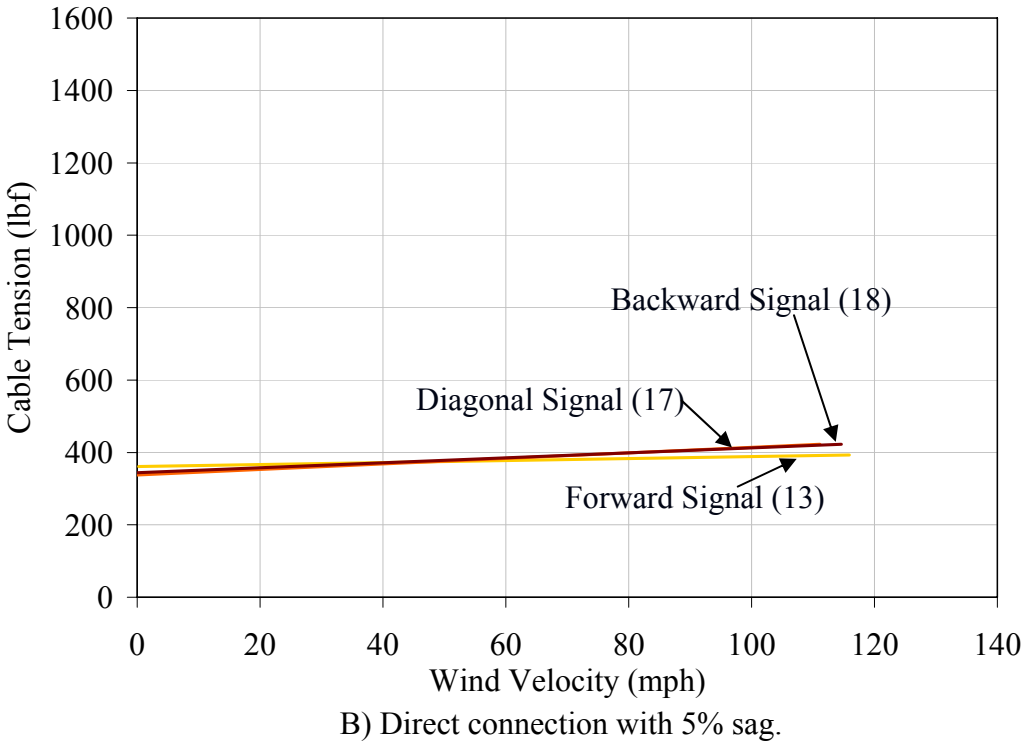

B) Direct connection with 5% sag.

Figure 4-8. Cable tension for signal with different orientation supported by single cable system.

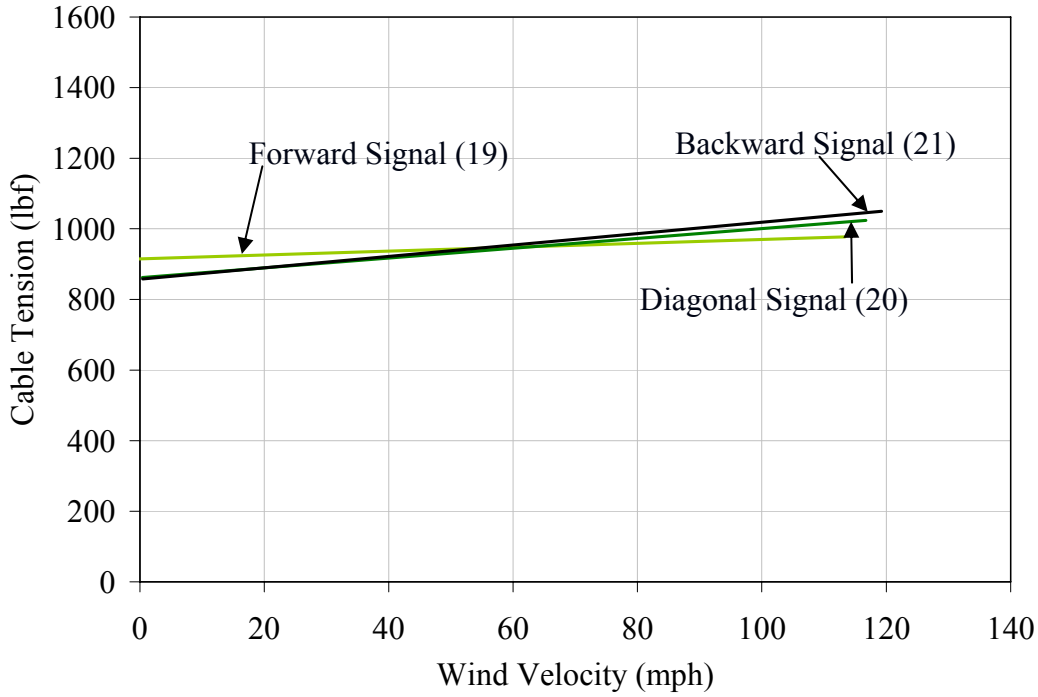

C) Direct connection with 2% sag.

Figure 4-8. Cable tension for signal with different orientation supported by single cable system, continued.

4.2.1.2 Effect of Additional Weight on Cable Tension

Unlike the signal orientation, the added weight was expected to increase the cable tension.

Figure 4-9 shows that like the other tests, the increase in cable tension was directly proportional to the wind speed. Additionally, the initial tension in the cable did not increase appreciably with an increase in wind speed. The only difference between tests was the affect of additional weights on the initial cable tension. The linear plots for tension were nearly the same in all tests; however, for the directly connected signal, there was a slightly different slope for the signal without weights. The tests with additional weight indicate that the weight of the signal has little effect on the increase in cable tension with increased winds; instead, the initial tension in the cable is the only variable affected by the increased signal weight.

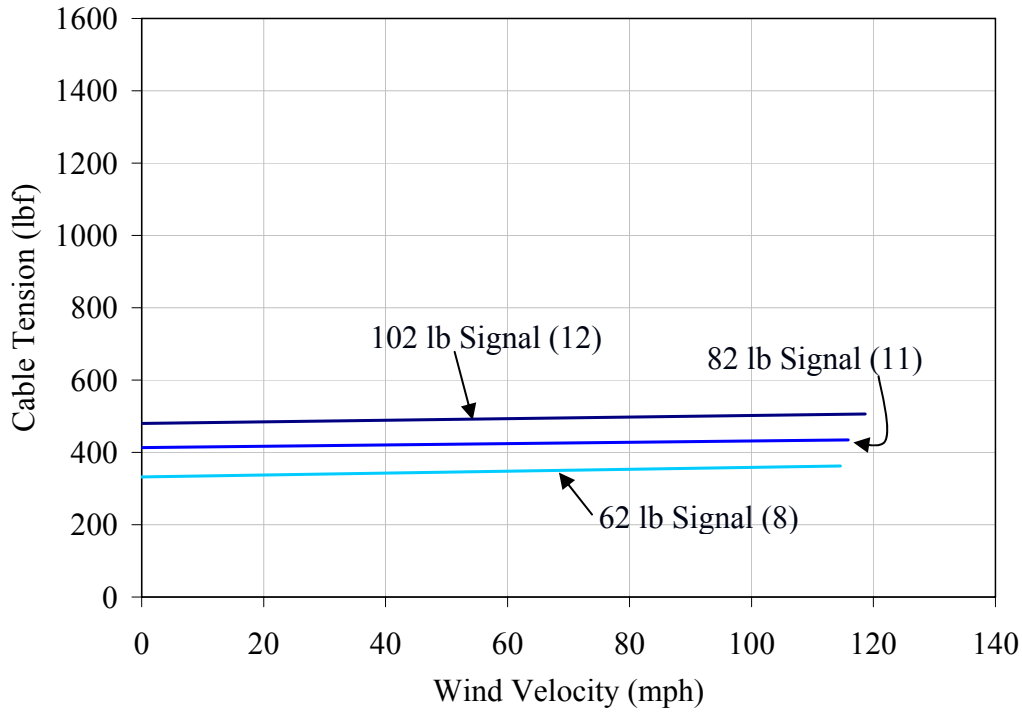

A) 40” pipe hanger with 5% sag.

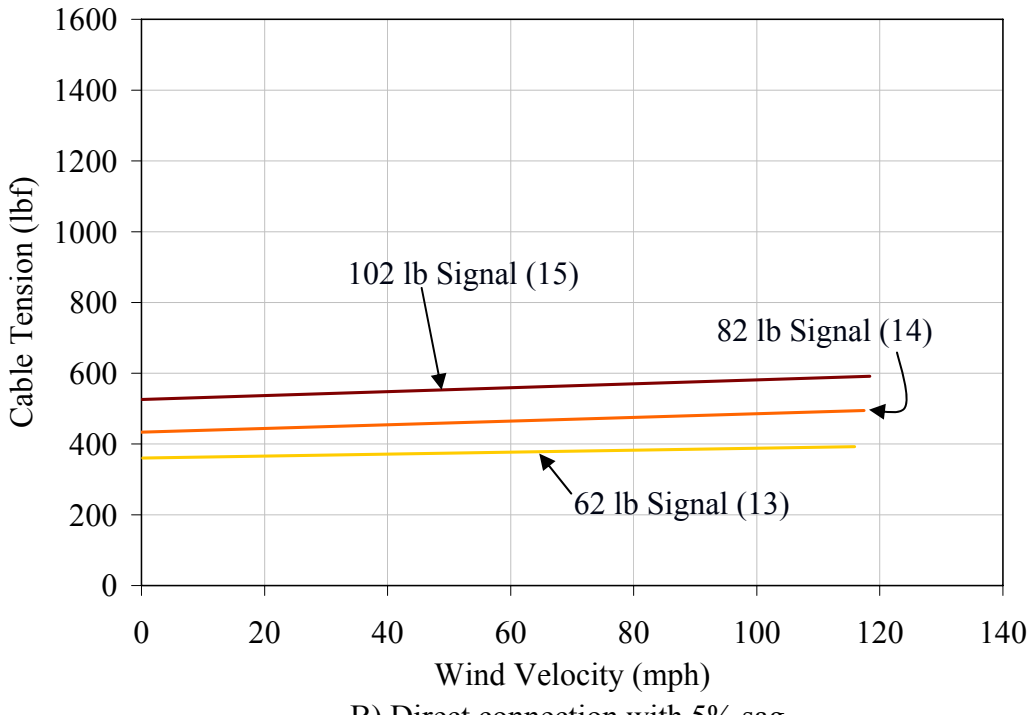

B) Direct connection with 5% sag.

Figure 4-9. Cable tension for signal with varying weight supported by single cable system.

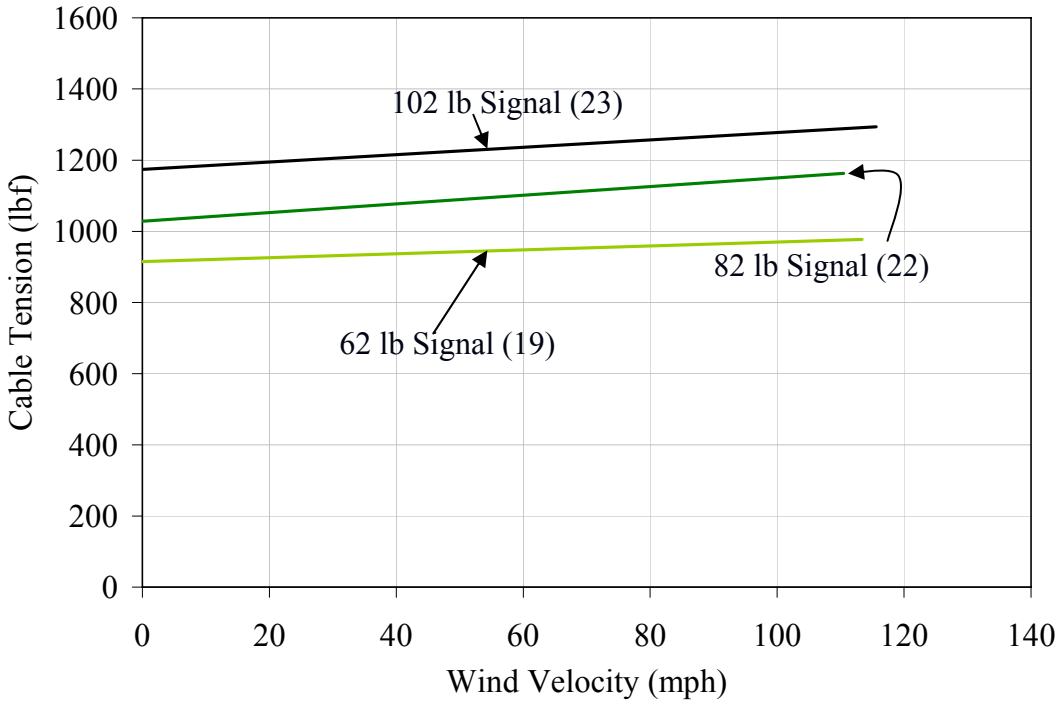

C) Direct connection with 2% sag.

Figure 4-9. Cable tension for signal with varying weight supported by single cable system, continued.

4.2.2 Dual Cable System

The difference in behavior between catenary and messenger cables was significant As the wind speed increased for both tests, the catenary cable reacts similar to the single cable system; however, the messenger cable resists the rotation of the hanger and experiences a large increase in tension associated with the increased resistance from high wind speeds.

While the catenary cables experience changes in tension of less than 100 pounds, the messenger cable tension increases by several hundred pounds. The messenger cable is initially tightened during installation, and regardless of the initial force observed at the beginning of the test, the force increases similarly as indicated in Figure 4-10. The length of hanger is indicated as 15

inches (for 7% sag) or 40 inches (for 5% sag). For both single and dual cable systems, the increase in tension in the catenary cable is similar, no matter the initial tension of the catenary cable.

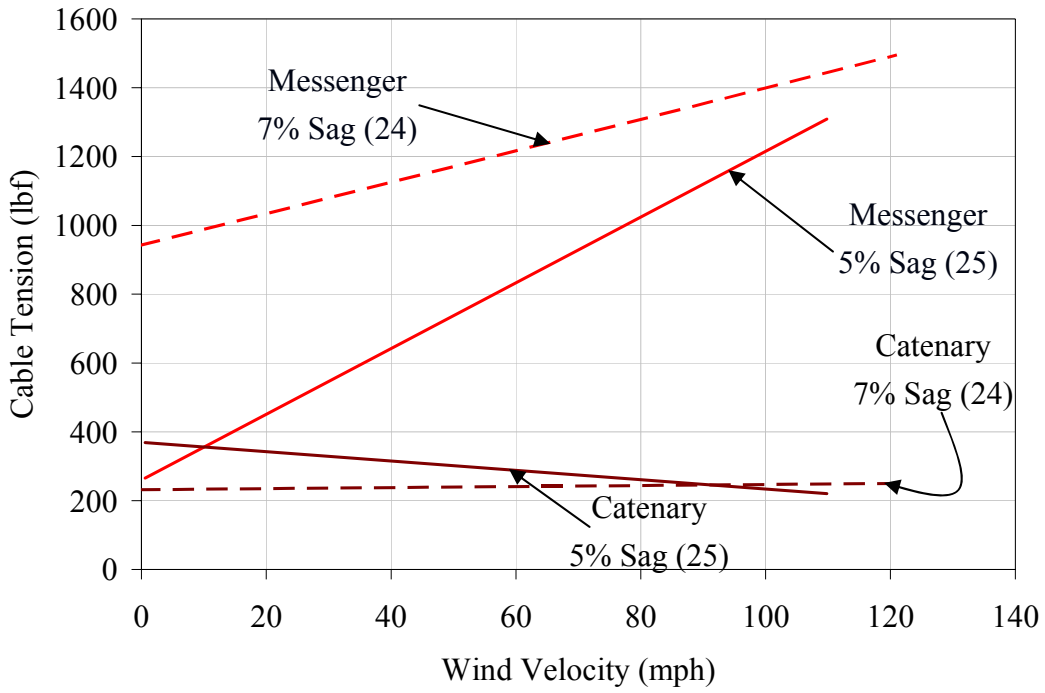

Figure 4-10. Cable tension for signal supported by dual cable system.

4.2.3 Repeated Tests

Figure 4-11 shows the results from each series of repeated tests. The tests were conducted approximately one week apart, and the cables were removed after the first round of tests. Figure 4-11 A shows that for test 25, both the messenger and catenary cables started at nearly the same initial tension. Test 1 had similarly close readings for the available data after the Wall of Wind was started. The catenary cables differed negligibly in behavior and the messenger cables experienced a similarly large increase in tension.

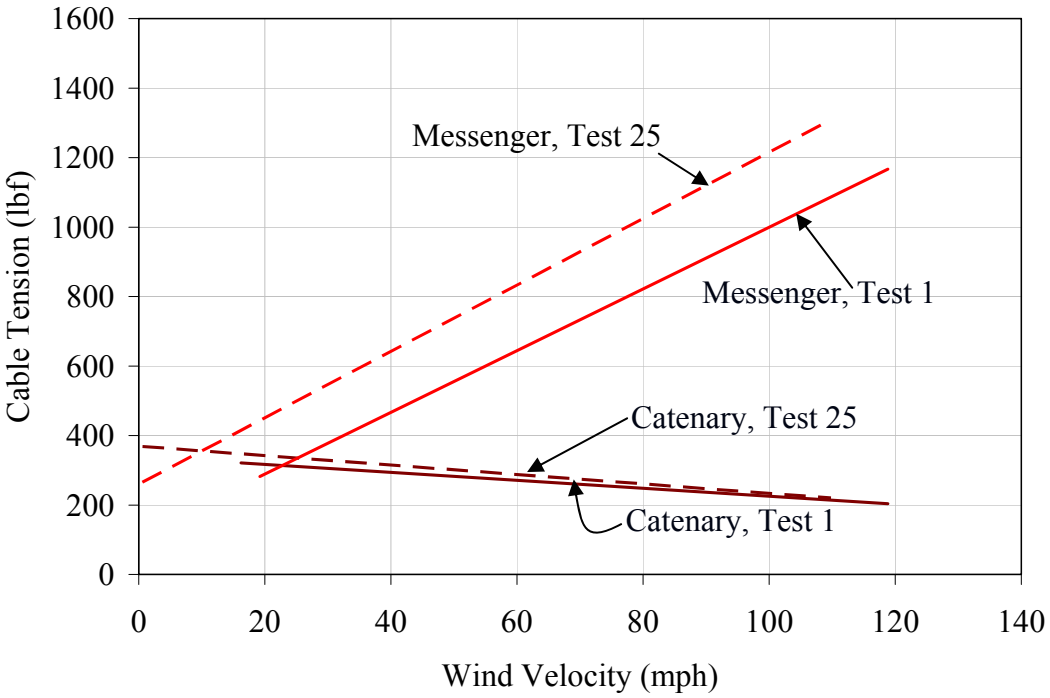

A) Dual cable system with 5% sag and 40”aluminum hanger.

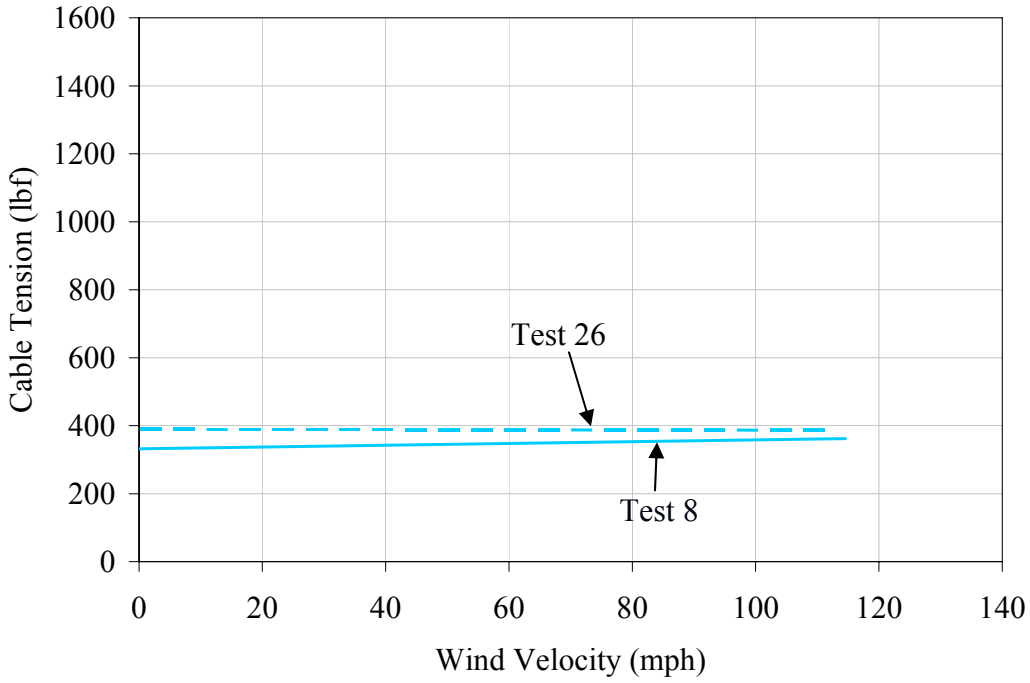

B) Single cable system with 5% sag and 40” pipe hanger.

Figure 4-11. Cable tension for forward facing signal—repeated tests.

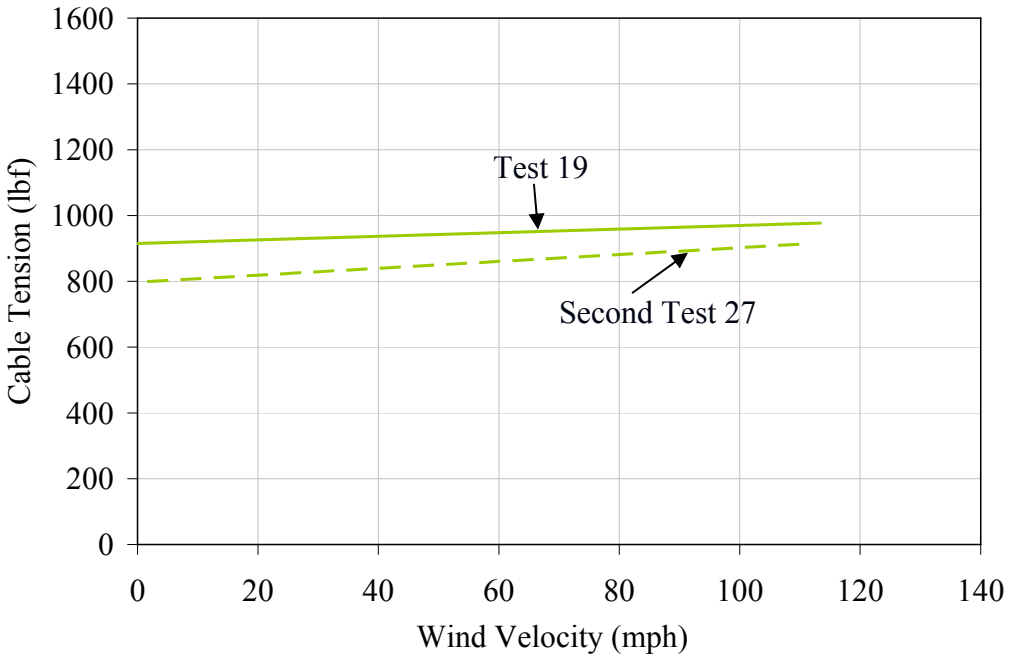

C) Single cable system with 2% sag and direct connection.

Figure 4-11. Cable tension for forward facing signal—repeated tests, continued.

The single cable test featuring the pipe hanger experienced an increased tension in the cable during the second test initially, but at the highest wind speeds the data indicate a similar cable tension. The increases in tension are shown to remain nearly parallel. Unlike the signal suspended by the pipe hanger, the one directly connected to the signal experienced a higher tension on the first test, and the second test had a lower tension.

4.2.4 Discussion of Cable Tension

Table 4-2 and Table 4-3 provide a summary of cable tension. As noted in Table 4-2, the cable tension in the single cable tests only increased between 4% and 21% above that observed under dead load. As shown in Table 4-3, the catenary cable in the dual cable systems experienced a moderate change in tension with respect to the initial readings while the messenger cable experienced a dramatic increase. It should be noted that the measured initial tension in the

cables was slightly less than the theoretical tension at the nominal sags of 5% and 2%. For example, at exactly 5% sag with a 62 lb signal, 14 lb cable, and 50 ft span, the theoretical cable tension is 382 lbs. As noted in Table 4-2, the initial tension values were slightly less indicating that the actual sag was somewhat greater than the nominal. This is evident in Tests 7-10 where the initial tension was 10% to 13% less and Tests 13-19 where the initial tension was 4% to 7% less indicating that the actual sag in Tests 13-19 were closer to the nominal cable sag. .

Table 4-2. Cable tension increase for single cable support systems at 115 miles per hour.

Test	Hanger	Nominal Sag (%)	Signal Orientation	Signal Weight (lbf)	Initial Tension (lbf)	Final Tension (lbf)	Force Increase (lbf)	%Force Increase
7	40” Strap	5	Backward	62	343	373	30	9%
8	40” Pipe	5	Forward	62	332	362	30	9%
9	40” Pipe	5	Diagonal	62	335	349	14	4%
10	40” Pipe	5	Backward	62	345	369	24	7%
11	40” Pipe	5	Forward	82	413	434	21	5%
12	40” Pipe	5	Forward	102	480	506	26	5%
13	Direct	5	Forward	62	365	391	26	7%
14	Direct	5	Forward	82	446	489	43	10%
15	Direct	5	Forward	102	532	588	56	11%
17	Direct	5	Diagonal	62	350	422	72	21%
18	Direct	5	Backward	62	356	420	64	18%
19	Direct	2	Forward	62	915	981	66	7%
20	Direct	2	Diagonal	62	883	1015	132	15%
21	Direct	2	Backward	62	888	1034	146	16%
22	Direct	2	Forward	82	1045	1164	119	11%
23	Direct	2	Forward	102	1197	1282	85	7%

Table 4-3. Cable tension increase for dual cable support systems at 115 miles per hour.

Test	Signal Orientation	Cable	Initial Tension (lbf)	Final Tension (lbf)	Change in Tension (lbf)	%Force Increase
1	Forward	Catenary	330	208	-122	-37%
1	Forward	Messenger	333	1132	799	240%
24	Forward	Catenary	243	250	7	2%
24	Forward	Messenger	943	1467	524	56%
25	Forward	Catenary	369	213	-156	-42%
25	Forward	Messenger	260	1358	1098	422%

The loads carried by the cables are transmitted to the foundation from the poles which are responsible for resisting the tensile forces. The poles develop an internal moment to resist the tension of the cables. Figure 4-12 shows the moments at the base of the poles for the single cable Test 8 and the dual cable system featured in Test 25. Both cases were analyzed with an assumed clearance of 17.5 feet for the traffic signal. As expected, because the tension in the messenger increases significantly, the poles in the dual cable system undergo a large increase in moment, while the single cable system shows the pole moment increase to be negligible.

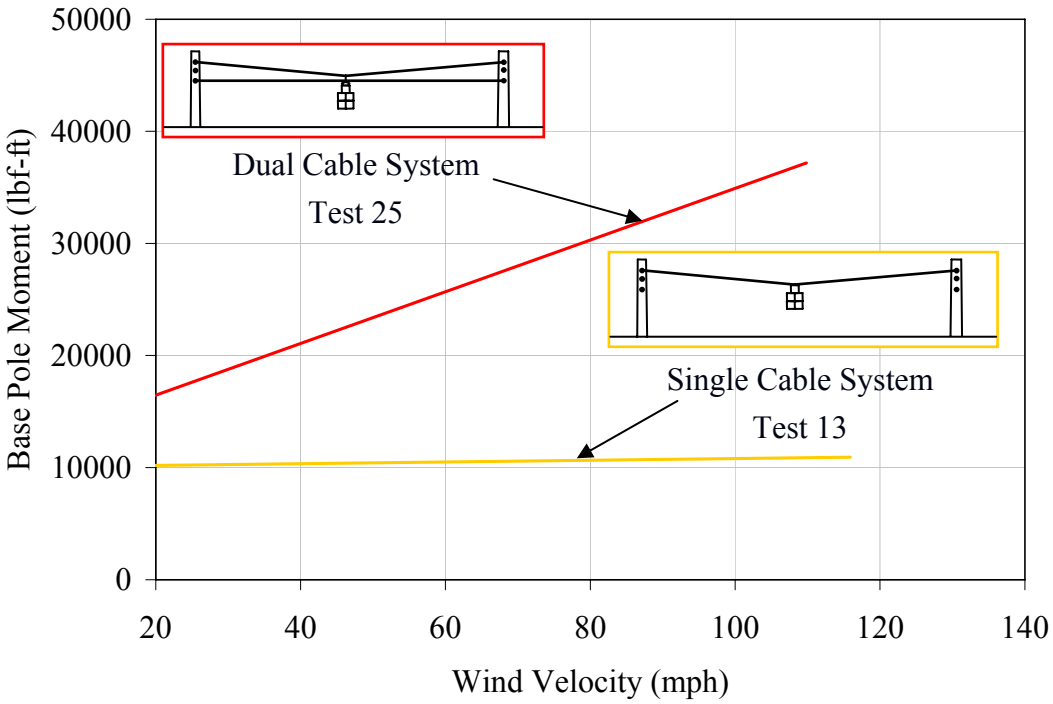

Figure 4-12. Moment in concrete poles with signal at minimum clearance height.

4.3 POLE MOVEMENT

A two-inch string pot was connected to the eyebolt on the west concrete pole and measured small displacements of the pole parallel to the wind direction. The pole displacement parallel to the wind direction and perpendicular to the cable span was deemed insignificant for the single cable tests that measured movement, as expected because the primary tensile forces were parallel to

the cable span. Visual inspection during testing verified that the poles did not experience significant movement. Because the poles were visually determined to be stable and consistent, the string pot was attached only to the west pole.

The recorded deflection was observed to be between 0.004 and 0.008 inches for each test, which is negligible by engineering standards. During the test featuring the rear-facing signal with 2% sag, the string pot returned a constant value of approximately 1.3, indicating that the equipment malfunctioned. Table 4-5 provides results from the tests measuring displacement parallel to the wind field. Displacements perpendicular to the wind field were not recorded.

Table 4-4. Pole displacement during testing

Test	Maximum Displacement During Test (in)
8	0.006
9	0.008
10	0.004
11	0.004
12	0.007
13	0.004
14	0.007
15	0.075*

*String pot malfunctioned during test

4.4 CABLE TRANSLATION

The movement of the cables for both the dual cable and single cable systems at the attachment of the traffic signal located at midspan shows how the system displaces in high winds.

4.4.1 Single Cable System

Figure 4-13 shows the horizontal translation (translation) of the single cable at the signal located at the midpoint of the span. At a wind velocity of 115 miles per hour, the signals supported by

the 5% sag cable did not vary much in translation. The signal with the 40 inch pipe hanger moved approximately 25 inches while the directly connected signal moved approximately 26 inches. The tighter cable caused half as much movement as the other two—the signal supported by the cable with 2% sag moved approximately 11 inches.

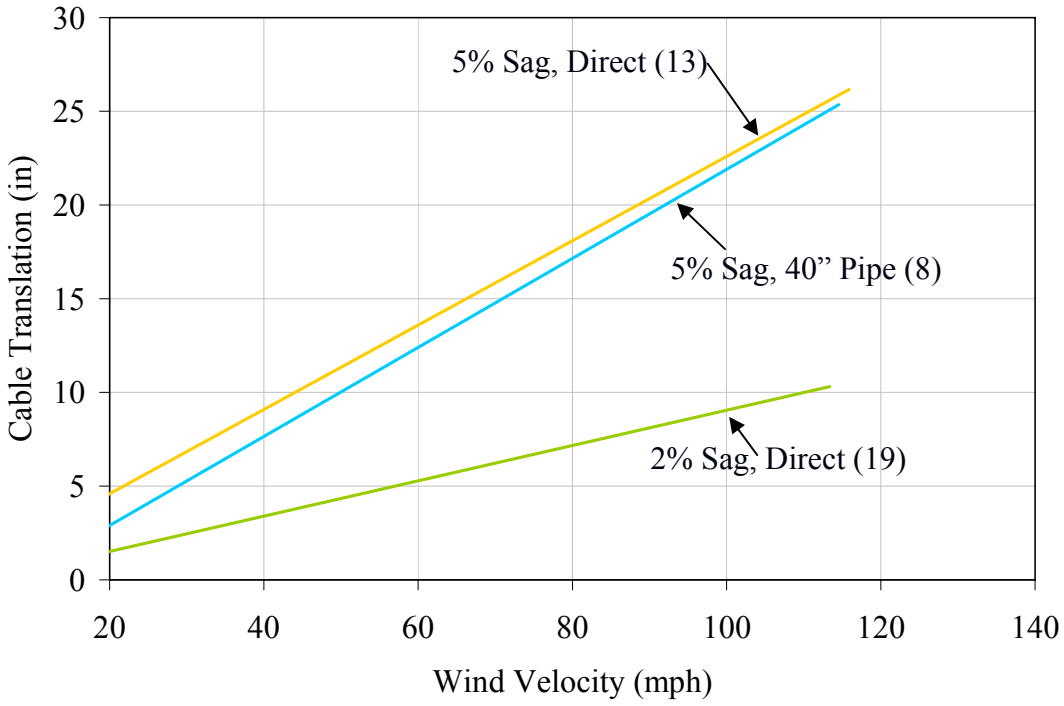

Figure 4-13. Cable translation for forward facing signal supported by single cable system.

4.4.1.1 Effect of Signal Orientation on Cable Translation

Figure 4-14 shows the cable translation for the single cable systems that featured various orientations with respect to the wind field. In nearly all cases, the cable experienced almost no difference in translation. The backward facing signal with pipe hanger and 5% cable sag experienced a slightly larger movement by approximately 3 inches from the forward and diagonal signal with same support.

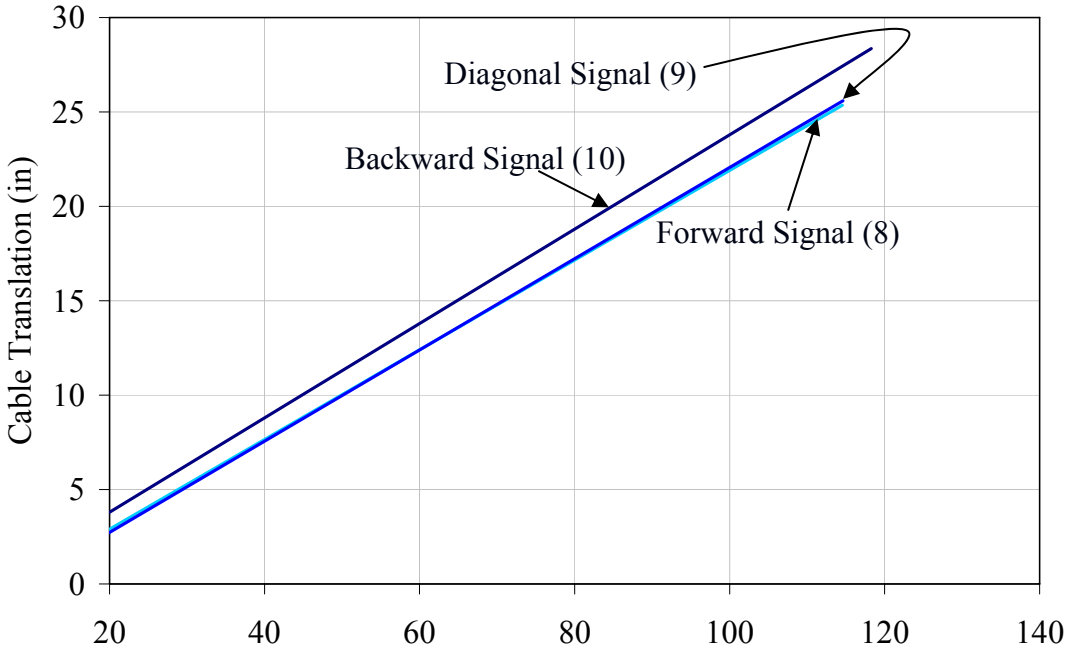

A) 40” pipe hanger with 5% cable sag.

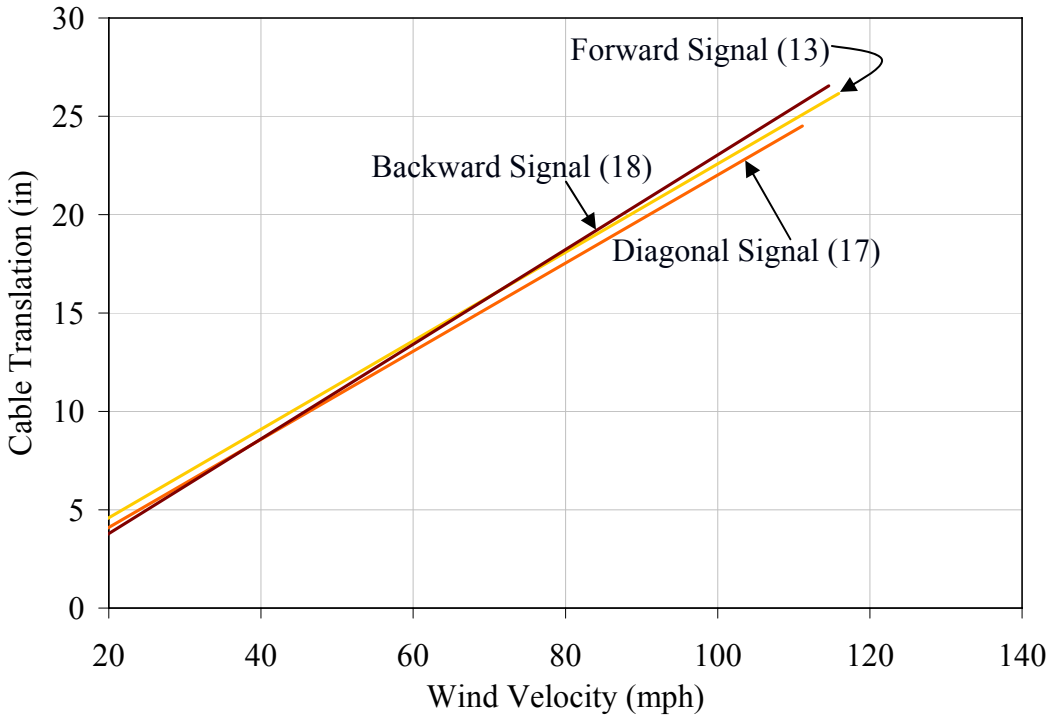

B) Direct Connection with 5% catenary sag.

Figure 4-14. Cable translation for signal with different orientation supported by single cable system.

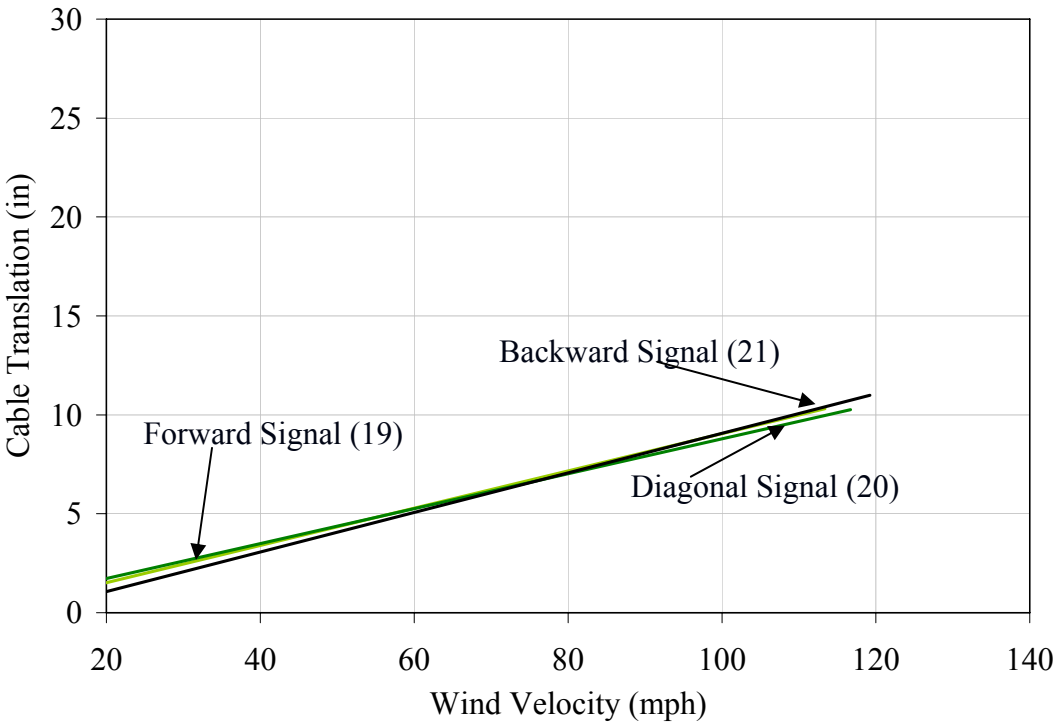

C) Direct connection with 2% catenary sag.

Figure 4-14. Cable translation for signal with different orientation supported by single cable system, continued.

4.4.1.2 Effect of Additional Weight on Cable Translation

Signals with various weights had slight differences in cable translation, as shown in Figure 4-15. In the tests featuring the 40 inch pipe hanger in the single cable system, the cable moved backward approximately 28 inches when the additional weights were added. The single cable system with 2% sag experienced slightly different results between the 82 pound signal and the 102 pound signal. The 102 pound signal moved the most, with a horizontal translation measured at approximately 13 inches. The 82 pound signal moved approximately 11 inches, and the 62 pound signal moved approximately 11 inches. In all cases, the variation in movement was less than 3 inches.

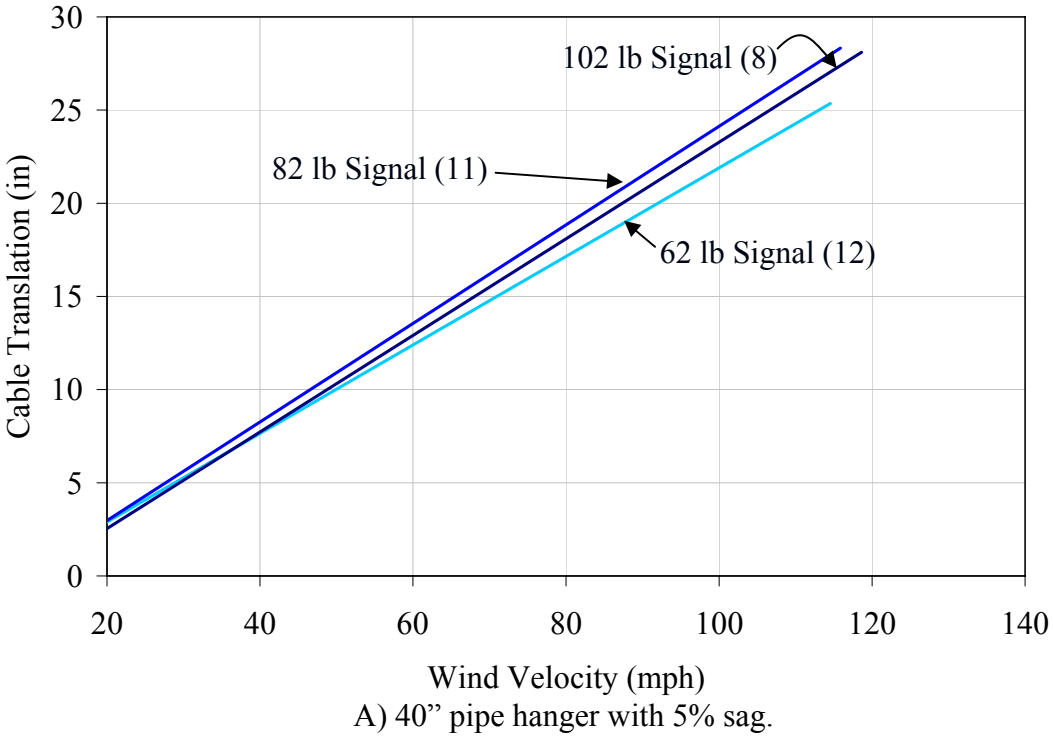

A) 40” pipe hanger with 5% sag.

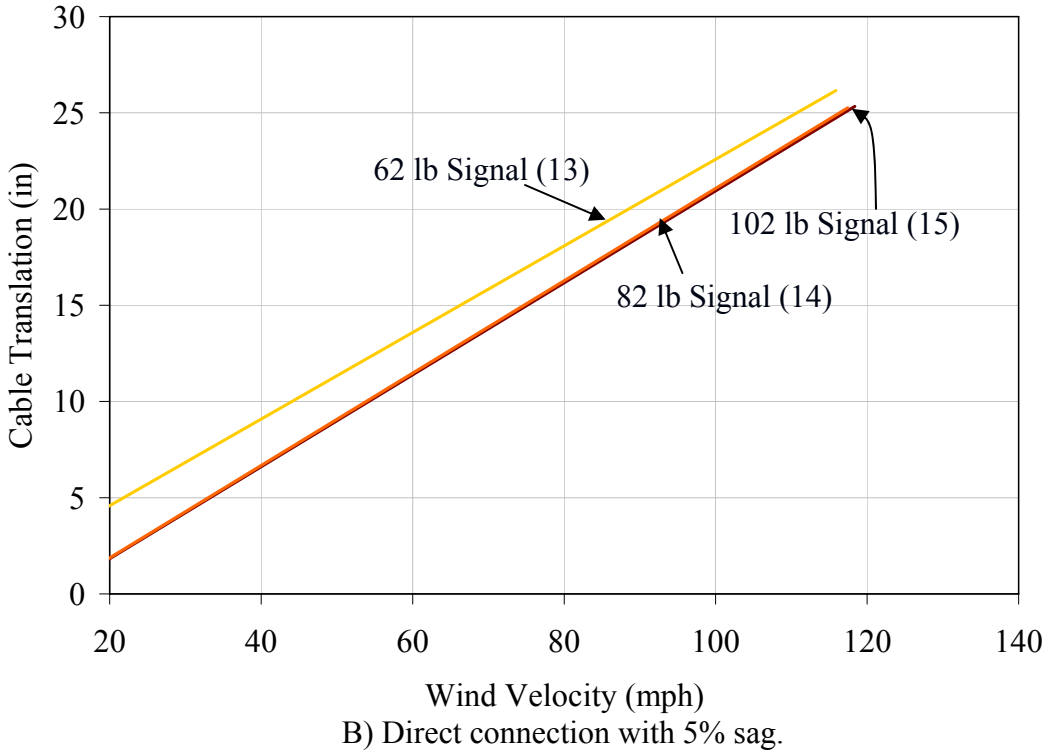

B) Direct connection with 5% sag.

Figure 4-15. Cable translation for signal with varying weight supported by single cable system.

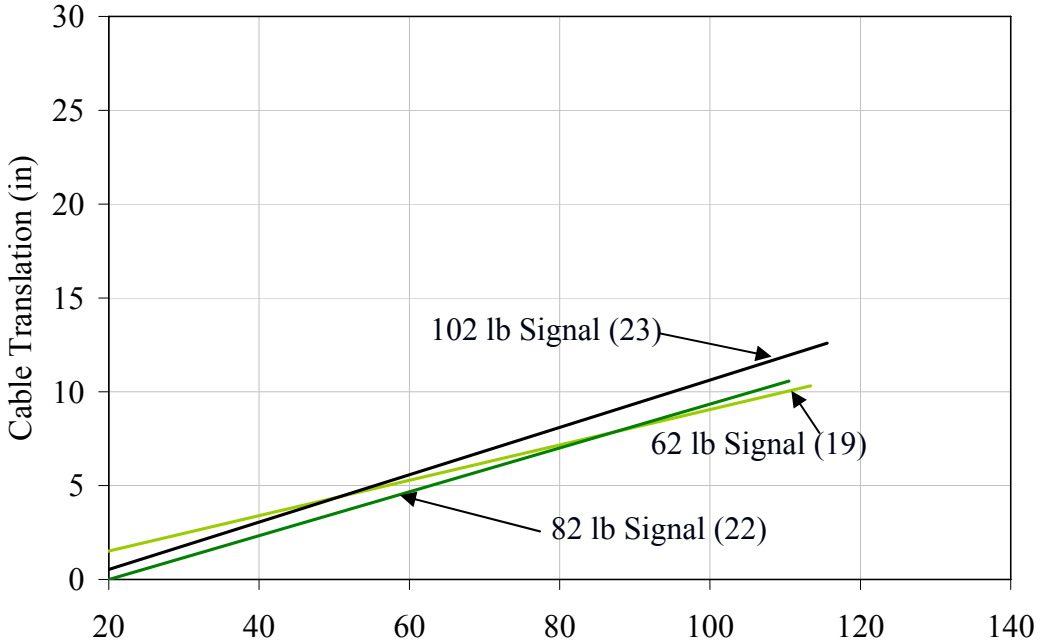

C) Direct connection with 2% sag.

Figure 4-15. Cable translation for signal with varying weight supported by single cable system, continued.

4.4.2 Dual Cable System

For the 5% sag, the catenary cable moved towards the wind source and reached a maximum translation of slightly more than 8 inches; the messenger cable moved in the opposite direction but displaced approximately the same distance as the catenary cable as shown in Figure 4-16.

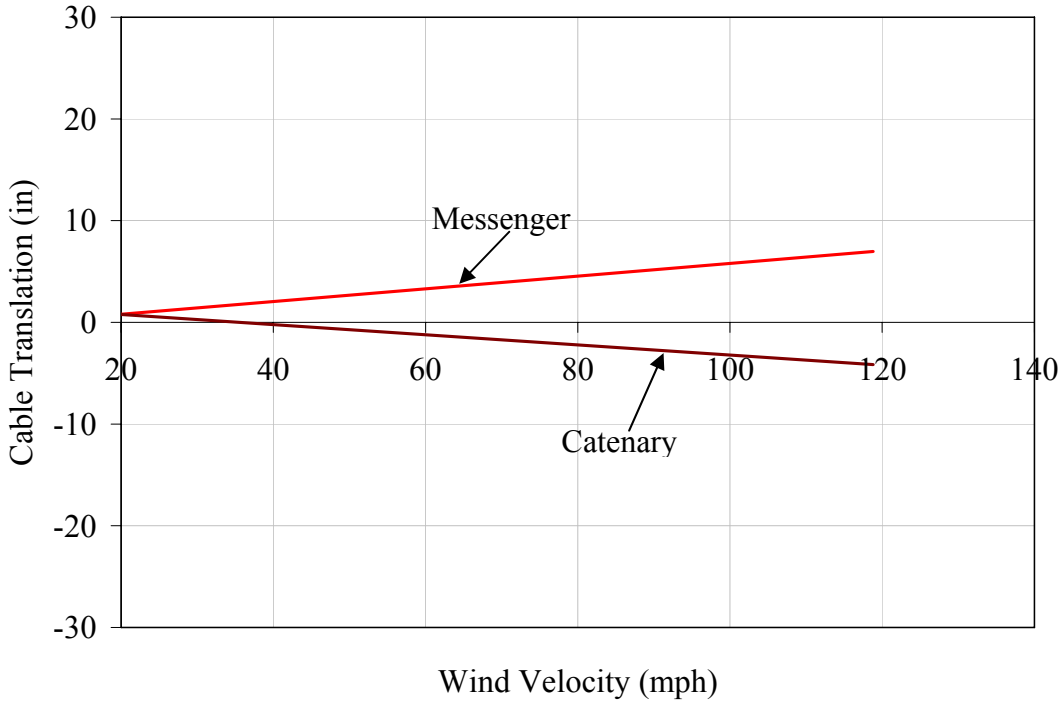

Figure 4-16. Cable translation for signal supported by dual cable system with 5% sag (test 1).

4.4.3 Repeated Tests

The second series of tests were conducted approximately one week after the first with various maintenance agencies present. The goal of the viewing was to offer the chance for authorities to view the behavior of the tests. Because a goal was to complete the tests within a day, time was limited to conduct each test. As a result, the test with the 2% catenary sag was the only test used to give results on cable translation that day.

Figure 4-17 shows the comparison between the two tests performed on the single cable system with 2% sag. Both cases yielded maximum cable translations below 15 inches, and both further show that the tighter cable had less movement than the cases with 5% sag. The data from the first test show that the catenary cable moved less compared to the second test. The difference in

movement was approximately 3 inches.

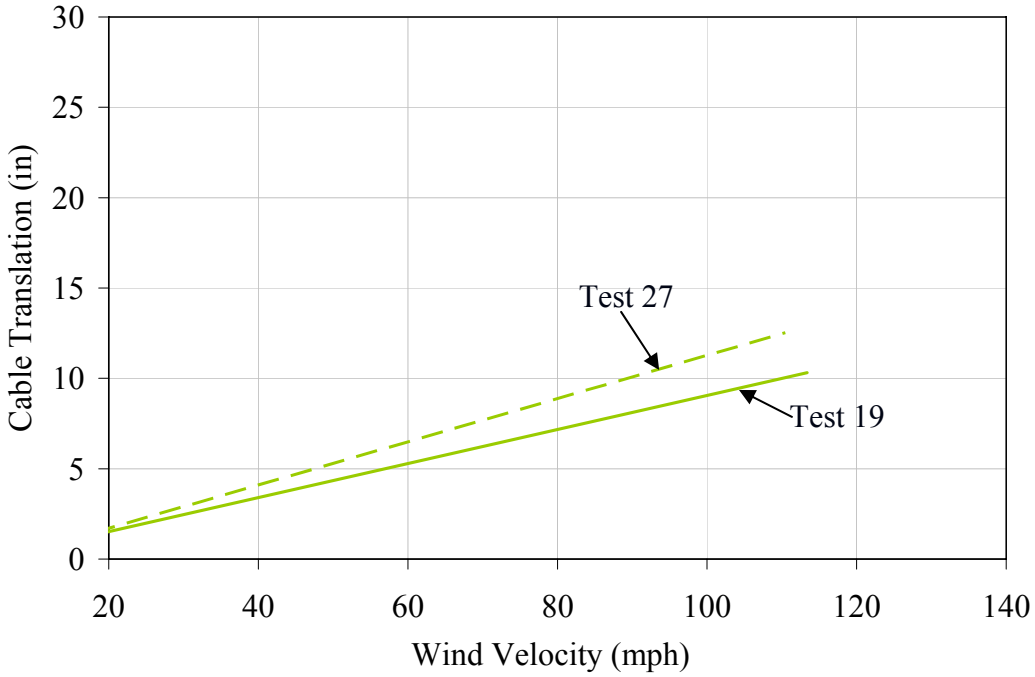

Figure 4-17. Cable translation for forward facing signal supported by single cable system with 2% cable sag.

4.4.4 Discussion of Cable Translation

The cable translation showed the horizontal movement the traffic signal cables underwent. In the single cable system cases, the movement was over 2 feet with the 5% catenary sag and approximately 1 foot with the tighter 2% catenary sag. The catenary and messenger cables experienced less movement with the dual cable system as the messenger cable works to restrain the motion of the system; although this may seem desirable, data has also shown that while the translation is limited, the hangers and disconnect boxes experience large forces often leading to yielding and eventual failure.

The measured cable translation at mid span was used to determine the rotation of the cable in the

single cable system. The angle the cable makes with the vertical plane,ϕ, is not assumed to be equal to the angle the signal makes with the vertical plane, θ, which was measured by inclinometers during testing. The cable angle ϕ is found using the cable translation measured by the string potentiometers along with the sag to determine the angle the cable makes with the vertical plane. Figure 4-18 shows the angles of both the cable (ϕ) and signal (θ) and the relationship used to determine cable angle, ϕ. Figure 4-19 A shows insignificant differences between the two rotations for the pipe hanger, while Figure 4-19 B shows that the signal rotates by at most 10 degrees more than the cable in the directly connected system.

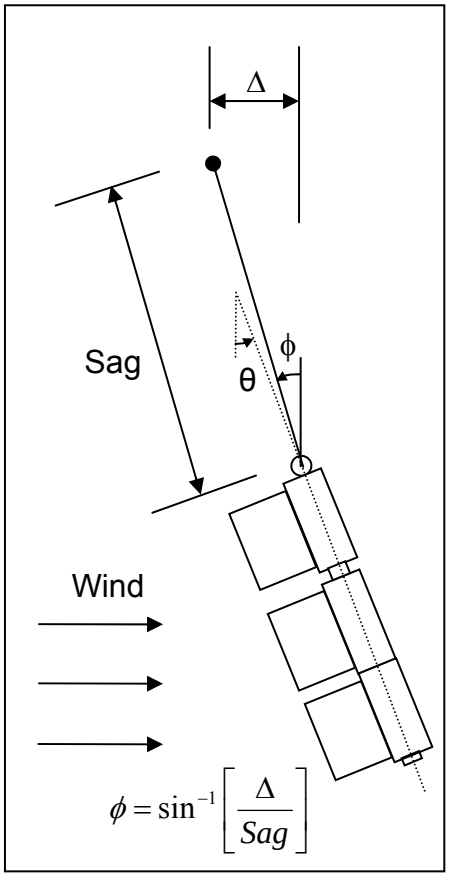

Figure 4-18. Rotation of cable and traffic signal.

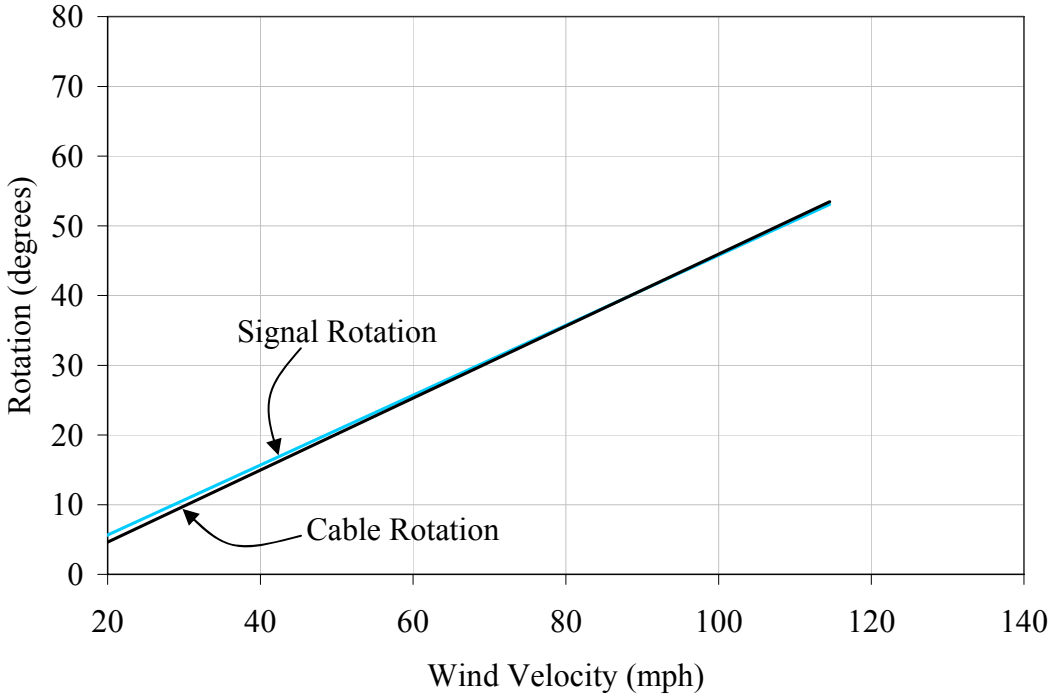

A) 40” pipe hanger with 5% sag.

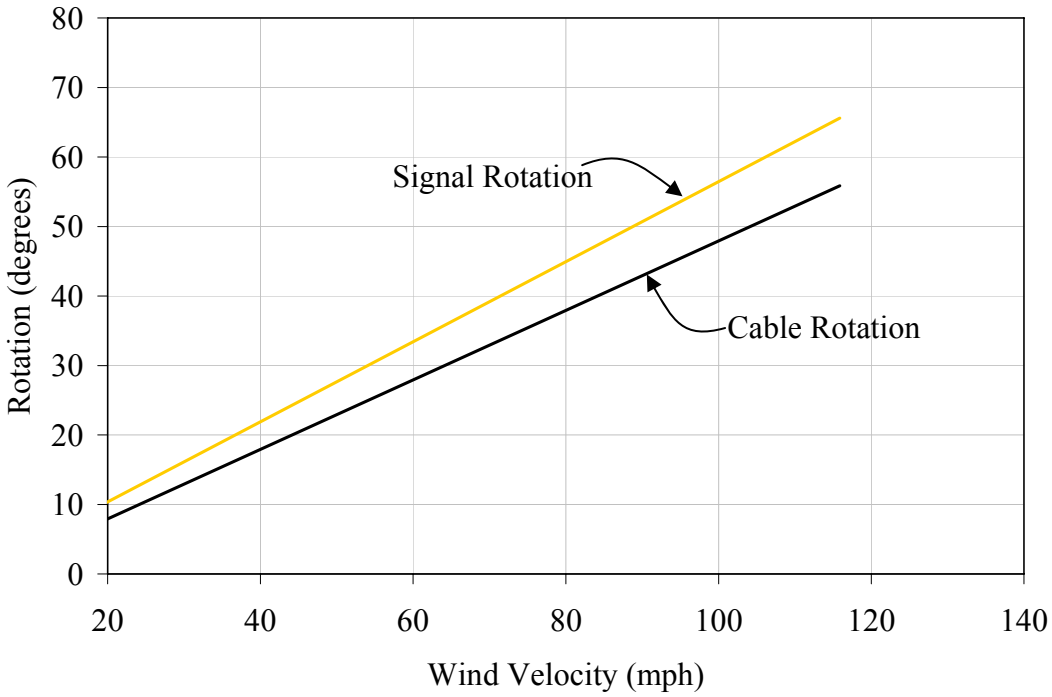

B) Direct connection with 5% sag.

Figure 4-19. Difference in rotation of traffic signal versus cable.

4.5 SUMMARY OF TEST RESULTS

The following provides a brief summary of test results based both on test data and visual observation of the tests.

4.5.1 Data Observation

The rotations experienced by the traffic signal are directly related to signal visibility. For 50% of the signal to remain visible, the maximum angle of rotation is 30 degrees. The signals tested experienced less than 50% visibility at wind velocities ranging from 54 to 79 miles per hour, which would rarely be present during typical driving conditions. The data shows that both single and dual cable systems perform well regarding signal rotation under normal operating conditions.

The cable tension did offer a good understanding of system performance in high velocity winds. The single cable system experienced little gain in cable tension with increased wind loading. These results agree with those reported in Alampalli 1998 as shown in Figure 2-3 for tests on signals supported by a single cable system. The ability of the single cable system to swing freely minimizes stresses in the hanger and signal; therefore, the hanger did not bend in high wind velocities. The dual cable system resists movement and the messenger cable experiences a high increase in tension. This load is transferred between the messenger cable and the signal by the hanger/disconnect box, which must be designed to transmit this load. In addition, the increased messenger cable tension causes significantly increased moments in the supporting pole resulting in larger pole sizes and deeper embedments.

The cable translation measurements help to understand the increase in tensile forces for the dual cable system. Because the messenger cable is provided, it limits the translation of the hanger and signal resulting in substantive increases in tension in the messenger cable, flexural stress in the hanger/disconnect, and moment in the concrete poles as the wind force increases. The single cable system allows both the cable and signal to move freely resulting in minimal buildup of resisting forces. The cable translation measurements also indicate that both the cable and signal rotate essentially the same with the system performing in a manner similar to a simple pendulum.

4.5.2 Visual Observation

All signals rotated gradually as a result of increased wind speed. However when the hanger was used, the primary difference between the single cable and dual cable system was that the messenger cable restricted movement and resulted in yielding of the aluminum hanger. This occurred in every test of the dual cable system. The pipe hanger, when connected by only the single cable, never experienced deformation.

5.0 FORCE COEFFICIENTS, DRAG COEFFICIENTS, AND LIFT COEFFICIENTS

The flow of air around traffic signals creates variances in pressure on the surface of the signal. A goal of this project is to determine the aerodynamic effects of a wind stream around the signal head.

The primary reference manuals for determining wind forces on structures—"Minimum Design Loads for Buildings and Other Structures" (ASCE 7) and "Standard Specifications for Structural Supports for Highway Signs, Luminaires, and Traffic Signals" (AASHTO 2001)—both define a coefficient for determination of the effect of bodies immersed in a flowing stream of air (ASCE 2005; AASHTO 2001). ASCE 7-05 makes use of a force coefficient in Section 6.5.15, "Design Wind Loads on Other Structures" (ASCE 2005). AASHTO uses a drag coefficient in the determination of the force acting on signals (AASHTO 2001). The force coefficient indicates the total force acting on the signal, while the drag coefficient and lift coefficient show the forces acting on the signal parallel and perpendicular to the wind stream, respectively.

The dynamic wind pressure in steady state is governed by the Equation 5-1 where ρ is the density of air, which is constant, and V is the velocity of the stream.

$$p = \frac{1}{2}\cdot\rho\cdot V^2 = 0.00256\cdot V^2 \qquad (5\text{-}1)$$

When air encounters a surface, the total pressure acting on the object is a result of the pressure of the face of the object in the oncoming stream, as well as from the slow moving stream of air that forms on the surface in the wake. A force coefficient (C_f) added to the Equation 5-1 accounts for the forces on all surfaces, and when multiplied by the surface area, the new equation shows the total wind force acting on a surface. Equation 5-2 is reflective of the total force acting on objects

in a wind stream, where the constants are replaced, the area of the object, A, is specified, and C_f is the force coefficient that accounts for the sum of the pressures acting on the surfaces of the object.

$$P_w = p \cdot C_f \cdot A = 0.00256 \cdot V^2 \cdot C_f \cdot A \tag{5-2}$$

The force coefficient, C_f, accounts for the total air force acting on the signal, and as shown by Equation 5-3, can be found by rearranging Equation 5-2.

$$C_f = \frac{P_w}{0.00256\ V^2\ A} \tag{5-3}$$

The total force acting on the traffic signal is composed of a drag force, which acts parallel to the wind direction, and a lift force which is perpendicular to the wind direction. The drag and lift can be found by using Equations 5-4 and 5-5, which are variations of Equation 5-2 that replace the force coefficient with a drag and lift coefficient.

$$D = 0.00256 \cdot V^2 \cdot C_d \cdot A \tag{5-4}$$

$$L = 0.00256 \cdot V^2 \cdot C_l \cdot A \tag{5-5}$$

The drag and lift coefficients are found similarly to the force coefficients and are expressed in Equations 5-6 and 5-7. The coefficients are found by normalizing the drag and lift forces with respect to the dynamic wind force.

$$C_d = \frac{D}{0.00256 \cdot V^2 \cdot A} \tag{5-6}$$

$$C_l = \frac{L}{0.00256 \cdot V^2 \cdot A} \tag{5-7}$$

Figure 5-1 A shows a free body diagram of the forces acting on a signal in a single cable support system. Using the summation of forces equilibrium equations, the drag force (D) and the lift force (L) can be determined by Equation 5-8 and Equation 5-9:

$$D = T'\sin\phi \tag{5-8}$$

$$L = W - T'\cos\phi \tag{5-9}$$

The moment equilibrium equation about the pinned connection between the cable and signal shown in Figure 5-1 A leads to Equation 5-10 where d_{weight} is the distance from the pinned connection to the center of weight (W) and d_{wind} is the distance from the pinned connection to the center of the drag and lift wind loads (D and L) as shown in Figure 5-1 A.

$$W\,d_{weight}\sin\phi - L\,d_{wind}\sin\phi - D\,d_{wind}\cos\phi = 0 \tag{5-10}$$

Figure 5-1 B shows the relationship between the measured tension force in the single cable system (T), with the resulting force (T') acting in the plane of the rotated single cable for all angles of cable rotation, this results in Equation 5-11 for determining T'.

$$T' = 2\cdot T\cdot\frac{sag}{\sqrt{sag^2 + \left(\frac{span}{2}\right)^2}} - W_{cable} \tag{5-11}$$

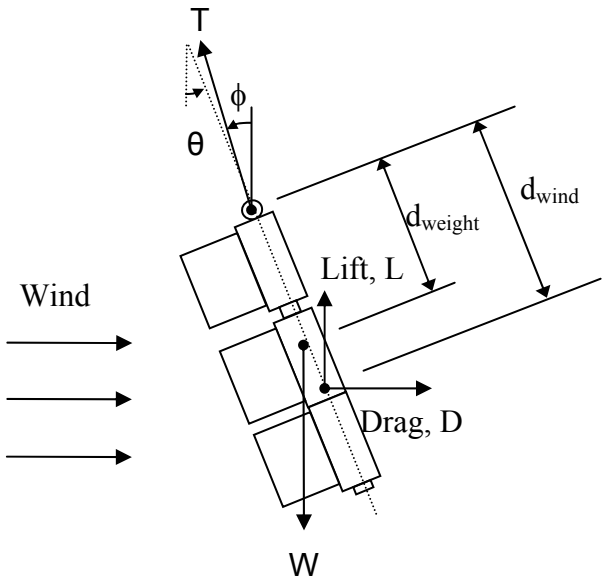

A) Free body diagram of signal supported by single cable system

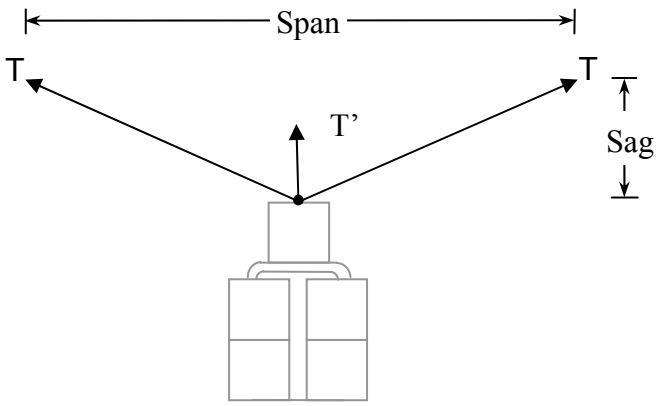

B) Relationship between measured cable tension (T) and resulting force (T') acting in the plane of the cable regardless of cable rotation ϕ

Figure 5-1. Forces acting on traffic signal in a single cable support system.

Using Equation (5-10), the center of action of the drag and lift wind load forces, d_{wind}, was found to coincide with the center of weight and center of geometry, d_{weight}. For example, using Test 13 with 5% cable sag, a direct signal connection with a 62 lb signal, and where the center of weight, d_{weight}, was located 31 inches below the cable (based on the 24 inch distance from the top of the signal to the center of weight/geometry as shown in Figure 3.3 plus an additional 7 inches due to the length of the hardware required for the direct signal connection to the cable) and at a wind velocity of 100 mph; the cable rotation (ϕ) determined from cable translation measurements was 47.9°, the tension force in the direction of cable rotation, T' was determined to be 63.2 lbs with the resulting drag force, D, of 46.9 lbs, and a lift force, L, of 19.6 lbs. The solution of Equation (5-10) for d_{wind} indicates that it is 31 inches below the cable, the same as d_{weight}, indicating the center of weight, center of geometry, and center of wind load all coincide. For design purposes the signal weight, drag load, and lift load should be assumed to act at the geometric center of the signal.

5.1 DRAG AND LIFT COEFFICIENTS

The drag force, D, and the lift force, L, act horizontally and vertically, as shown in Figure 5-1, and the presence of these forces causes the signal to rotate. Equations 5-8 and 5-9 are combined with Equations 5-6 and 5-7 to determine the drag and lift coefficients expressed in Equations 5-12 and 5-13.

$$C_d = \frac{D}{0.00256 \cdot V^2 \cdot A} = \frac{T' \cdot \sin(\phi)}{0.00256 \cdot V^2 \cdot A} \tag{5-12}$$

$$C_l = \frac{L}{0.00256 \cdot V^2 \cdot A} = \frac{W - T' \cdot \cos(\phi)}{0.00256 \cdot V^2 \cdot A} \tag{5-13}$$

The total area of the signal faces is used to normalize the drag and lift coefficients because the

drag and lift forces expressed by Equations 5-4 and 5-5 are most easily computed using the total area of the signal heads. The addition of the hood configuration or signal rotation into the force coefficient, which affect the projected area in the wind field, makes the use of the equations difficult without data on such parameters. The drag and lift coefficients shown in the following figures and in Appendices F and G are based on Equation 5-12 and 5-13 using Equation 5-11 for T' with the nominal cable sag. The following figures also show drag and lift coefficients for a five head signal based on ASCE 1961 (see Figure 2-1). Equations 5-12 and 5-13 are sensitive to T' while Equation 5-11 is very sensitive to sag. Use of the nominal cable sag in Equation 5-11 indicates that tests where the measured initial tension was very close to the calculated initial cable tension based on nominal sag provide the best estimation of the drag and lift coefficients. As noted in Section 4.3, the tests with the signals directly connected to the single cable provided this. The figures below show the results for these tests, all single cable system raw data for the drag coefficient is provided in Appendix F and the lift coefficient data is presented in Appendix G.

5.1.1 Effect of Signal Orientation on Drag and Lift Coefficients

The drag coefficients are presented in Figure 5-2 for various rotations of the traffic signal. The drag coefficients vary by at most 0.1 and decreases as the signal rotates.

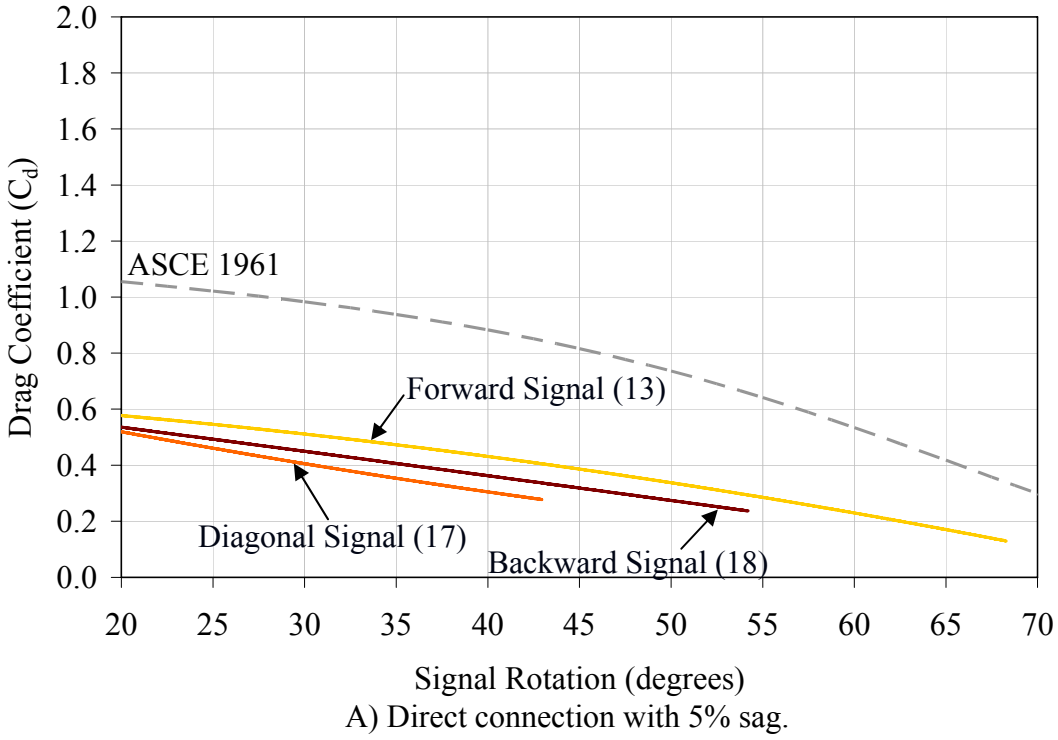

A) Direct connection with 5% sag.

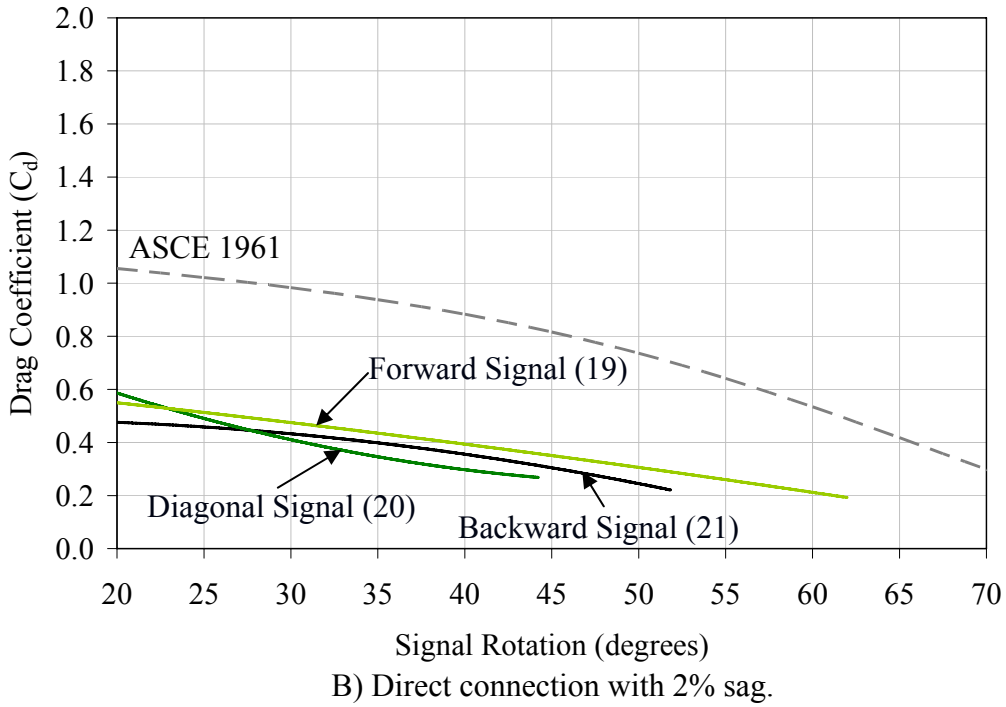

B) Direct connection with 2% sag.

Figure 5-2. Orientation effect on drag coefficients.

Figure 5-3 shows the lift coefficients for the same tests presented in Figure 5-2. The lift coefficient did not display any significant deviations between tests as they decrease. The orientation of the signal plays an insignificant role in the effect of the drag and lift coefficients.

5.1.2 Effect of Additional Weight on Drag and Lift Coefficient

Figures 5-4 and 5-5 show the effect of additional weight on the drag and lift coefficients. Figure 5-4 displays the drag coefficients. The results are similar to the values shown for various signal orientations. Figure 5-5 displays the lift coefficients for the traffic signal. Both the drag and lift are not shown to be significantly different due to differences in the weight of the traffic signal. Additionally, both the drag and lift coefficients decrease as the signals rotate. Test 23 experienced slightly higher drag and coefficients than similar tests.

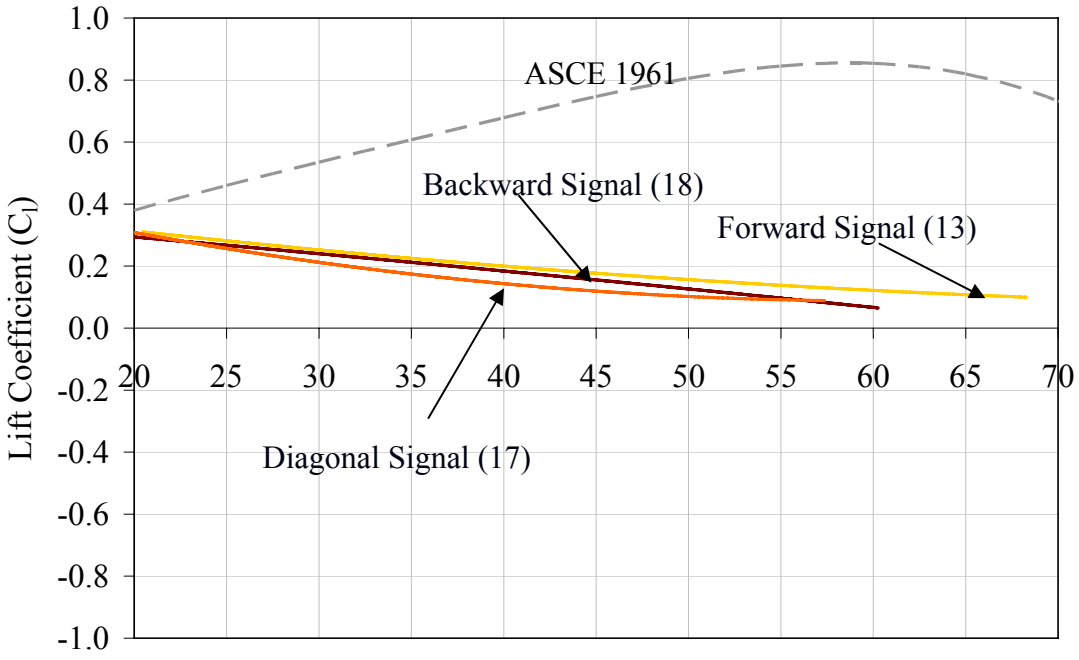

A) 5% Direct Connection with 5% sag.

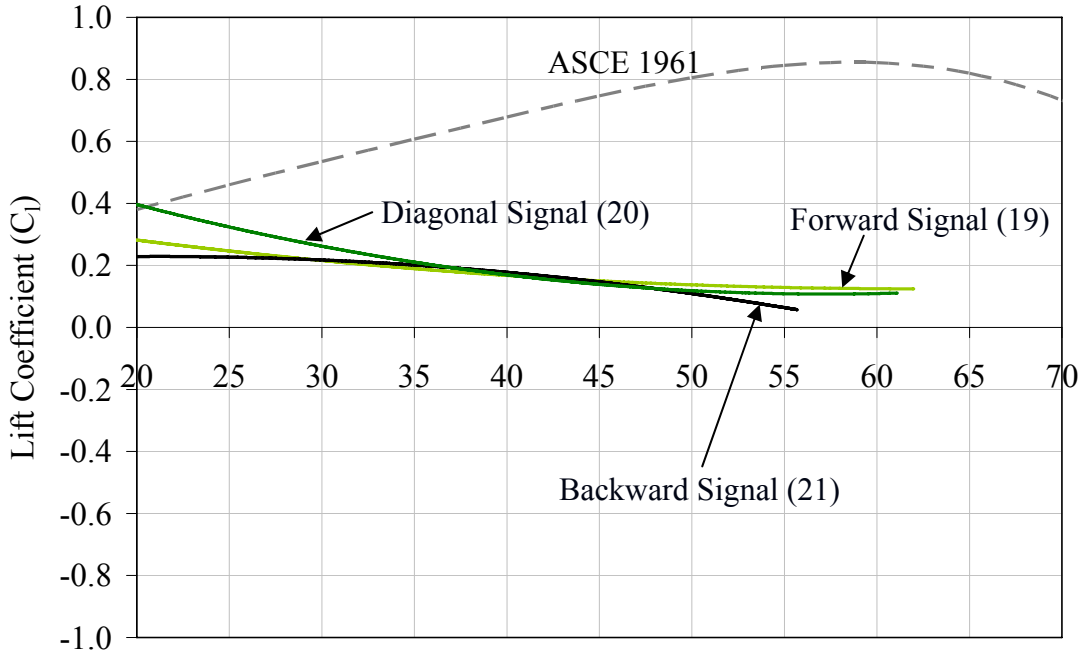

B) Direct connection with 2% sag.

Figure 5-3. Orientation effect on lift coefficients.

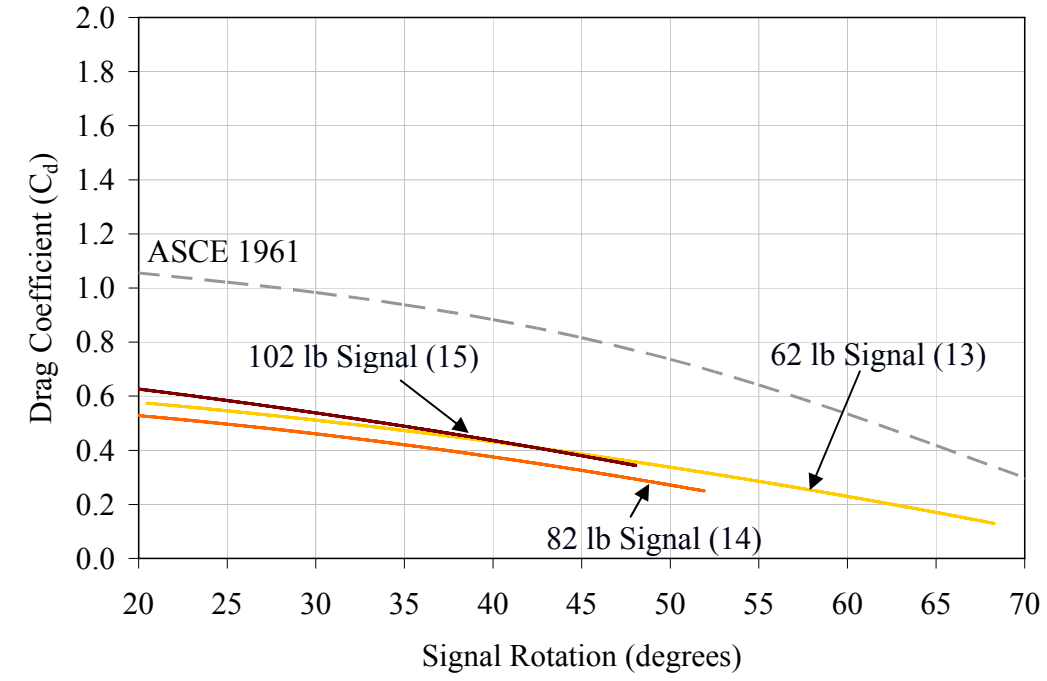

A) Direct connection with 5% sag.

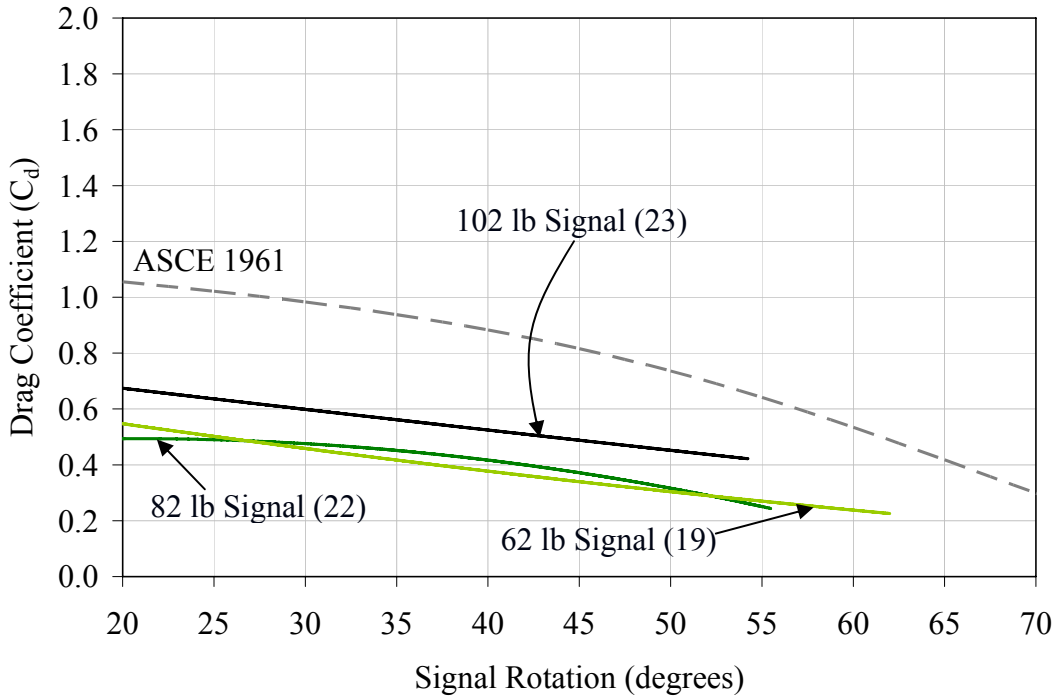

B) Direct connection with 2% sag.

Figure 5-4. Weight effect on drag coefficients.

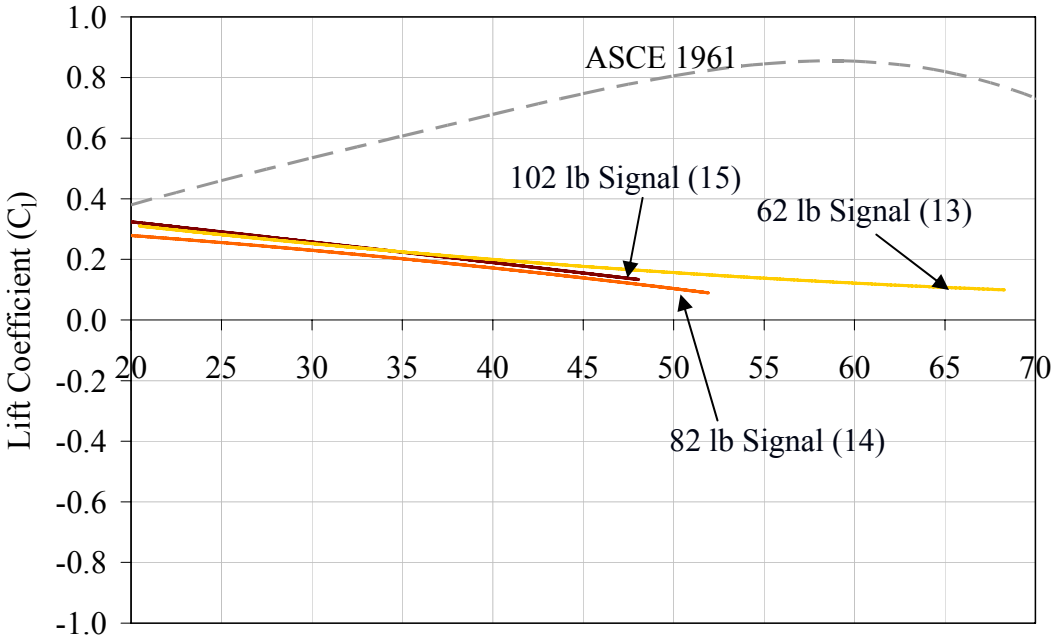

A) Direct connection with 5% sag.

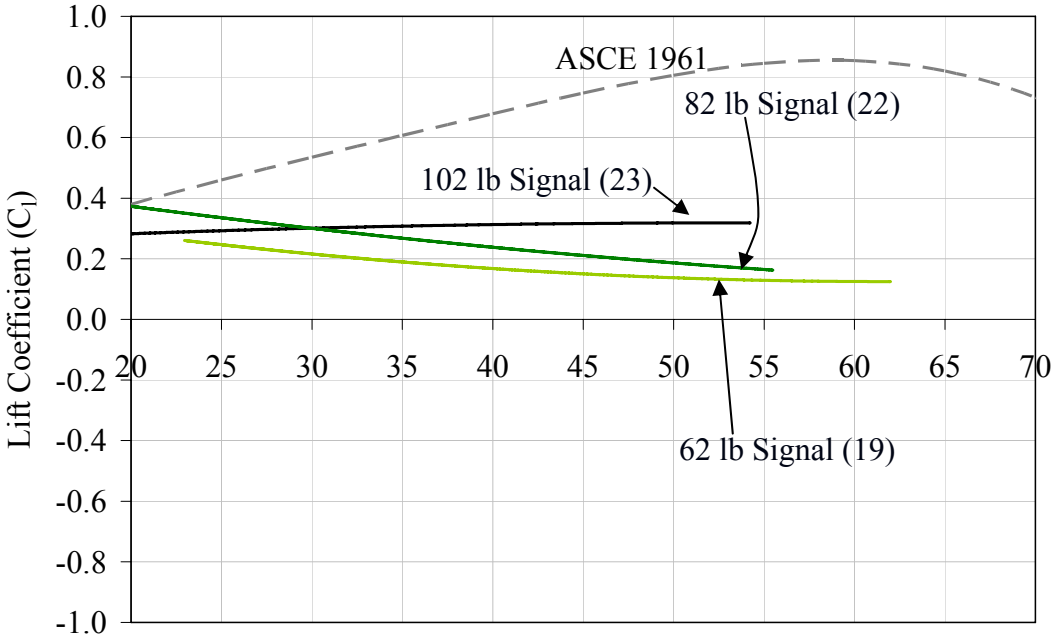

B) Direct connection with 2% sag.

Figure 5-5. Weight effect on lift coefficients.

5.2 DISCUSSION OF FORCE, DRAG, AND LIFT COEFFICIENTS

Drag and lift forces combine to act on the traffic signal; drag acts parallel to the wind field, while the lift is perpendicular to the wind field. The constant drag coefficient of 1.2 presented in AASHTO does not account for the varying drag coefficient experienced by a rotating signal supported by a single cable system and is conservative (AASHTO 2001). For low wind velocities, the drag makes up a large portion of the total force acting on the signals in testing, as expected. As the wind speed increases, the rotation increases, causing the drag to decrease. In all cases, the drag coefficient from testing is lower than the ASCE curves.

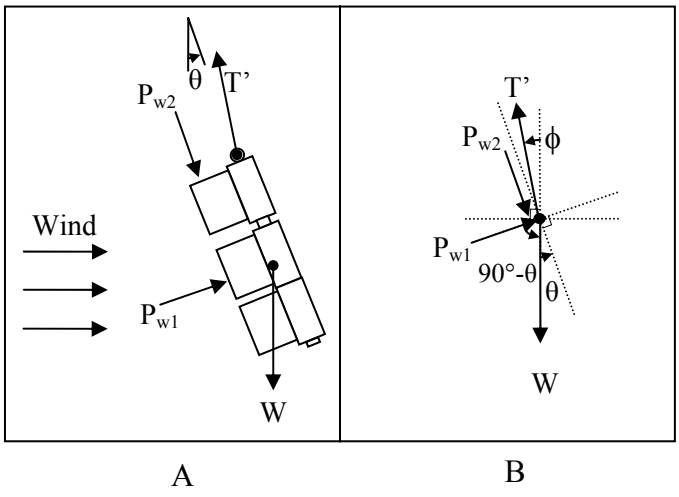

Figure 5-6. Wind forces acting on the traffic signal.

The lift coefficient from ASCE increases as the rotation increases, but the test results of the single cable system indicate that the signal lift coefficient decreases with increasing rotation. Figure 5-6 presents the primary wind forces acting on the traffic signal. The wind forces of significance act on the face of the signal, P_{w1}, as well as the top of the visors, P_{w2}. As the signal rotates, the projected area of the visors increases, causing a force that has a component that acts downward on the signal. The ASCE curves were created using a flat plate, which would not experience this force. As a result, the lift acting on the signal is expected to be lower and is in

fact shown to decrease.

5.3 COMPARISON OF DRAG FORCES

As previously mentioned, Marchman conducted tests on traffic signals (Marchman 1971). Figure 5-7 shows the drag force measured by Marchman for tests which have a projected cross sectional area of 6.3 ft^2. Tests 6 and 7 featured 3-way signals with a total weight of 107 pounds, and Tests 8-10 featured 4-way signals with a total weight of 135 pounds. These tests were compared to forward facing signals of 62 and 102 pounds with a cross sectional area of 6.35 ft^2. Marchman's tests reveal higher drag forces, even when compared to signals of similar cross sectional area and weight, as shown in Figure 5-7.

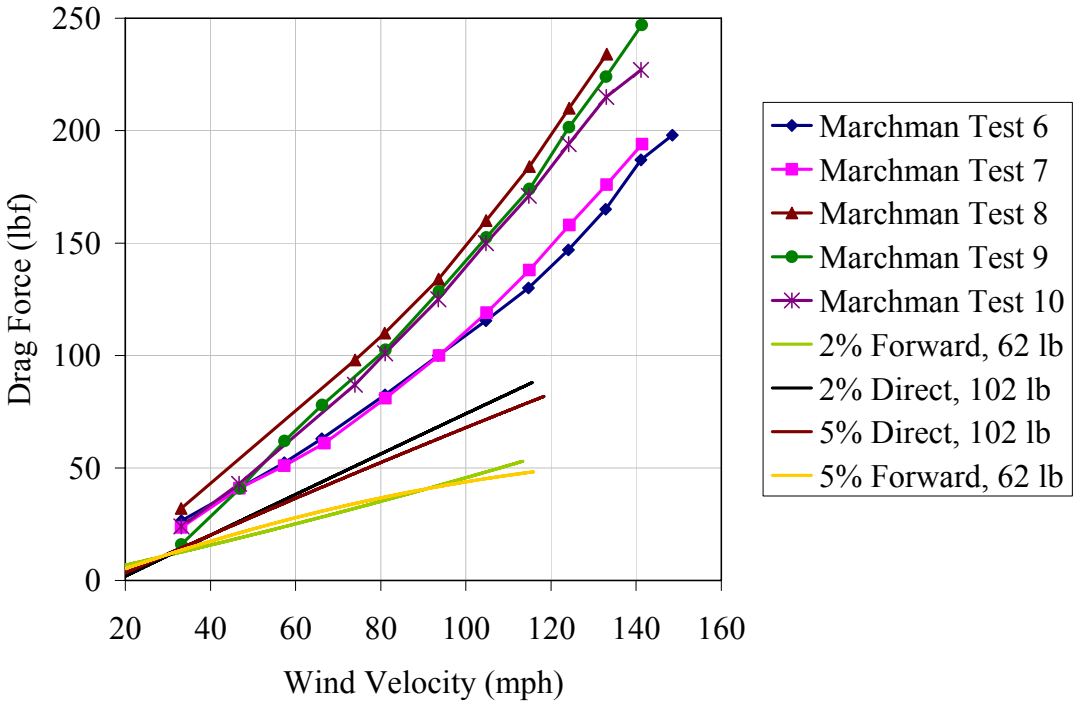

Figure 5-7. Drag forces from University of Florida tests and Marchman 1971.

Marchman's tests featured signals that were allowed to rotate but were suspended by a fixed support. Similar tests performed during this research project were performed using traffic signals suspended by the single cable system. Similar to a simple pendulum, the single cable signal support system freely swings back and results in minimal forces in the cable, support pole, hanger and signal. As shown in Figure 5-8, the force required to hold the weight at a certain rotation in a simple pendulum support system is always less than the weight. The single cable tests performed in this research project and tests results reported in Alampalli 1998 (Figure 2-3) indicate that this is how signals supported by a single cable system perform. The slight increase in initial cable tension measured in the single cable system tests is likely due to the fact that the signal hoods pick up wind load as the signal rotates.

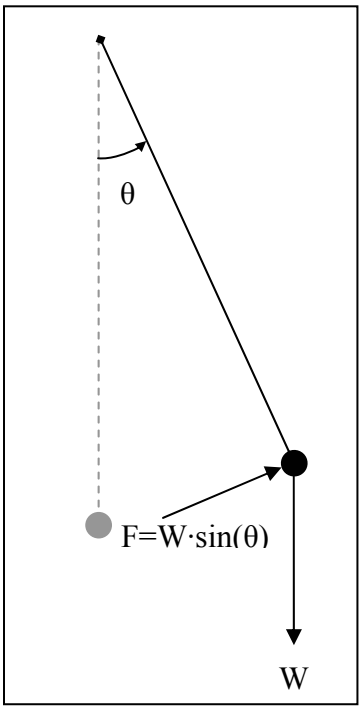

Figure 5-8. Forces required to maintain equilibrium of a simple pendulum.

6.0 ANALYSIS OF SPAN WIRE DESIGN METHODS

The flow of air around traffic signals creates variances in pressure on the surface of the signal. This chapter presents comparisons of the results of the testing program to loads determined in accordance with AASHTO 2001. ATLAS also provides assistance with the determination of wind forces on dual cable traffic signal support systems.

6.1 SPECIFICATIONS FOR WIND LOADS ON SIGNS, LUMINAIRES AND TRAFFIC SIGNALS

AASHTO's document is used to determine the forces on signs, signals, and luminaries. Section 3.8 in particular presents the specifications and commentary for the design of wind forces. Equation 6-1 defines the wind force on traffic signals where K_z is the height and exposure factor, G is the gust effect factor, V is the basic wind speed to be determined from the wind speed map in AASHTO Figure 3-2, I_r is the wind importance factor, and C_d is the drag coefficient (AASHTO 2001). Equation 6-1 is derived from Bernoulli's expression for fluid flow.

$$P_z = 0.00256\, K_z\, G\, V^2\, I_r\, C_d \qquad (6\text{-}1)$$

6.1.1 Height and Exposure Factor

Wind profiles vary according to elevation, and the roughness experienced at the boundary layer directly influences the wind speed away from the boundary. The height and exposure factor is used to categorize the upwind surface conditions and account for the surface friction which is responsible for altering the wind profile near the ground. The height and exposure factor in AASHTO 2001 is analogous to the velocity exposure coefficient presented in ASCE 7-05. Because ASCE 7-95 was the standard referenced in AASHTO 2001, exposure category A, which

was used for dense urban areas, remains in AASHTO 2001 while being discontinued in ASCE 7-02. Category B is defined as suburban and urban areas with obstructions the size of a single family dwelling; Category D is defined as a flat, unobstructed surface, not to include coastal zones in hurricane prone regions; and exposure category C is described as open terrain with scattered obstructions and applies where exposures B and D do not apply.

The commentary of AASHTO's design specifications notes that exposure C has been adopted for use in the specifications because it provides a conservative approach to the estimation of surface roughness (AASHTO 2001). Therefore the surface roughness coefficients that appear in Table 3-5 of the specifications are for a reference exposure category C, and the commentary also offers Equation C 3-1 as an alternative to calculate the height and exposure factor

$$K_Z = 2.01 \left(\frac{z}{z_g} \right)^{\frac{2}{\alpha}} \tag{6-2}$$

where z is the height above the ground or 15 feet, whichever is greater, and α and z_g are constants which vary with the exposure condition. For exposure C—the recommended condition— z_g is taken as 900 feet and α is 9.5, as in ASCE 7-95 (AASHTO 2001). This equation corresponds to equations C6-4a and C6-4b in ASCE 7-05 and the constants are unchanged from ASCE 7-95 (ASCE 2005). For a height of 32.8 feet, the factor is equal to unity, which corresponds to the reference height and exposure category for the wind speed map in Figure 3-2 of AASHTO 2001.

6.1.2 Gust Effect Factor

The gust effect factor accounts for the dynamic response of the structure exposed to fluctuations

in wind velocity. The gust effect factor presented in AASHTO 2001 is not based on the derivation from ASCE 7.

ASCE 7 presents the gust factor for two types of structures: flexible and rigid. The basis of calculations is based on wind variations and the dynamic response of the structural system. AASHTO approach sites the requirements for flexible structures in ASCE 7-95 as a structure that has a fundamental frequency less than 1 hertz or a ratio of height to least horizontal dimension as greater than 4; accordingly, all sign and signal structures are considered flexible. AASHTO 2001 mentions the application of the procedure provided in ASCE 7 would be cumbersome, requiring detailed information about the site and construction methods. Because details regarding the structures are not considered to be known with good precision, the code determines that the use of the "…calculation procedure does not outweigh the complexities and confusion introduced by its use" (AASHTO 2001).

The gust effect presented is based on a modified recommended gust factor by R. H. Sherlock in 1947. After recording wind speeds in 3 winter storms in Michigan, Sherlock used the values obtained from a storm on January 19, 1933, and divided the wind data into 5 minute intervals. He then took the fastest gust for a given time frame and divided that velocity by the average for the storm's duration. The points were drawn below Pearson Type III curves. The intervals of 5 minutes had gust durations of 0.5, 1.0, 2.0, 3.0, 5.0, and 10.0 seconds; the curves were combined and Sherlock decided that the 5 minute interval should be based on a 20% increase over the average. For a 3 second gust at 1.2 times the storm's average wind velocity, the gust factor from the Pearson Type III curve is 1.3, but his recommendation was for more conservative gust factor

of 1.385. The value of 1.3 has remained in the AASHTO specifications. Because this value is greater than for rigid structures and "resulted in successful designs," the value would continue to be used for fastest mile wind speeds but would differ with the inclusion of the 3-second gust (AASHTO 2001).

The gust factor was previously applied to the fastest mile wind speed, and the standard's conversion to a 3-second wind gust resulted in a conversion of the gust factor. Previously the gust effect factor was multiplied by the wind speed before squaring. Using the Durst model for wind gusts in ASCE 7-05 Figure C6-4 for a wind velocity of 85 miles per hour, the gust factor was to be multiplied by 0.82 and then squared to remove the gust effect factor from the wind velocity (ASCE 2005). The product of the gust effect factor and the Durst factor, once squared, and results in the recommended value of 1.14 found in AASHTO 2001.

6.1.3 Importance Factor

The importance factor is analogous to the importance factor presented in ASCE 7. The wind speed maps provided in Figure 3-2 of the AASHTO specifications are associated with the annual probability of occurrence of 2%, representing a 50-year mean recurrence interval. All transportation structures do not have a design life of 50 years and may require either a shorter or longer recurrence rate based on expected lifespan and consequences of failure. AASHTO 2001 Table 3-2 provides the importance factors for 3 cases: wind velocities of 85 to 100 miles per hour, wind velocities of 100 miles per hour or greater in hurricane prone regions, and Alaska. While these are representative of ASCE 7 values, AASHTO provides Table 3-3, specifically recommending a minimum design life for transportation structures.

6.1.4 Drag Coefficient

The drag force is the vector component of the total force in the direction of wind flow. The drag coefficient may be represented by Equation 6-3 where D is the drag force, ρ is the density of air, V is the wind velocity, and A is the area of the cross section (Holmes 2001).

$$C_d = \frac{D}{\frac{1}{2} \rho V^2 A} \tag{6-3}$$

The drag force varies according to the aerodynamic properties of the structure, including shape and dimensions. The drag coefficients for various shapes and structures are presented in Table 3-6 of the AASHTO specifications; however, the drag represents only one component of the resultant force acting on traffic signals that are allowed to rotate.

6.2 COMPARISON OF RESULTS FROM WIND TESTS AND AASHTO 2001

The drag force calculated by AASHTO 2001 uses a constant value of 1.2 for the drag coefficient. As a result, the expected drag on a signal would increase at the rate of the second order equation. Testing has shown, however, that when normalized over the area of the signal, the drag coefficient instead decreases with increased wind velocity as the signal rotates. For the rotations shown in Chapter 5, the drag coefficient is well below unity, and the use of a constant value would lead to drag forces several times larger than what is seen by the signal. Although conservative, the increased wind force could also result in support systems designed for unnecessary forces.

6.3 ATLAS

ATLAS is a program used to assist in the design of dual cable signal systems. Output from the

computer program is compared to results from tests using the catenary and messenger cables.

6.4 COMPARISON OF RESULTS FROM ATLAS AND WIND TESTS

Figure 6-1 shows the recorded readings for cable tension compared to ATLAS. ATLAS reveals an increase in messenger cable tension similar to the observed data for high wind velocities. At the maximum wind speed, the design value more closely represents the second test while the first test has a final cable tension more than 200 pounds less than the ATLAS value. The catenary cable tension more closely follows the ATLAS design values. The cable tension at the maximum wind speed matches the ATLAS results for both tests.

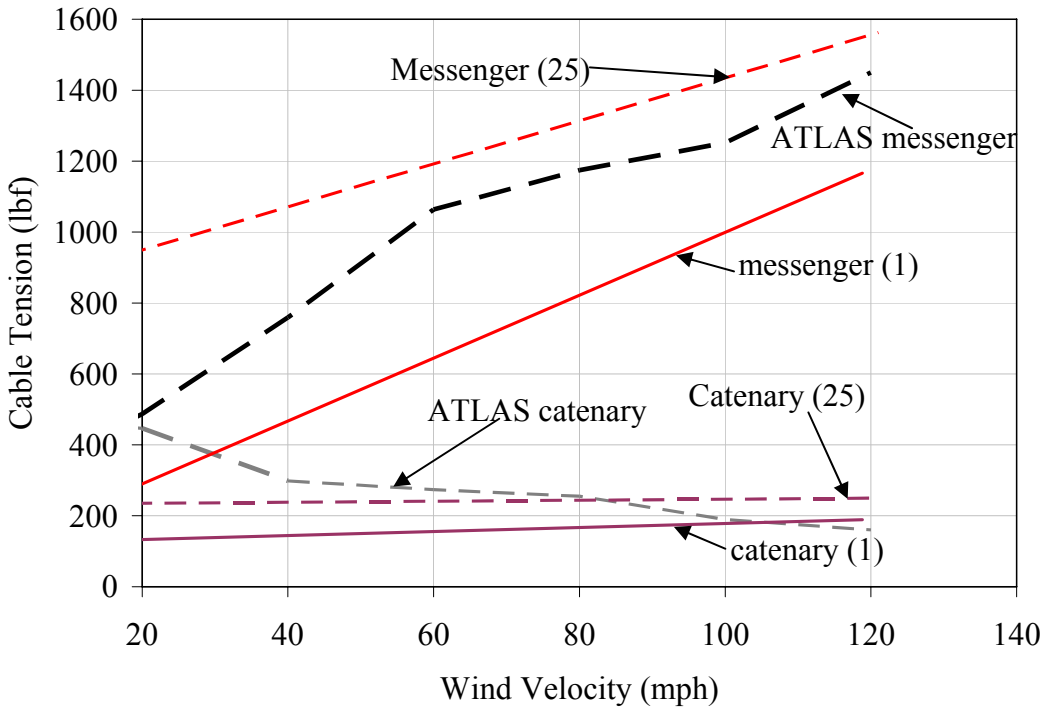

Figure 6-1. Comparison between ATLAS design values and cable tension from testing of dual cable systems.

6.5 DISCUSSION OF DESIGN METHODS

AASHTO 2001 makes use of a constant drag coefficient for design of traffic signals for wind speed. However, as shown in Chapter 5, the drag coefficient does not remain constant throughout testing because the signal rotates; as a result, the use of constant value is inaccurate. Whether comparing to a constant drag coefficient of 1.2, the coefficients provided in ASCE 1961 (shown in Figure 2-1), or to Marchman's tests (Marchman 1971), the wind forces and coefficients measured during testing using the single cable support system were lower at high wind loads agreeing with the results of single cable tests reported in Alampalli 1998. This is due to the single cable support system acting like a single pendulum.

ATLAS may be used as a reference for the design of dual cable systems. For the tests conducted, the forces predicted by ATLAS were accurate for the catenary cable at high wind velocities, and the measured messenger cable tension rose in magnitude similar to that predicted by ATLAS.

7.0 SUMMARY, CONCLUSIONS, AND RECOMMENDATIONS

Wind testing was conducted to determine how dual and single cable support systems for traffic signals experience wind force and transfers the force to the supporting structure.

7.1 SUMMARY

A series of wind tests were performed to compare the behavior of dual cable and single cable traffic signal support systems. In the dual cable system tests the distance between the catenary and messenger cables was varied. In the single cable system tests, the signal orientation, signal weight, distance of the signal from the cable, and cable sag were varied. The wind velocity, cable tension, signal rotation, and cable translations were measured. For the single cable system tests, test data was used to determine the drag and lift forces acting on the signal.

7.2 CONCLUSIONS

Regarding signal rotation, both dual and single cable support systems maintained 50% visibility of the signal to a wind velocity equal or exceeding 54 miles per hour. The average wind velocity for 50% visibility was 72 miles per hour for the dual cable system tests and 68 miles per hour for the single cable system tests. Tests of the single cable system experienced an insignificant increase in cable tension with increased wind load indicating that the system acts similar to a simple pendulum. Tests of the dual cable system exhibited a significant increase in the tension of the messenger cable with increased wind load and with the accompanying increase in stresses in the hanger/disconnect and moment in the pole support structure. For dual cable support systems, the design of the support poles must include the large increase in moment with the resulting increase in cost of the pole support structure. Single cable support systems do not

require this since the cable force remains relatively constant.

For design of the dual cable system, drag (C_d) and lift (C_l)coefficients should be the same as those reported in Cook et al. 1996 and based on ASCE 1961 as shown in Figure 2-1 (maximum values: $C_{d,max} = 1.2$, $C_{l,max} = 0.8$). For the single cable system, these same drag and lift coefficients provide a conservative estimation of the forces acting on the system but the results of this study indicate that for a 5 head signal, a maximum drag coefficient of 0.7 and maximum lift coefficient of 0.4 would be reasonable.

Based on previous field performance in hurricanes, the dual cable system is unreliable in high wind environments. The results of the tests performed in this project indicate that the dual cable system increases the likelihood of failure of hangers/disconnects, cables, and poles with increased wind speed. Test results for the single cable system indicate that it operates as a simple pendulum resulting in no significant increase in the forces carried by the hanger, cables, and poles with increased wind speed over those carried in the dead load condition. The single cable system should be adopted to minimize failures associated with span wire support systems.

7.3 RECOMMENDATIONS

To reveal a complete picture of all possible design loads, more signal configurations should be tested. Signals with different configurations and number of heads should be tested, as well as with and without visors. Combinations of signals on a single span may also reveal the dynamic nature of the system, resulting in a more complete analysis of the design procedure. Future tests should also subject the traffic signals to higher wind speeds. The maximum speed obtained

during testing was approximately 115 miles per hour, while the AASHTO design wind speed in Florida is as high as 150 miles per hour. At higher speeds, the appropriate drag, and lift coefficients can be determined for the higher rotations expected. The goal of future testing should be to understand the behavior of traffic signals with varying cross sectional area, alternative hangers, number of signals, as well as varying span lengths.

APPENDIX A
REHABILITATION OF DUAL CABLE TRAFFIC SIGNAL TEST SYSTEM

The following provides a summary of the work done regarding rehabilitation and testing using the apparatus designed for the qualification of dual cable traffic signal support systems (Cook et al. 1996). When returned to the University of Florida, the testing apparatus was fully operational. The computer program performs tasks as designated, loading the traffic signal until a specified force is reached over a number of cycles. The load cell records data accurately, and the actuator arm is in working order.

In the test, the actuator arm places a force at the centroid of traffic signals for a specified number of cycles unless failure of the support system occurs. Because the load cell measures the applied force caused by the messenger cable's restraint on the system, the dual cable system is the only type which can be tested by the apparatus. From code review, the method of calculating the forces to be applied to the traffic signal contained in the system software remains current and may be used for testing of components in the dual cable system. Note that testing of components to be used in the dual cable system does not warrant the use of the reduced drag and lift coefficients observed from the wind tests conducted on traffic signals supported by the single cable pendulum system.

APPENDIX B
SIGNAL ROTATION GRAPHS

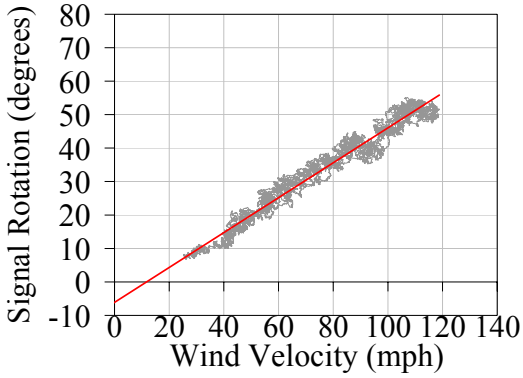

A) Test 1

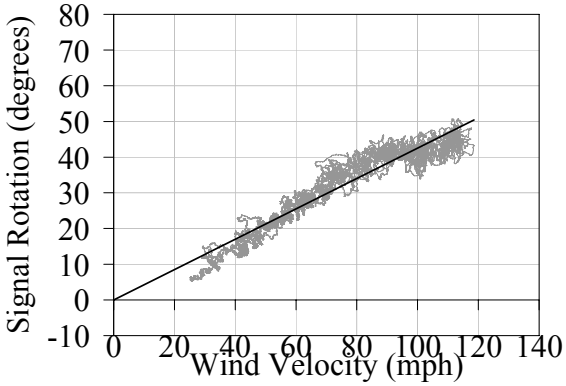

B) Test 2

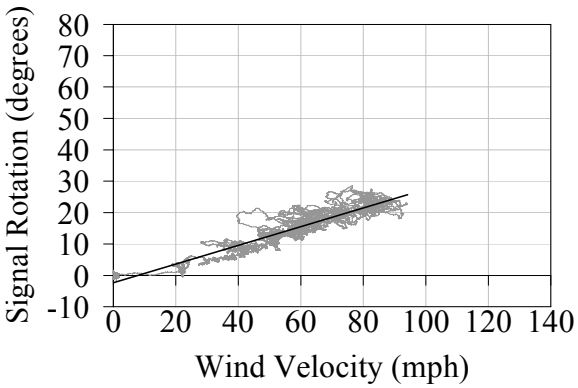

C) Test 4

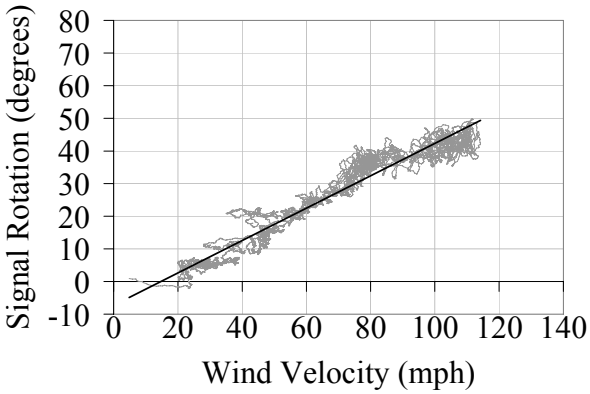

D) Test 7

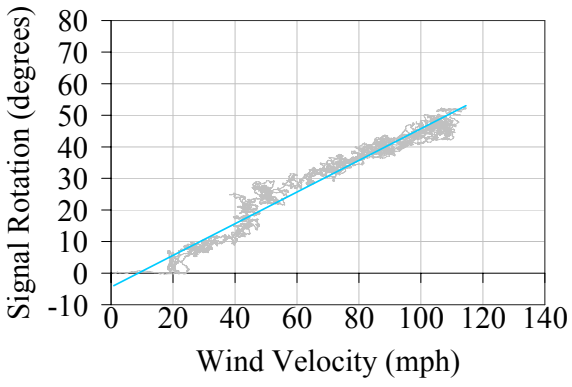

E) Test 8

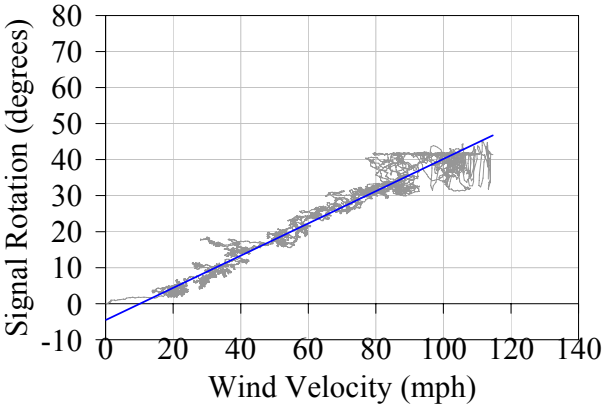

F) Test 9

Figure B-1. Signal Rotation.

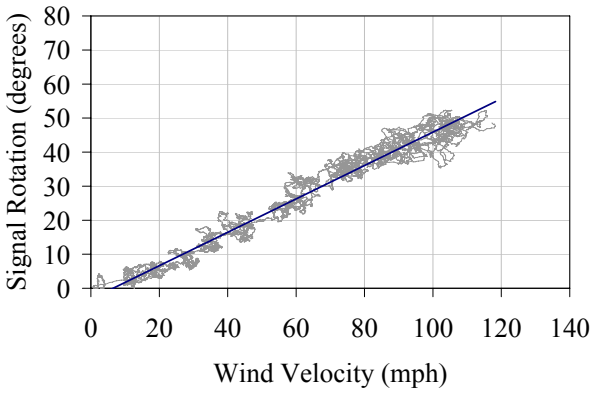

G) Test 10

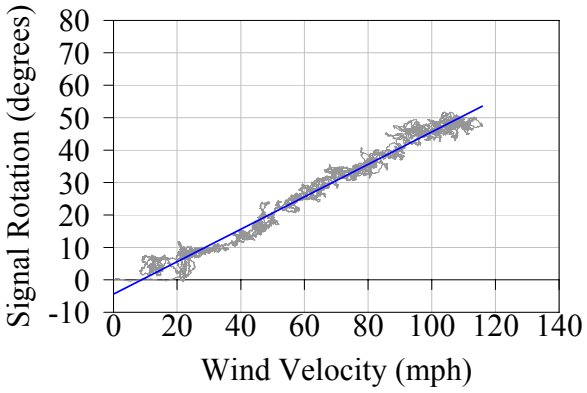

H) Test 11

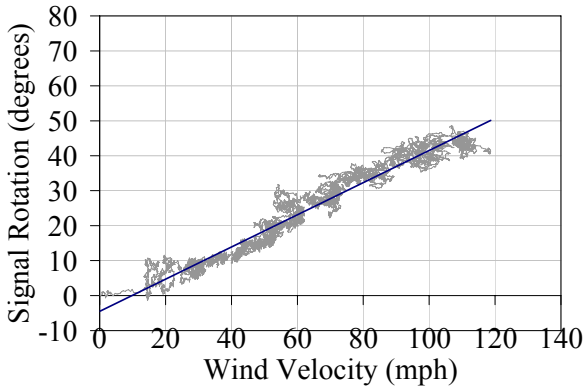

I) Test 12

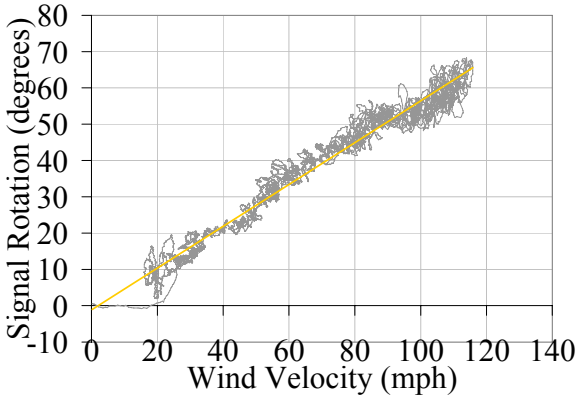

J) Test 13

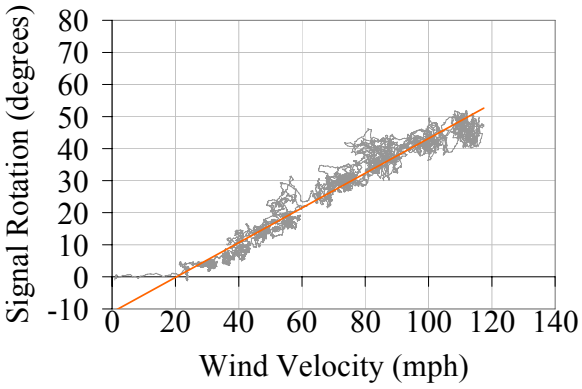

K) Test 14

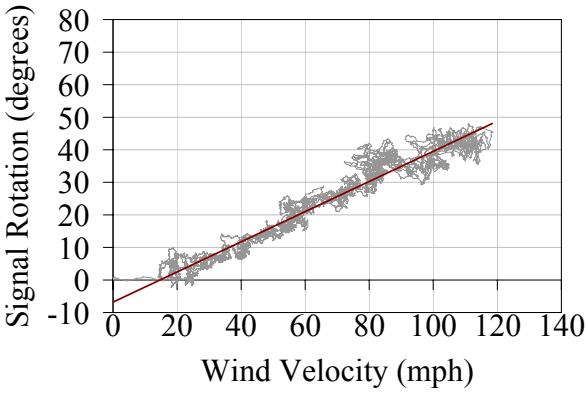

L) Test 15

Figure B-1. Signal rotation, continued.

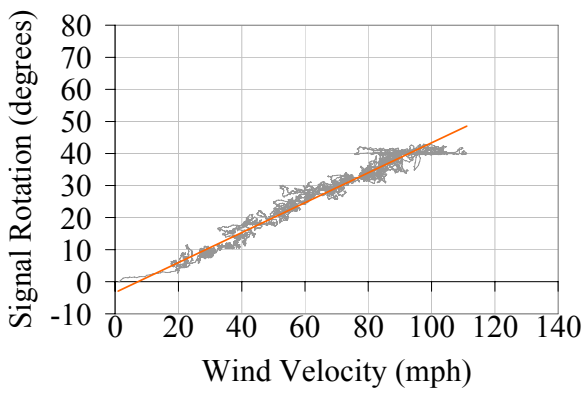

M) Test 17

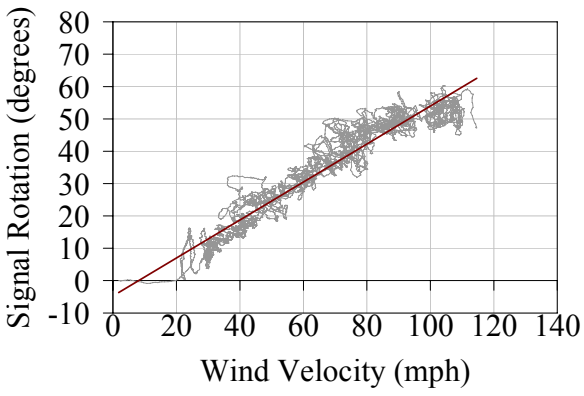

N) Test 18

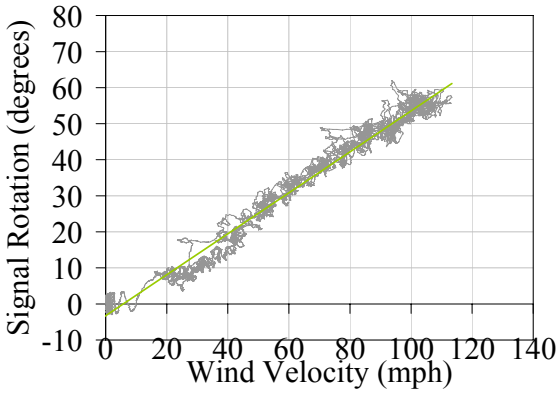

O) Test 19

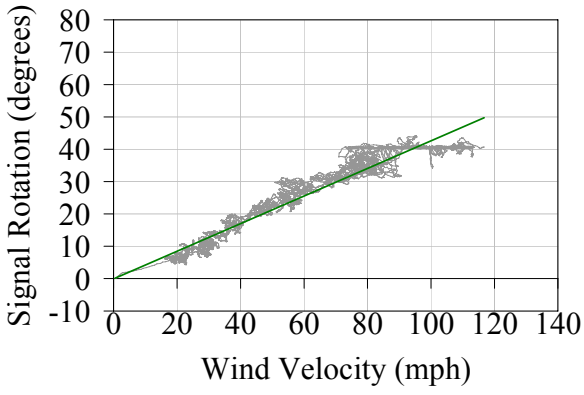

P) Test 20

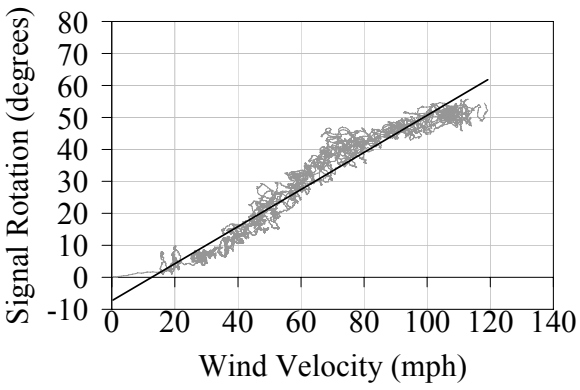

Q) Test 21

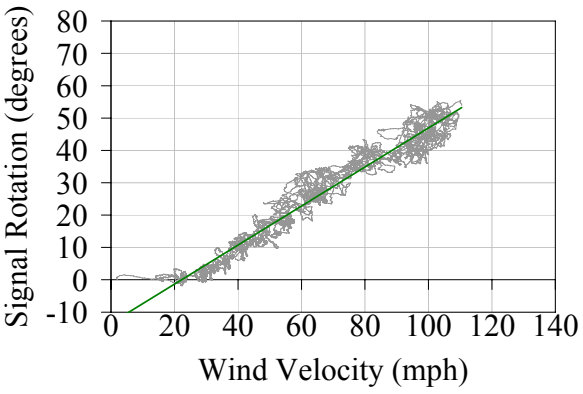

R) Test 22

Figure B-1. Signal rotation, continued.

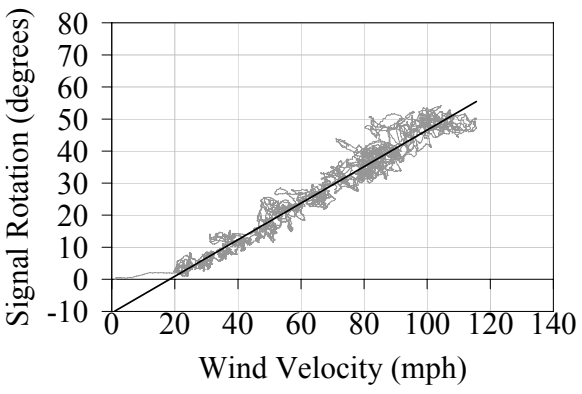

S) Test 23

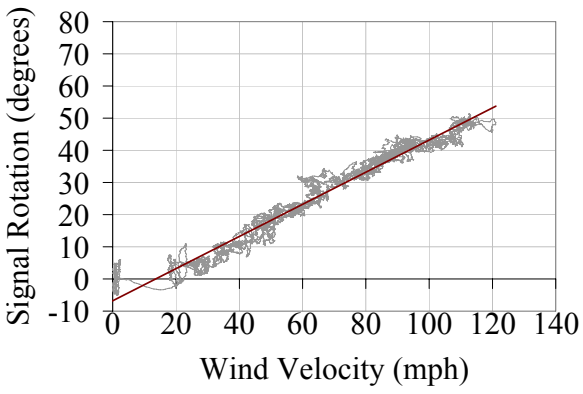

T) Test 24

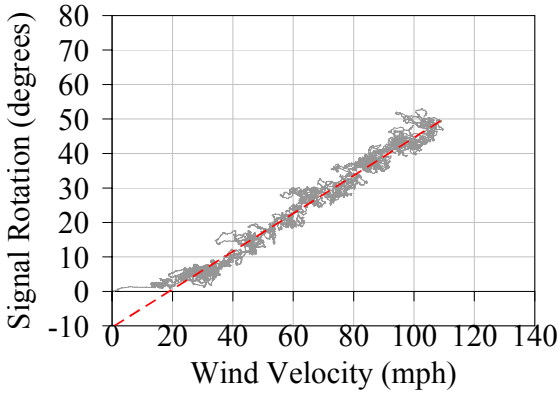

U) Test 25

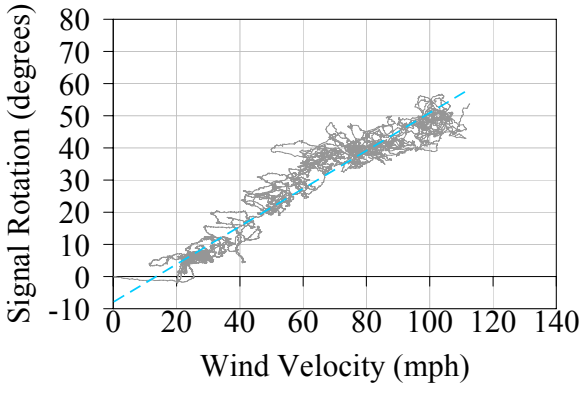

V) Test 26

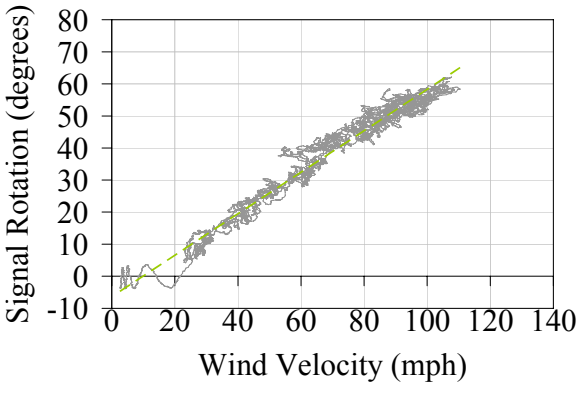

W) Test 27

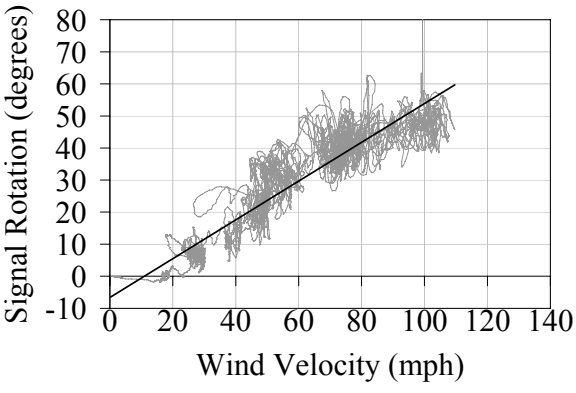

X) Test 28

Figure B-1. Signal rotation, continued.

APPENDIX C
CABLE TENSION GRAPHS

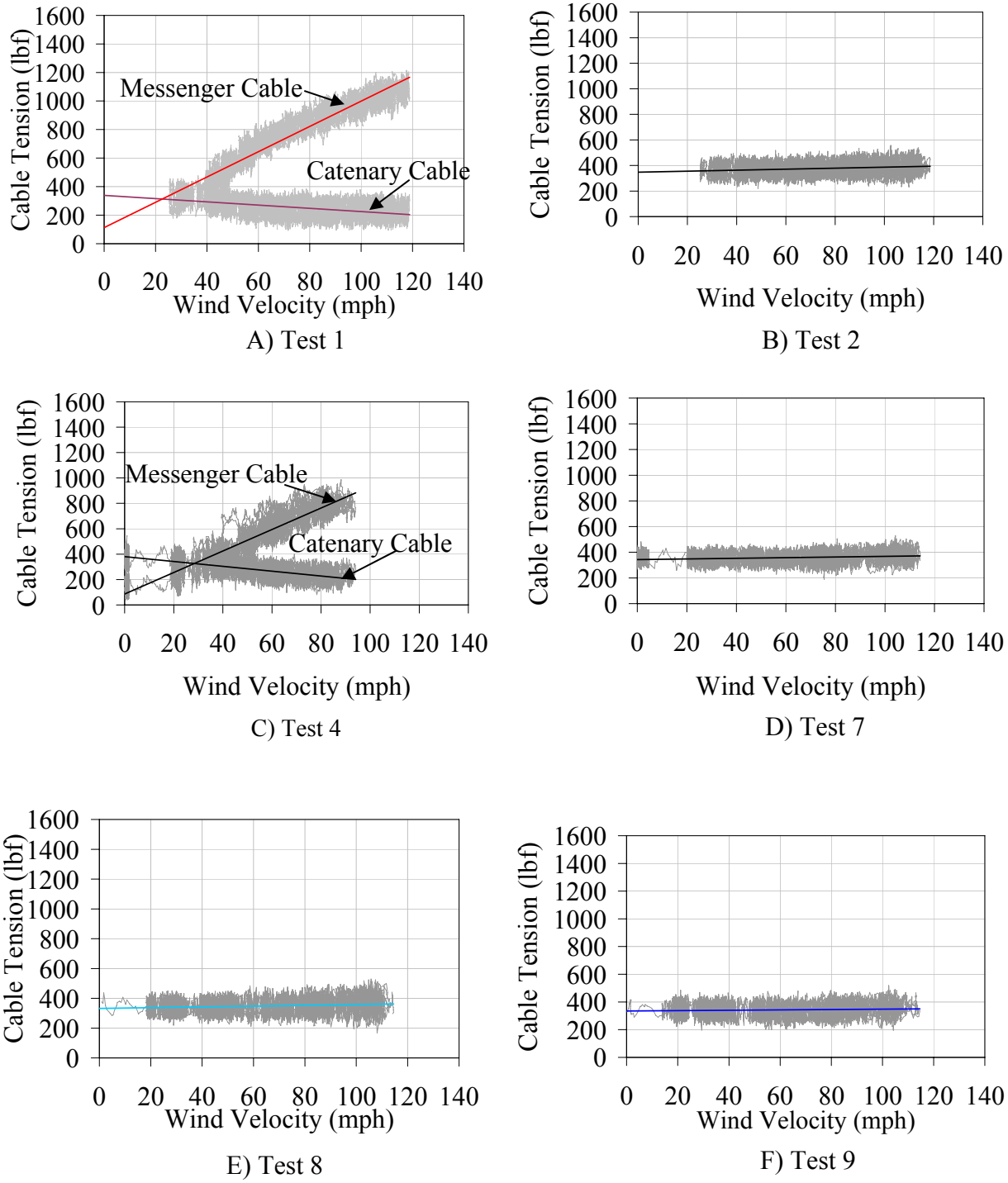

Figure C-1. Cable Tension.

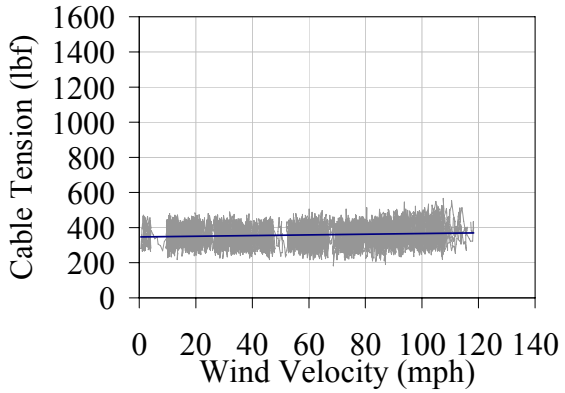

G) Test 10

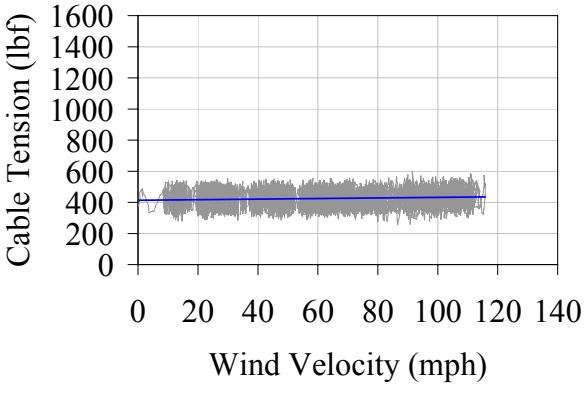

H) Test 11

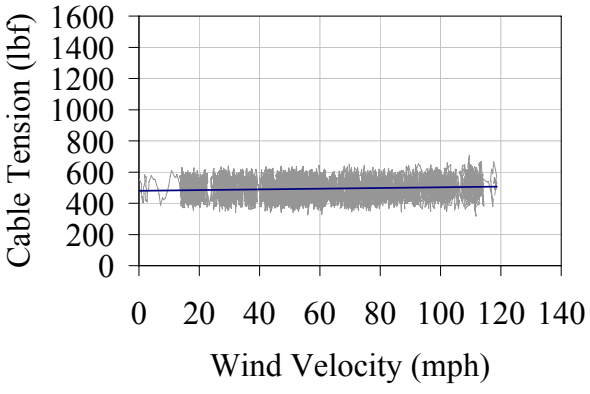

I) Test 12

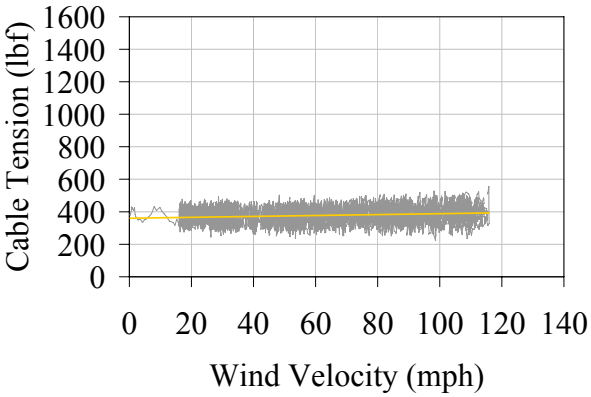

J) Test 13

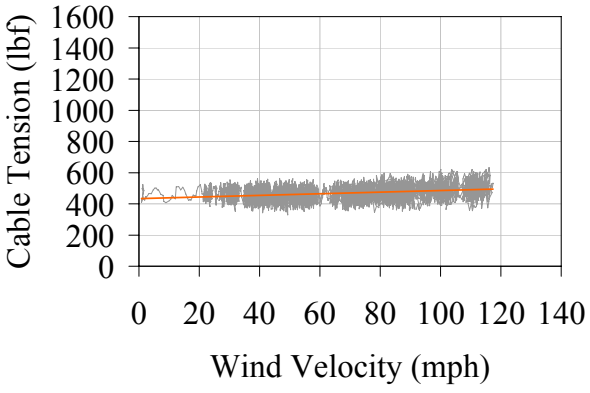

K) Test 14

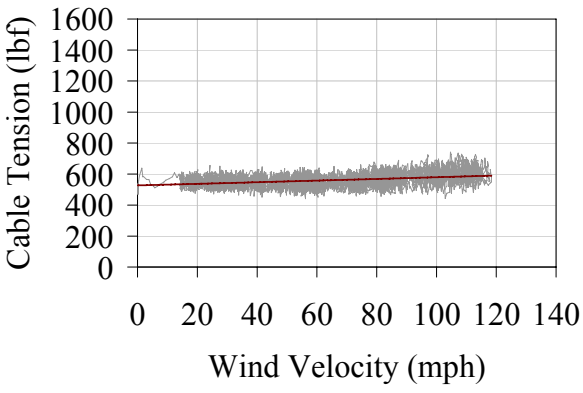

L) Test 15

Figure C-1. Cable tension, continued.

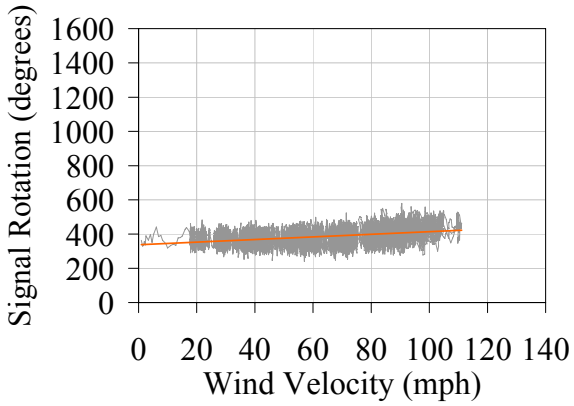

M) Test 17

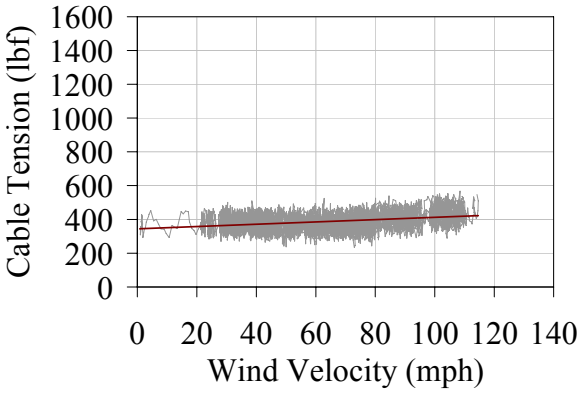

N) Test 18

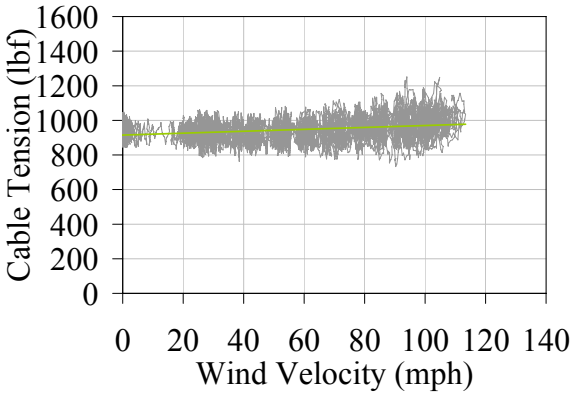

O) Test 19

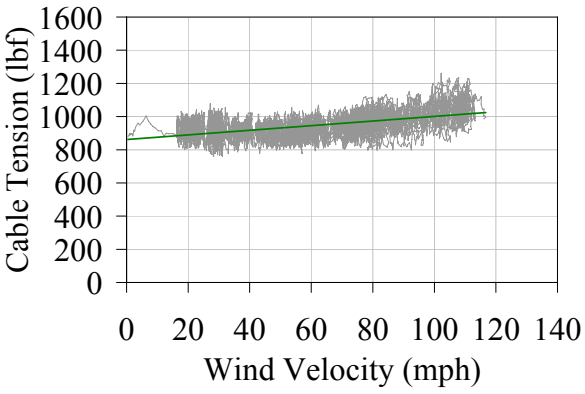

P) Test 20

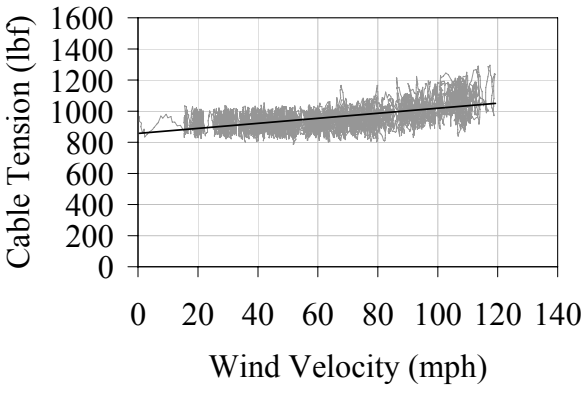

Q) Test 21

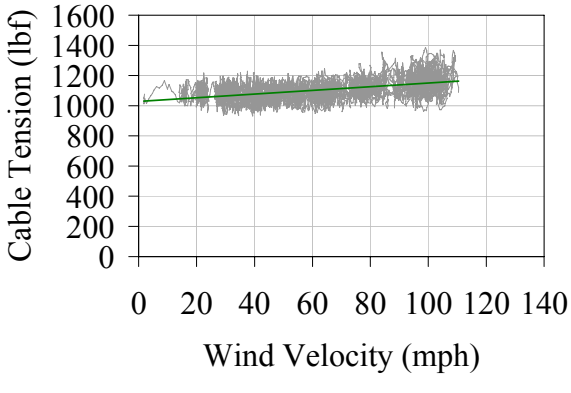

R) Test 22

Figure C-1. Cable tension, continued.

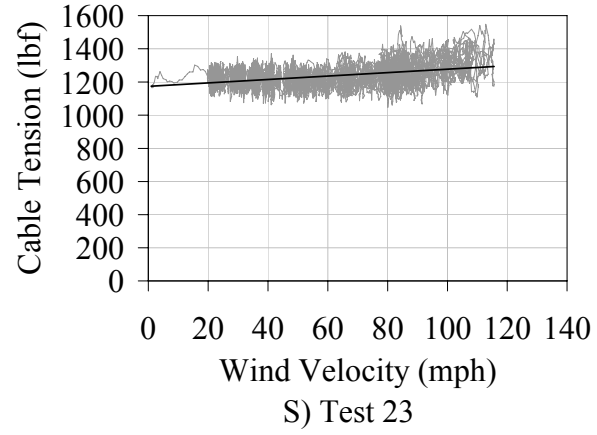

S) Test 23

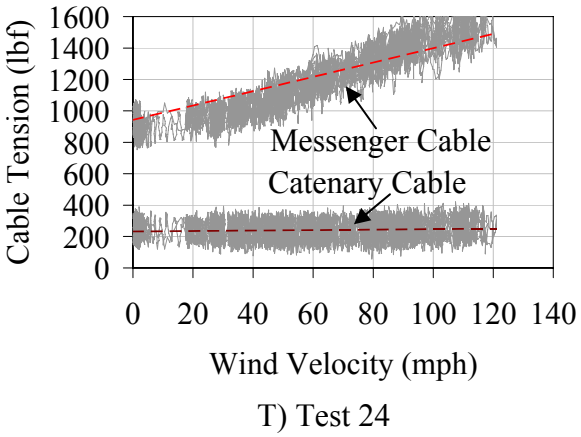

T) Test 24

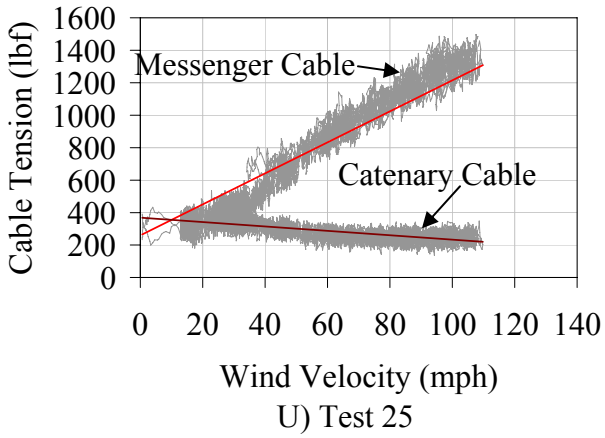

U) Test 25

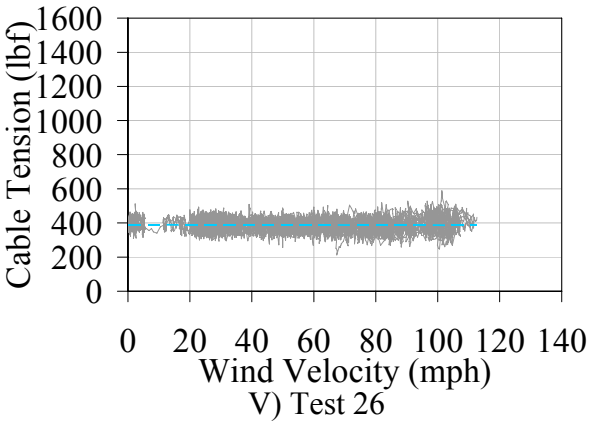

V) Test 26

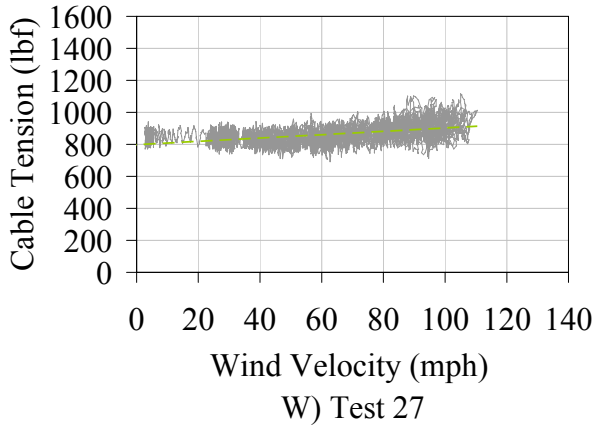

W) Test 27

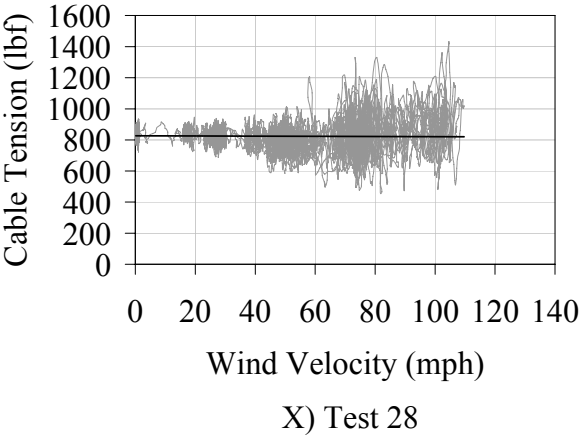

X) Test 28

Figure C-1. Cable tension, continued.

APPENDIX D
CABLE TRANSLATION GRAPHS

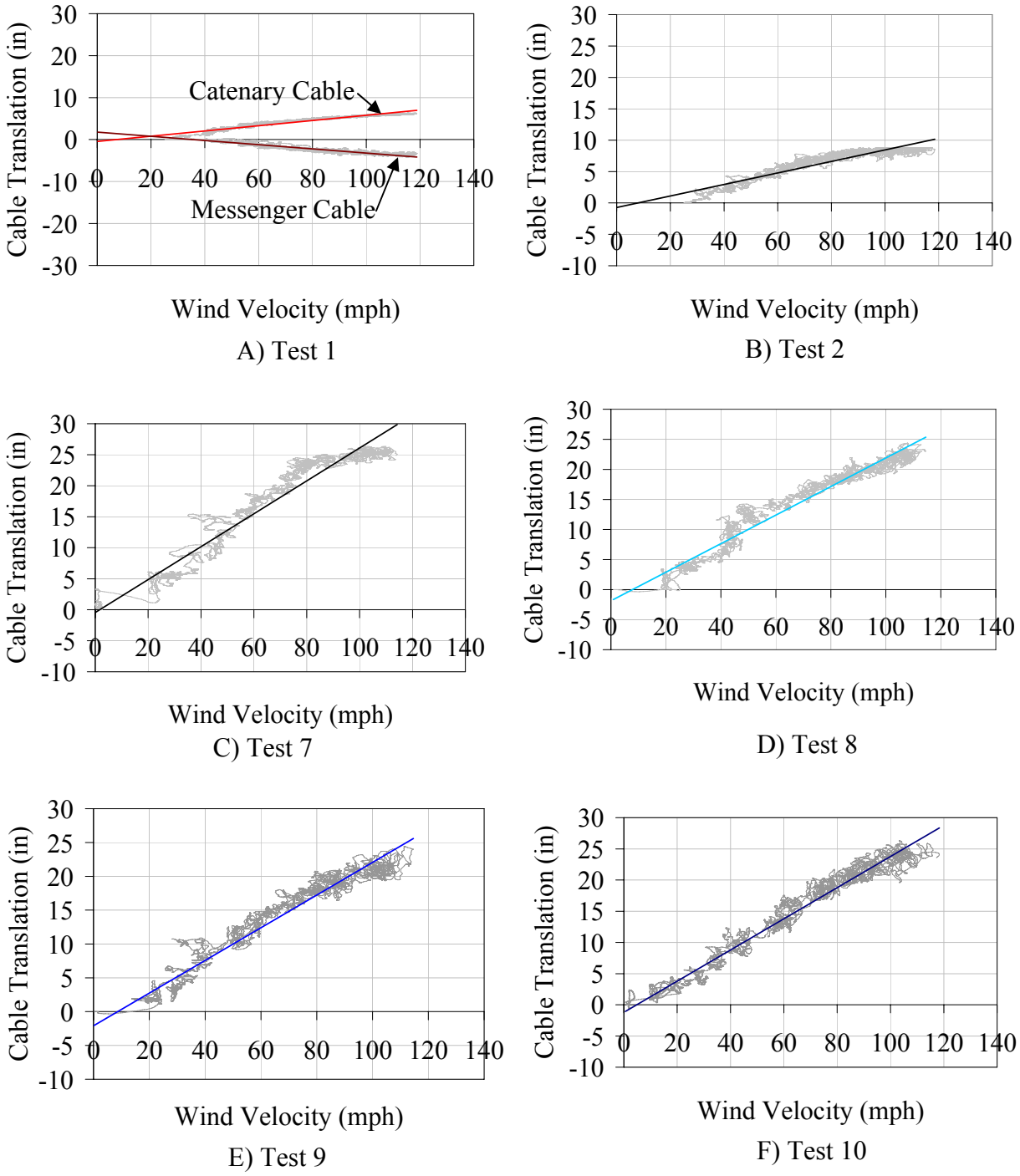

Figure D-1. Cable translation.

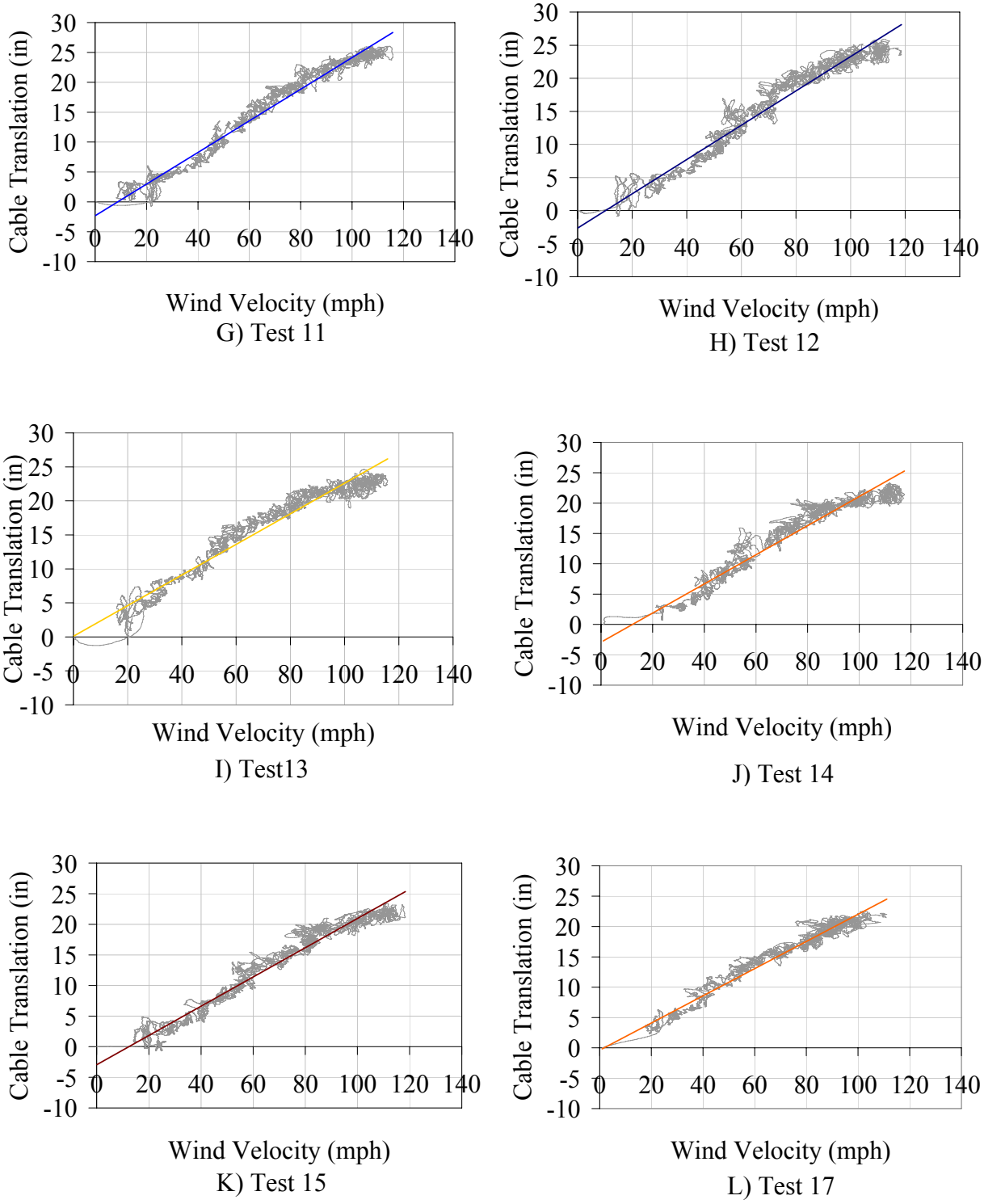

Figure D-1. Cable translation, continued.

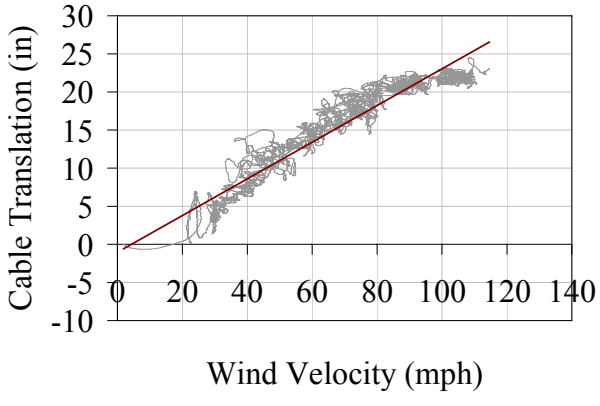

M) Test 18

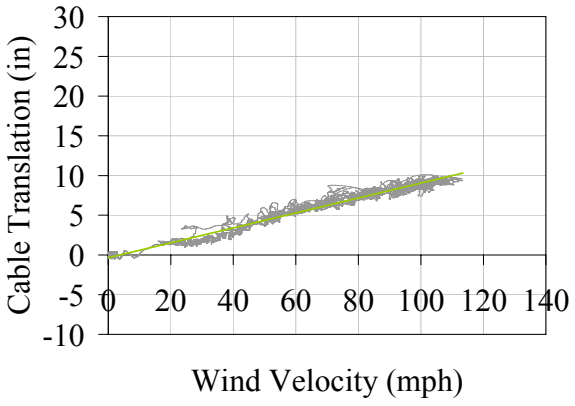

N) Test 19

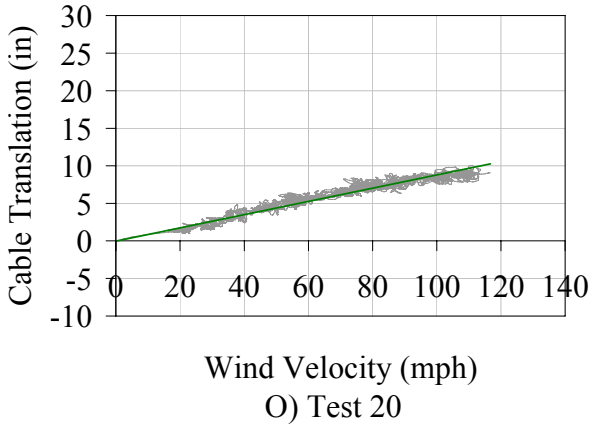

O) Test 20

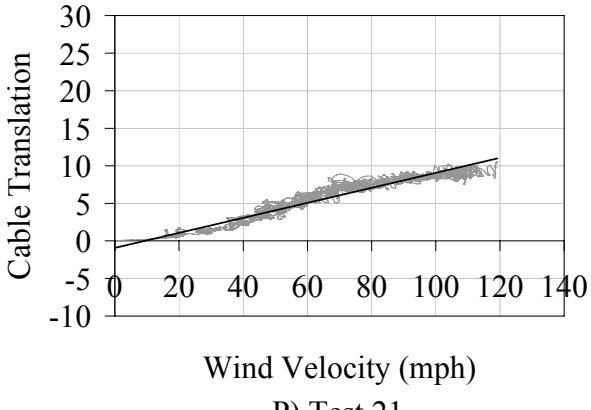

P) Test 21

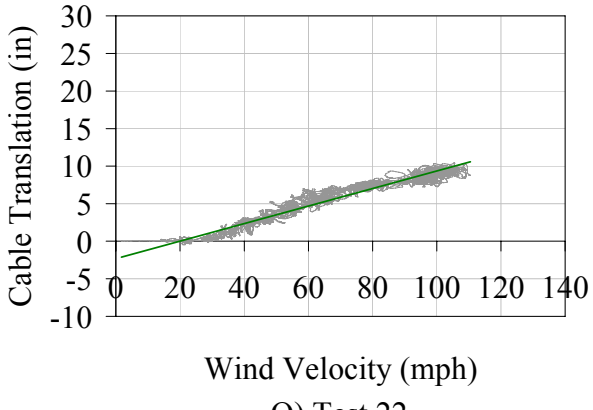

Q) Test 22

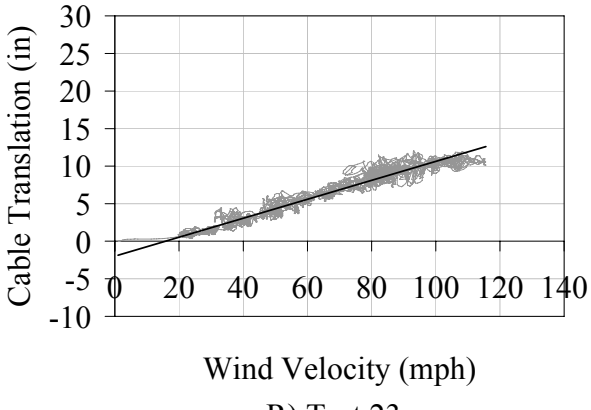

R) Test 23

Figure D-1. Cable translation, continued.

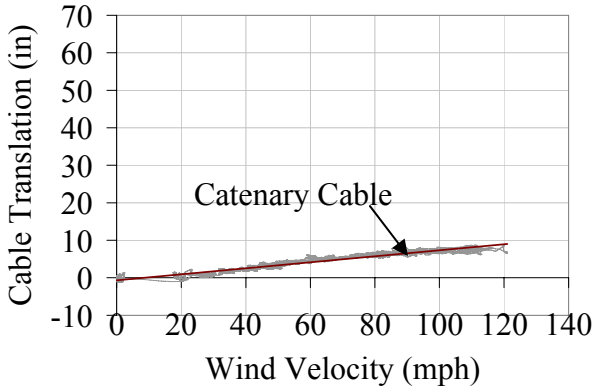

S) Test 24

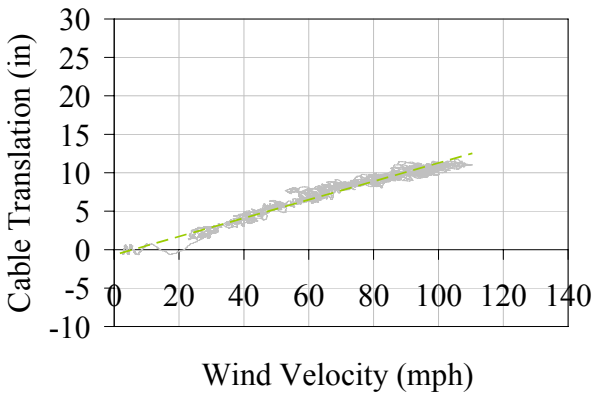

T) Test 27

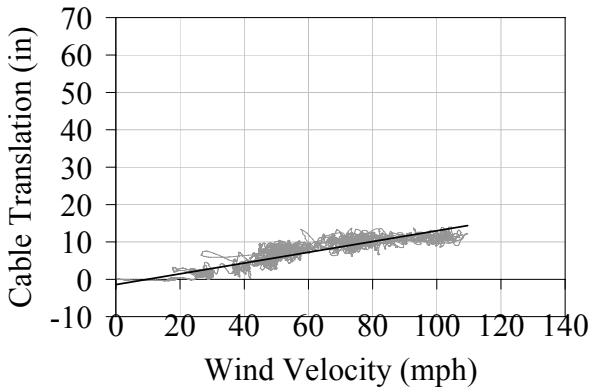

U) Test 28

Figure D-1. Cable translation, continued.

APPENDIX E
POLE DEFLECTION GRAPHS

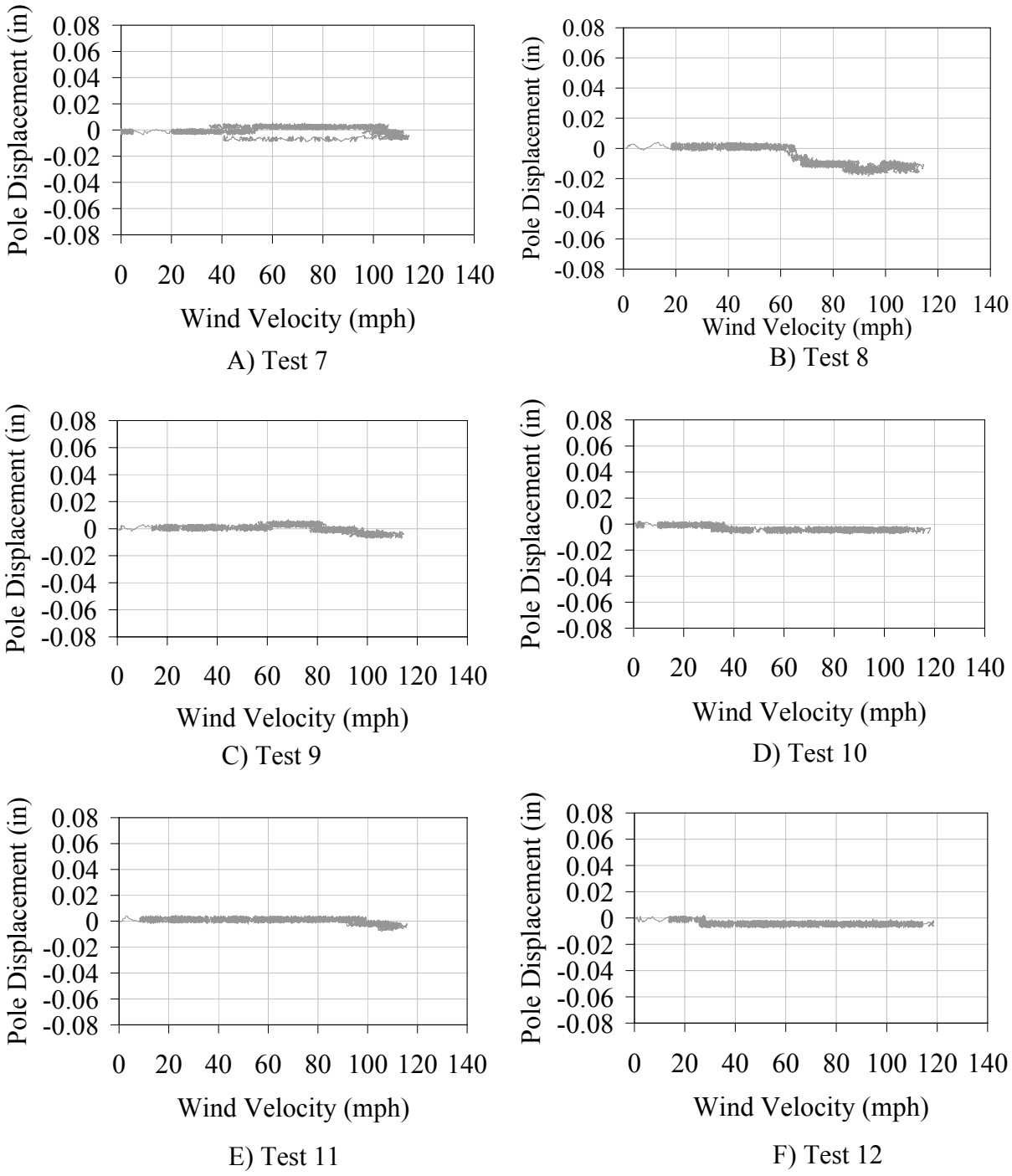

Figure E-1. Pole deflection.

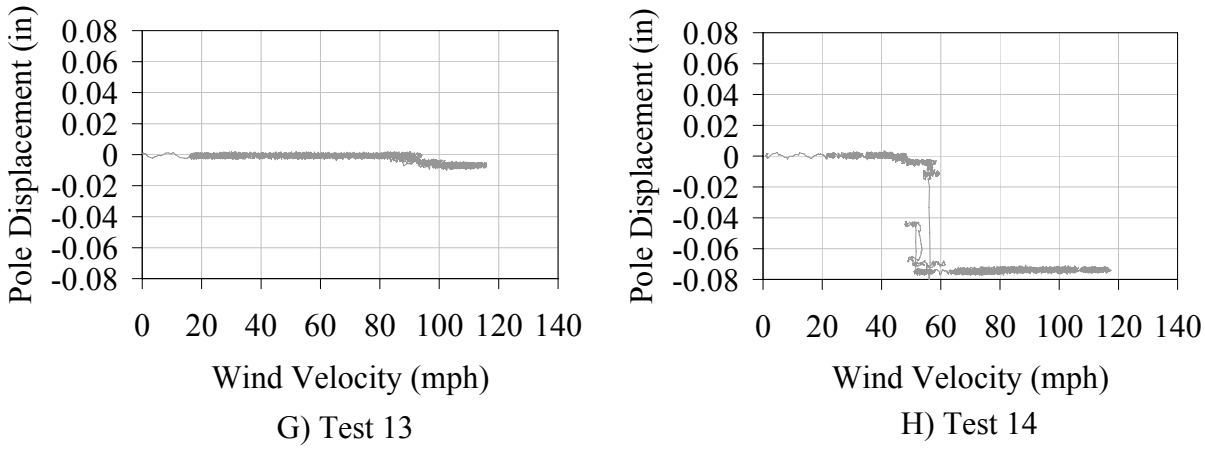

Figure E-1. Pole deflection, continued.

APPENDIX F
DRAG COEFFICIENT GRAPHS

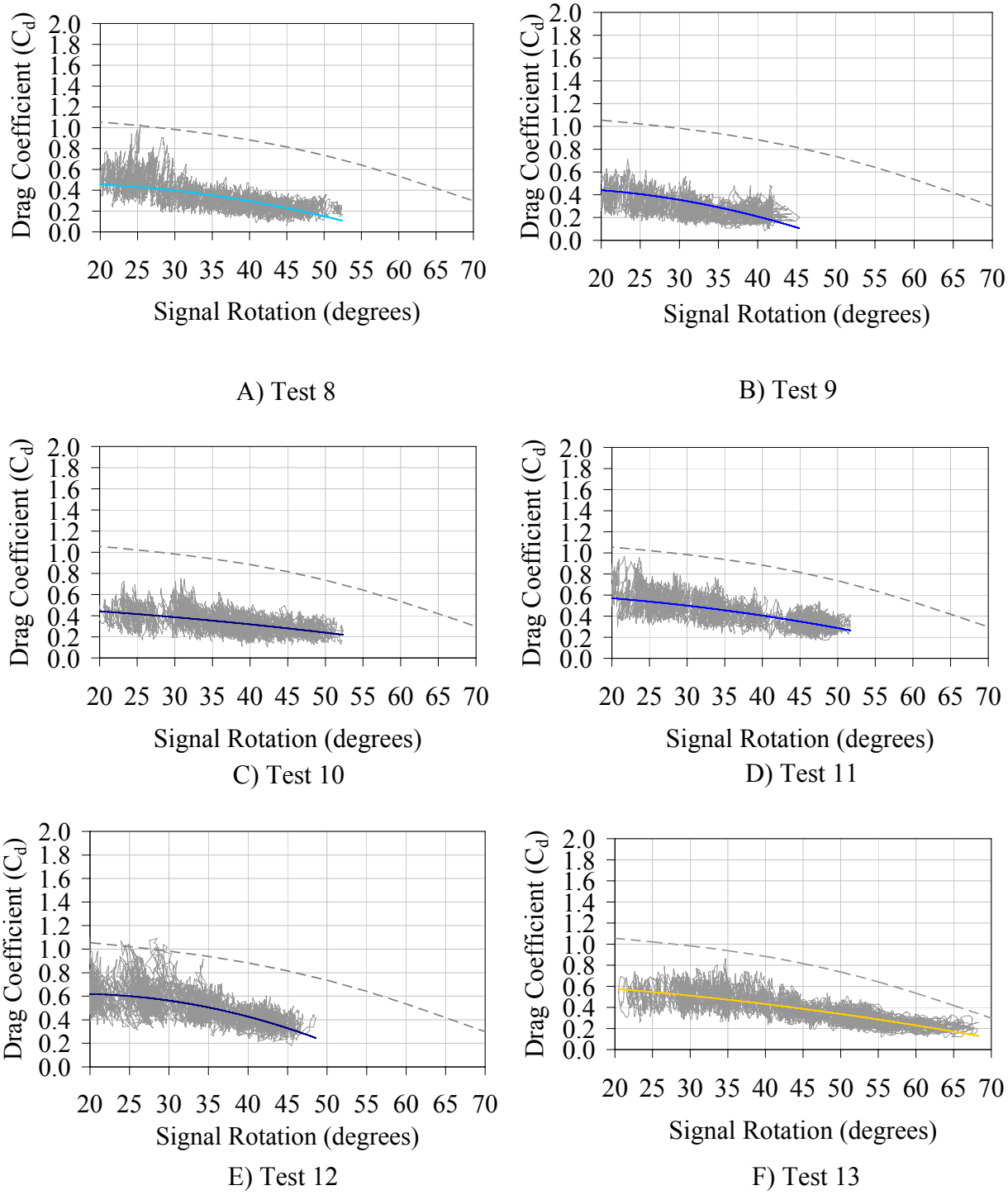

Figure F-1. Drag Coefficient.

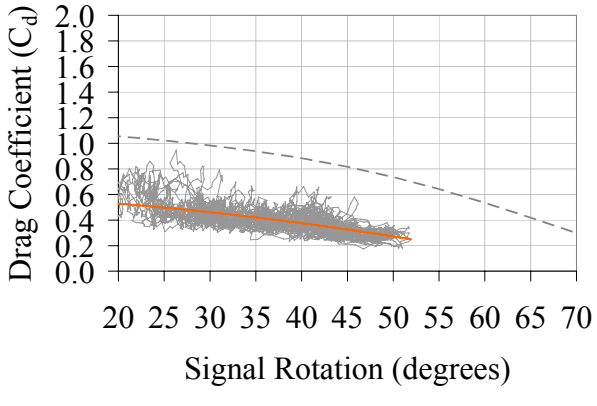

G) Test 14

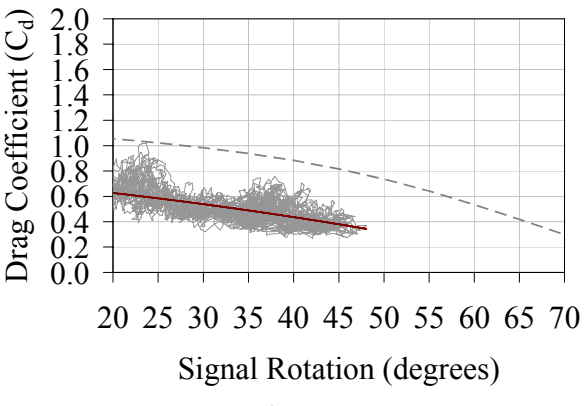

H) Test 15

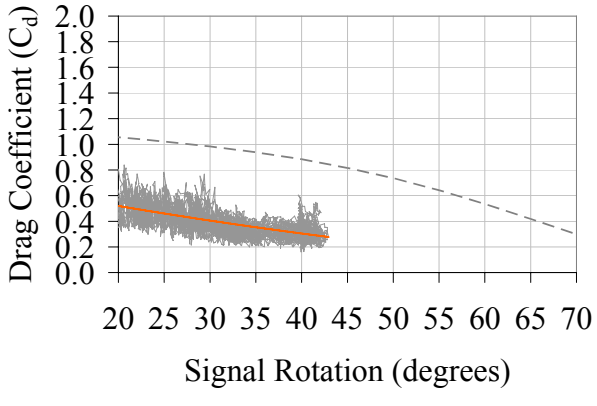

I) Test17

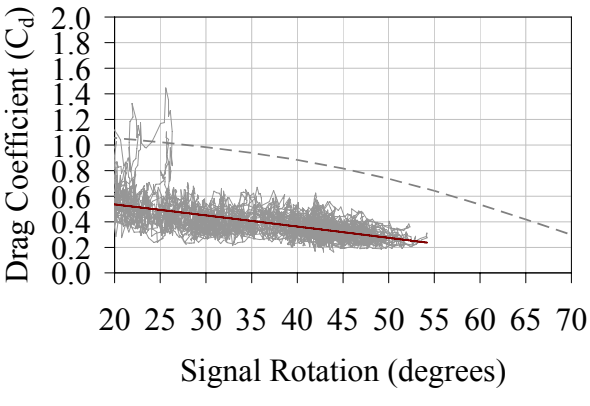

J) Test 18

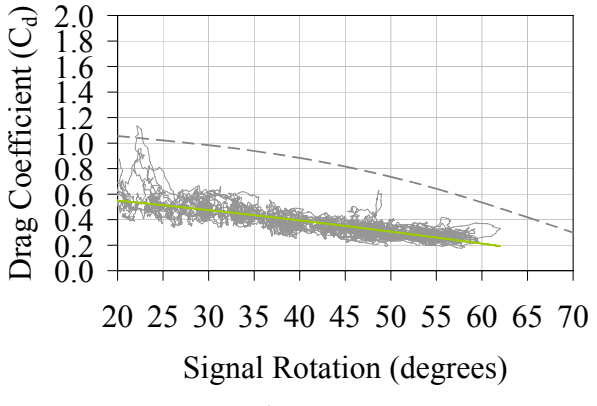

K) Test 19

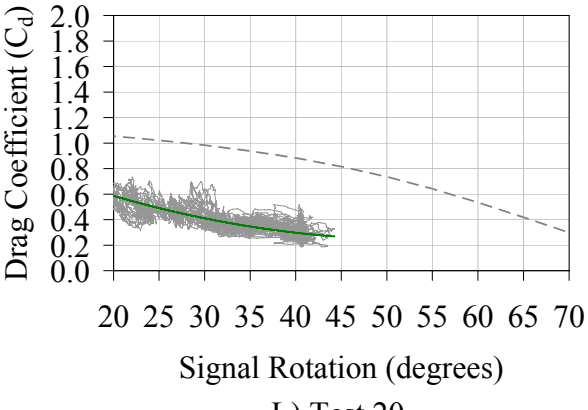

L) Test 20

Figure F-1. Drag Coefficient, continued.

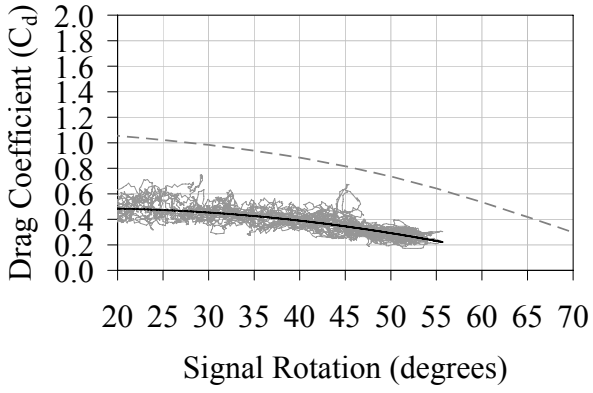

M) Test 21

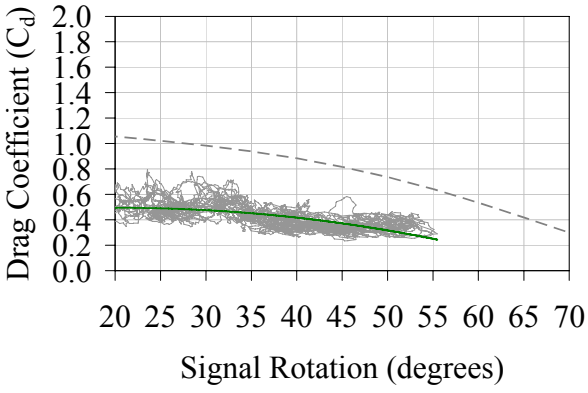

N) Test 22

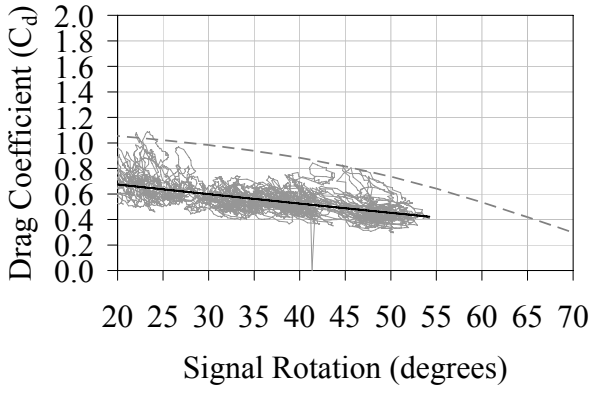

O) Test 23

Figure F-1. Drag Coefficient, continued.

APPENDIX G
LIFT COEFFICIENT GRAPHS

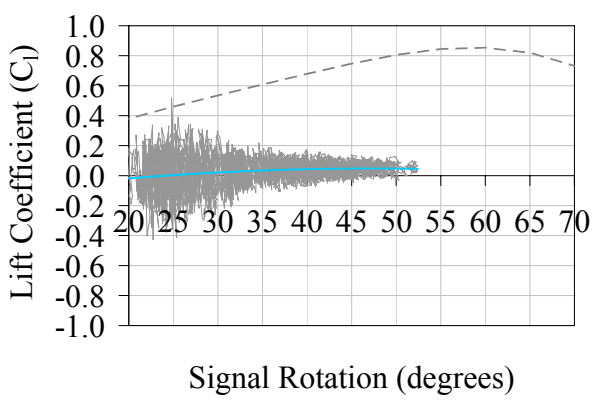

A) Test 8

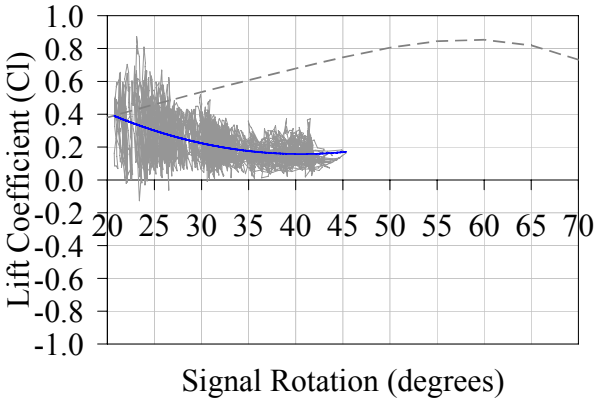

B) Test 9

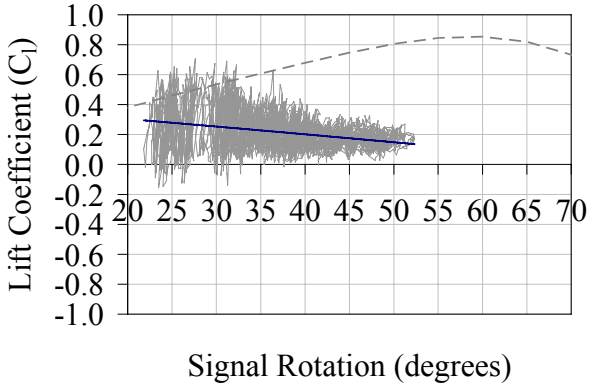

C) Test 10

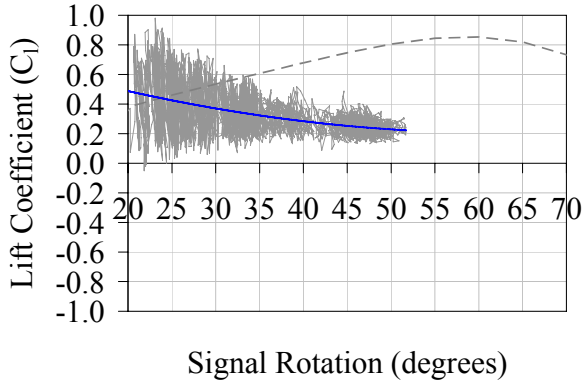

D) Test 11

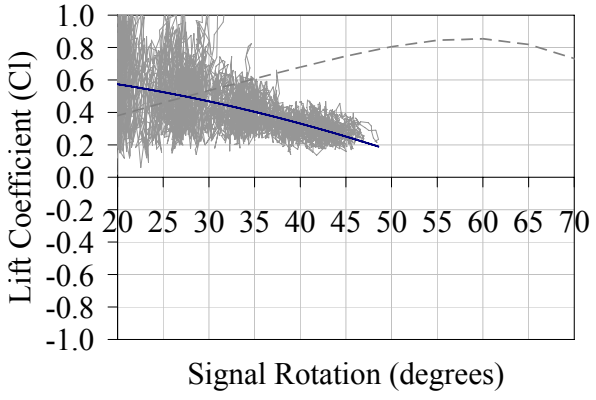

E) Test 12

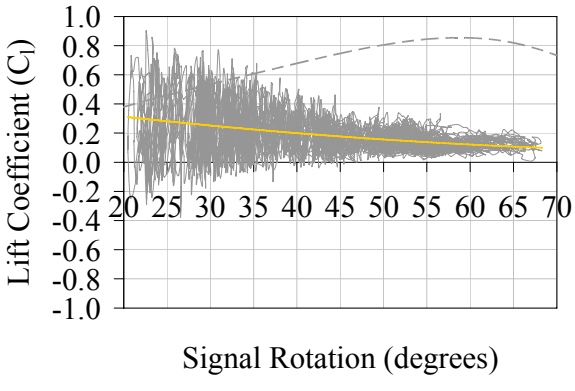

F) Test 13

Figure G-1. Lift Coefficient.

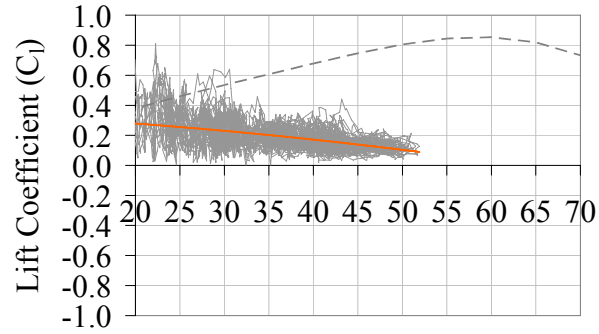

G) Test 14

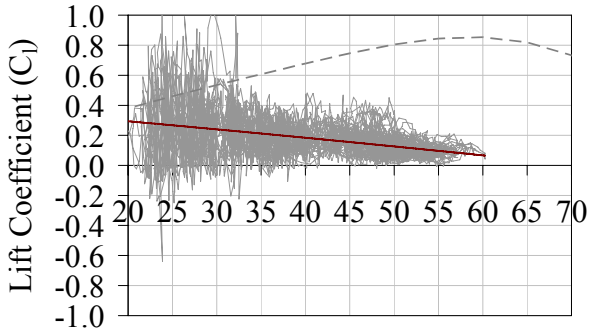

H) Test 15

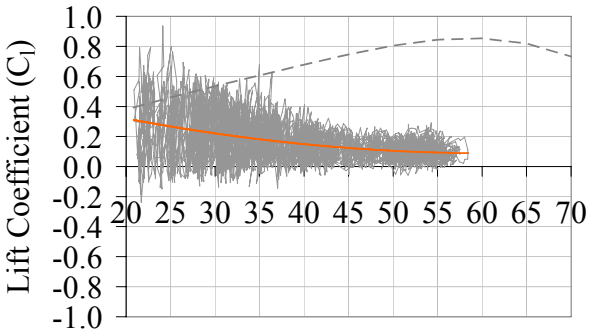

I) Test 17

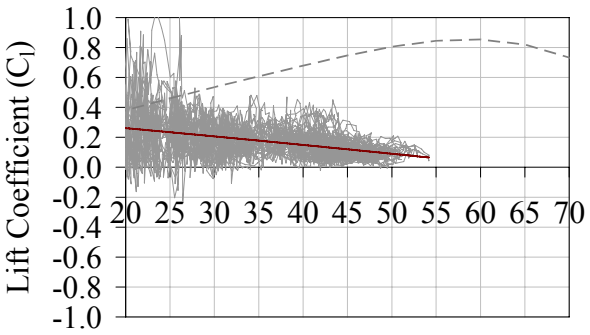

J) Test 18

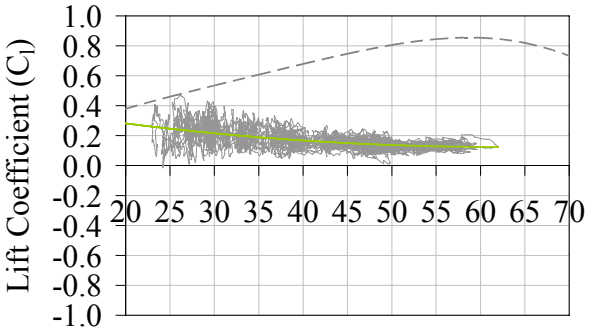

K) Test 19

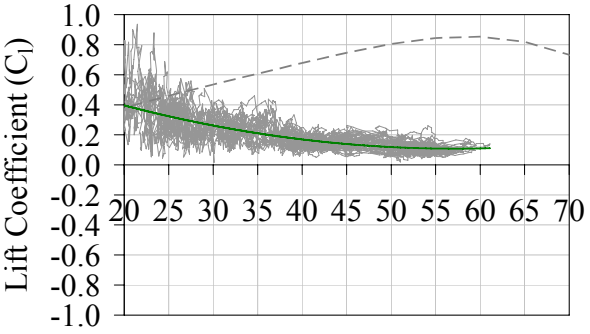

L) Test 20

Figure G-1. Lift Coefficient, continued.

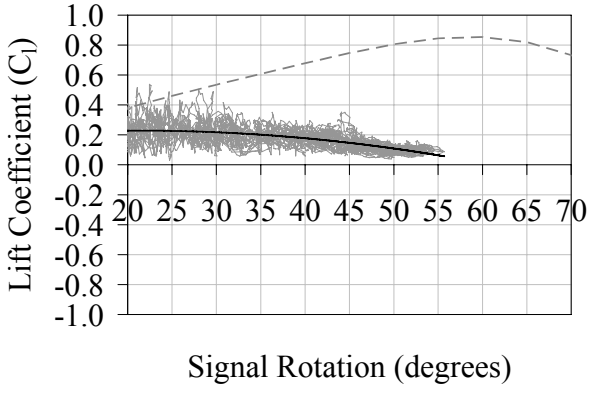

M) Test 21

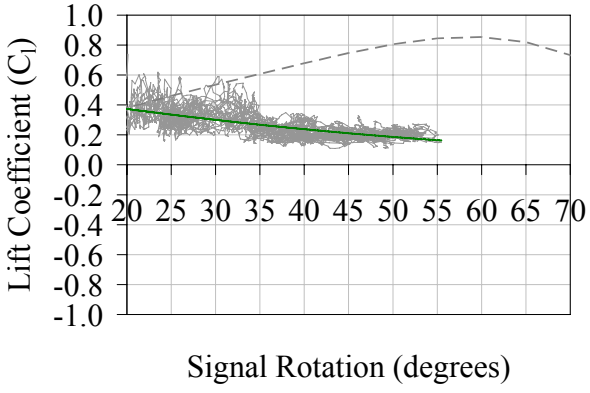

N) Test 22

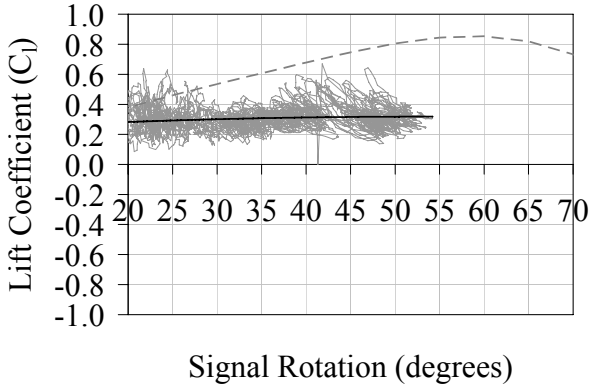

O) Test 23

Figure G-1. Lift coefficient, continued.

REFERENCES

Alampalli, S. (1998). Response of Untethered-Span-Wire Signal Poles to Wind Loads. *Journal of Wind Engineering and Industrial Aerodynamics*, 77&78, 73-81.

American Association of State Highway Transportation Officials (2001). *Standard Specifications for Structural Supports for High Signs, Luminaires and Traffic Signals* (4th Ed.). Washington, D.C.: American Association of State Highway Transportation Officials.

American Society of Civil Engineers Task Committee on Wind Forces (1961). Wind Forces On Structures. *Transactions of the American Society of Civil Engineers*, 126(2), 1124-1198.

ASCE 7-05 (2005). *Minimum Design Loads for Buildings and Other Structures*. Reston, VA: American Society of Civil Engineers.

Branick, Michael (2006). "A Comprehensive Glossary of Weather Terms for Storm Spotters." *NOAA Technical Memorandum NWS SR-145*, <http://www.srh.noaa.gov/oun/severewx/glossary.php> (February 3, 2007).

Cook, R.A., Bloomquist, D., & Long, J.C. (1996). Structural Qualification Procedure for Traffic Signals and Signs (FDOT WPI No. 0510731). Gainesville, Florida: University of Florida, Engineering and Industrial Experiment Station.

Durst, C.S. (1960). Wind Speeds Over Short Periods of Time. *The Meteorological Magazine*, 89(1056), 181-186.

Hoit, M.I., Cook, R.A., Christou, P.M., & Adediran, A.K. (1997). *Computer Aided Design Program For Signal Pole and Span Wire Assemblies With Two Point Connection System* (FDOT WPI No. 0510653). Gainesville, Florida: University of Florida, Engineering and Industrial Experiment Station.

Hoit, M.I., Cook, R.A., Wajek, S.L., & Konz, R.C. (1994). *Static and Dynamic Tests On Traffic Signal and Sign Dual Cable Support Systems* (FDOT WPI No. 0510653). Gainesville, Florida: University of Florida, Engineering and Industrial Experiment Station.

Holmes, J.D. (2001). *Wind Loading of Structures*. New York, NY: Spon.

Krayer, W.R., & Marshall, R.D. (1992). Gust Factors Applied to Hurricane Winds. *Bulletin of the American Meteorological Society*, 73(5), 613-617.

Liu, H. (1991). *Wind Engineering: A Handbook for Structural Engineers*. Englewood Cliffs, NJ: Prentice-Hall.

Marchman, J.F., III. (1971). Wind Loading On Free-Swinging Traffic Signals. *Transportation Engineering Journal*, 98, 237-246.

McDonald, J.R., Mehta, K.C., Oler, W.W., & Pulipaka, N. (1995). *Wind Load Effects on Signs, Luminaires and Traffic Signal Structures* (Research Study No. 11-5-92-1303). Lubbock, Texas: Texas Tech University, Wind Engineering Research Center.

Sherlock, R.H. (1947). Gust Factors for the Design of Buildings. *Publications: International Association for Bridge and Structural Engineering*, 8, 205-236.

Simiu, E., & Miyata, T. (2006). *Design of Buildings and Bridges for Wind*. Hoboken, NJ: John Wiley & Sons.

Solari, G. (1993). Gust Buffeting I: Peak Wind Velocity and Equivalent Pressure. *Journal of Structural Engineering*, 119(2), 365-382.

Solari, G. (1993). Gust Buffeting II: Dynamic Alongwind Response. *Journal of Structural Engineering*, 119(2), 383-398.

Solari, G. (1992). Alongwind Response Estimation: Closed Form Solution. *Journal of the Structural Division*, 108, 225-244.

Solari, G., & Kareem, A. (1998). On the Formulation of ASCE 7-95 Gust Effect Factor. *Journal of Wind Engineering and Industrial Aerodynamics*, 77&78, 673-684.

Transportation Research Board (1998). *Structural Supports for Highway Signs, Luminaires, and Traffic Signals* (NCHRP Rep. No. 411) Washington, D.C.: Transportation Research Board.

Transportation Research Board (2003). *Structural Supports for Highway Signs, Luminaires, and Traffic Signals* (NCHRP Rep. No. 494) Washington, D.C.: Transportation Research Board.